LAPPEENRANTA-LAHTI UNIVERSITY OF TECHNOLOGY LUT

School of Engineering Science

Degree programme in Chemical and Process Engineering

Sonja Kauppi

SIMULATION AND TECHNO-ECONOMIC ANALYSIS OF SYNTHETIC NATURAL GAS PRODUCTION

Examiners: Professor Tuomas Koiranen

Docent Arto Laari

ABSTRACT

Lappeenranta-Lahti University of Technology LUT
School of Engineering Science
Degree programme in Chemical and Process Engineering

Sonja Kauppi

Simulation and techno-economic analysis of synthetic natural gas production

Master's Thesis
2020
93 pages, 19 figures, 31 tables, 46 equations and 2 appendices

Examiners: Professor Tuomas Koiranen and Docent Arto Laari
Supervisors: Professor Tuomas Koiranen and Docent Arto Laari

Keywords: Power-to-X, Power-to-Gas, P2X, P2G, synthetic natural gas, biogas, methane, renewable fuel, process simulation, Aspen Plus

Alternative fuels, such as synthetic natural gas (SNG) and biogas, are considered a way to mitigate climate change. Politics and environmental concerns are driving forces for industry to join the alternative fuel research. It is important to find techno-economically feasible solutions to replace conventional fuels. Power-to-X (P2X) technologies are seen promising as they utilize renewably sourced energy, carbon dioxide (CO_2) captured from emissions and hydrogen (H_2) produced via water electrolysis. The technology required to utilise SNG as transport fuel and the required infrastructure are already available. SNG also has various utilisation options besides as transport fuel, which makes it an attractive option.

Literature research in P2X technologies and SNG and biogas production processes was carried out. The results were used as a basis to design catalytic and biological methanation processes on conceptual design level. The processes were simulated using Aspen Plus. Hydrogen purification with deoxo process was also studied. Techno-economic analysis was conducted for both processes based on the simulation results.

The product purity targets (max. 3 mol-% H_2 and 6 mol-% CO_2) were met in the catalytic process model (CH_4 82.15; H_2 2.84; CO_2 1.62; H_2O 13.38 mol-%) but not in the biological model (CH_4 90.7; H_2 4.87; CO_2 1.13; H_2O 3.29 mol-%) due to high hydrogen conversion requirements that exceeded the methanation archaea's maximum conversion. The total fixed capital costs were 37.4 M€ for catalytic methanation and 34.1 M€ for biological methanation at 40 MW capacity. The necessity of deoxo process needs further research as it increases the investment and operational costs for both processes considerably.

Before more detailed design is possible, experimental results are required to find out how they correlate to the simulation results to confirm the accuracy of the models. The results of this thesis can be considered as conceptual design and evaluation for both methanation processes.

TIIVISTELMÄ

Lappeenrannan-Lahden teknillinen yliopisto LUT
School of Engineering Science
Kemiantekniikan koulutusohjelma

Sonja Kauppi

Synteettisen maakaasun tuotannon simulointi ja teknillistaloudellinen arviointi

Diplomityö
2020
93 sivua, 19 kuvaa, 31 taulukkoa, 46 yhtälöä ja 2 liitettä

Tarkastajat: Professori Tuomas Koiranen ja dosentti Arto Laari
Ohjaajat: Professori Tuomas Koiranen ja dosentti Arto Laari

Avainsanat: Power-to-X, Power-to-Gas, P2X, P2G, synteettinen maakaasu, biokaasu, metaani, uusiutuva polttoaine, prosessisimulointi, Aspen Plus

Vaihtoehtoisten polttoaineiden, kuten synteettisen maakaasun (SNG) ja biokaasun, käyttöä pidetään keinona hillitä ilmastonmuutosta. Poliittiset päätökset ja ympäristötekijät kannustavat teollisuutta osallistumaan vaihtoehtoisten polttoaineiden tutkimukseen. Tavanomaiset polttoaineet tulisi korvata ratkaisuilla, jotka ovat teknillistaloudellisesti toteutettavissa. Power-to-X (P2X) -teknologiat vaikuttavat lupaavilta, koska ne hyödyntävät uusiutuvaa energiaa, päästöistä kaapattua hiilidioksidia (CO_2) sekä veden elektrolyysillä tuotettua vetyä (H_2). SNG:n käyttö liikennepolttoaineena on jo mahdollista teknologian sekä infrastruktuurin kannalta. Liikennepolttoainekäytön lisäksi SNG:tä voi hyödyntää myös muihin tarkoituksiin, minkä takia se on houkutteleva vaihtoehto.

Kirjallisuuskatsauksessa perehdyttiin P2X-teknologioihin sekä SNG:n ja biokaasun valmistusprosesseihin. Tulosten perusteella suunniteltiin alustavasti sekä katalyyttinen että biologinen metaanin valmistusprosessi. Prosessit simuloitiin Aspen Plus – simulointiohjelmalla. Työssä perehdyttiin myös vedyn puhdistukseen deoxo-menetelmällä. Molemmista prosesseista tehtiin teknillistaloudellinen arviointi simulointitulosten perusteella.

Tuotteen puhtausvaatimukset (enintään 3 mol-% H_2 ja 6 mol-% CO_2) täyttyivät katalyyttisen prosessin mallissa (CH_4 82.15; H_2 2.84; CO_2 1.62; H_2O 13.38 mol-%). Biologinen malli ei yltänyt puhtausvaatimuksiin (CH_4 90.7; H_2 4.87; CO_2 1.13; H_2O 3.29 mol-%), koska siihen tarvittava vedyn konversio on korkeampi, kuin metanointiarkeonien enimmäiskonversio. Katalyyttisen prosessin kokonaisinvestointikustannukset olivat 37.4 M€ ja biologisen prosessin 34.1 M€ 40 MW kapasiteetilla. Deoxo-prosessin tarpeellisuutta on tutkittava lisää, koska se nostaa investointi- ja käyttökustannuksia huomattavasti.

Simulointitulosten tarkkuuden vahvistamiseen vaaditaan kokeellisia tuloksia. Mallin korrelointi kokeellisiin tuloksiin on selvitettävä, ennen kuin prosessisuunnittelua voidaan tehdä yksityiskohtaisemmin. Tämän diplomityön tuloksia voidaan käyttää esiselvityksenä kummallekin metaanin valmistusprosessille.

ACKNOWLEDGEMENTS

This master's thesis was carried out at Lappeenranta-Lahti University of Technology LUT in Lappeenranta between March and August 2020.

I thank my examiners and supervisors Professor Tuomas Koiranen and Docent Arto Laari for their input and guidance during this thesis project. Thank you Tommi Rintamäki and Anna Shigina from Wärtsilä for this interesting thesis topic and for guidance. Besides Tommi and Anna, I would also like to thank Petri Laakso and Cyril Bajamundi from Soletair Power for introducing me to the world of power-to-X. Your enthusiasm has been inspiring.

The past six months have been unusual globally. Social distancing, remote work and changes to our daily lives have affected everyone. Thank you to my parents and brothers for your support and keeping up even though we couldn't meet as normal for most of the duration of my thesis work. Thanks to my friends around the globe for staying close despite the physical distance, and for the extempore video calls, chats and hang outs.

It is important not to stop going on and always try to do our best, even when unexpected things happen. I'm glad I was able to carry on with my thesis as planned and play my part in making sure that scientific research doesn't stop at any inconvenience. This thesis is focused on making the future brighter, and I'm looking ahead to see what comes up next!

Lappeenranta, 31.8.2020

Sonja Kauppi

Contents

Symbols

T	temperature	°C
p	pressure	bar
STY	space-time yield	$dm^3_{product}/cm^3_{catalyst}$ h
T_c	critical temperature	K
p_c	critical pressure	bar
R	ideal gas constant	J/mol K
H	upper value	€
ML	most likely value	€
L	lower value	€
$\bar{x}$	mean value	€
$\bar{x}_{ISBL}$	mean value for ISBL	€
$\bar{x}_{OSBL}$	mean value for OSBL	€
S_x	standard deviation	€
$S_{x,ISBL}$	standard deviation for ISBL	€
$S_{x,OSBL}$	standard deviation for OSBL	€
C_{ISBL}	ISBL cost	€
C_e	equipment cost	€
C_{FC}	total fixed capital cost	€
ISBL	cost factor for ISBL cost	-
OS	cost factor for OSBL cost	-
D&E	cost factor for design and engineering costs	-
X	cost factor for contingency charges	-

Δp_b	pressure drop	Pa
f_m	modified coefficient of friction	-
ρ	fluid density	kg/m^3
v	superficial linear velocity	m/s
d_p	diameter of the catalyst particle	m
ε_b	bed voidage	-
H_b	bed height	m
R_e	Reynolds number	-
μ	viscosity of the fluid	Pa s
a	coefficient	-
b	coefficient	-
h	reactor height	m
Q	feed flowrate	m^3/s
A	cross-sectional area of reactor	m^2
GHSV	gas hourly space velocity	h^{-1}
$V_{catalyst}$	catalyst volume	cm^3; m^3
$V_{reactor}$	reactor volume	m^3
$V_{product}$	product flowrate	dm^3/h
V_{feed}	flowrate of feed	m^3/h
ω	acentric factor for the species	-
Δ H	enthalpy	kJ/mol

Abbreviations

AWE	Alkaline water electrolysis
CSTR	Continuous stirred tank reactor
DAC	Direct air capture
DC	Direct current
DME	Dimethyl ether
EOS	Equation of state
ETS	Emission trading system
GHG	Greenhouse gas
GHSV	Gas hourly space velocity
ISBL	Inside battery limits
LBG	Liquefied biogas
LNG	Liquefied natural gas
MEC	Microbial electrolysis cell
MFR	Methane formation rate
NPV	Net present value
OSBL	Outside battery limits, off-site
P2G	Power-to-gas
P2M	Power-to-methane
P2X	Power-to-X
PEM	Polymer electrolytic membrane; proton exchange membrane
SNG	Synthetic natural gas
SOEC	Solid oxide electrolysis cell
STY	Space-time yield

1 Introduction

1.1 Background of the work

Alternative fuels are considered a way to mitigate climate change. Renewable alternatives for fossil fuels used in transportation, heating and electricity production are broadly studied. (Semelsberger et al. 2006; Bassano et al. 2019) Fuel consumption increases as the world population grows and international trade and shipment of goods increases (Brummelkamp & Sardjoepersad 2007; IEA 2019). Transport sector has the fastest growing CO_2 emissions globally (Pearson et al. 2012). Climate change, resource scarcity and ecological sustainability are global megatrends in 2020 (Solovjew-Wartiovaara 2019; PwC 2020). This shows that climate change mitigation is of great importance. In the Paris agreement of United Nations, it was decided that the global average temperature rise should be limited to 2 °C, but aimed at 1.5 °C, and annual greenhouse gas (GHG) emissions should be reduced (UNFCC 2016). It should also be noted that the Finnish Government aims to achieve carbon neutrality by 2035 (Finnish Government 2020).

Politics and environmental concerns are driving forces for industry to join the alternative fuel research. It is important to find techno-economically feasible solutions to replace conventional fuels. Power-to-X (P2X) technologies are seen promising as they utilize renewably sourced energy, such as solar, wind or hydro power, carbon dioxide (CO_2) captured from emissions and hydrogen (H_2) produced via water electrolysis. (Götz et al. 2016; Bassano et al. 2019) CO_2 is captured from flue gas, biogas or directly from air. The aim is to store energy by using renewably sourced energy to produce something that can be used as energy later, e.g. synthetic fuel (Lehner et al. 2014). Synthetic fuels can be produced using power-to-gas (P2G) processes.

1.2 Goals and delimitations

The objective of this work is to conduct a techno-economic feasibility study to evaluate the potential of methane as a fuel in maritime transportation. Both biological and catalytic methanation processes are studied. Another object is to design biological and catalytic methane production processes and simulate them using Aspen Plus simulation software.

The focus of this thesis is on the methanation process. The process should utilise captured carbon dioxide and hydrogen produced via water electrolysis. The produced fuel is meant to be used in marine engines.

1.3 Structure of the thesis

In the literature part of this thesis the available technologies for carbon capture and water electrolysis are discussed. Available synthetic methane production technologies using catalytic and biological process routes are discussed and methane market development and production cost are studied. The parameters of techno-economic analysis are presented. This part is based on literature survey.

In the applied part, the methanation processes are designed and simulated using Aspen Plus simulation software. The results are analysed, and a closer look is taken to the techno-economic feasibility of synthetic methane production.

2 Power-to-gas technologies

In a typical power-to-gas process the required precursors are carbon dioxide and hydrogen (Figure 1). The by-product oxygen (O_2) from electrolysis can preferably be used in other industrial applications but it can also be released to the atmosphere. CO_2 and H_2 are used in the synthesis step. (Lehner et al. 2014) Possible synthetic fuel options are for example methanol, dimethyl ether and methane which is also called synthetic natural gas (SNG) (Lehner et al. 2014; LUT 2018). Another possibility is to capture nitrogen (N_2) from air and apply N_2 and H_2 in synthesis to produce ammonia (LUT 2018). Even though the recycled CO_2 will be released during some of the fuels' combustion, the idea, as Pearson et al. (2012) have stated, is that there will be no net increase in the CO_2 levels.

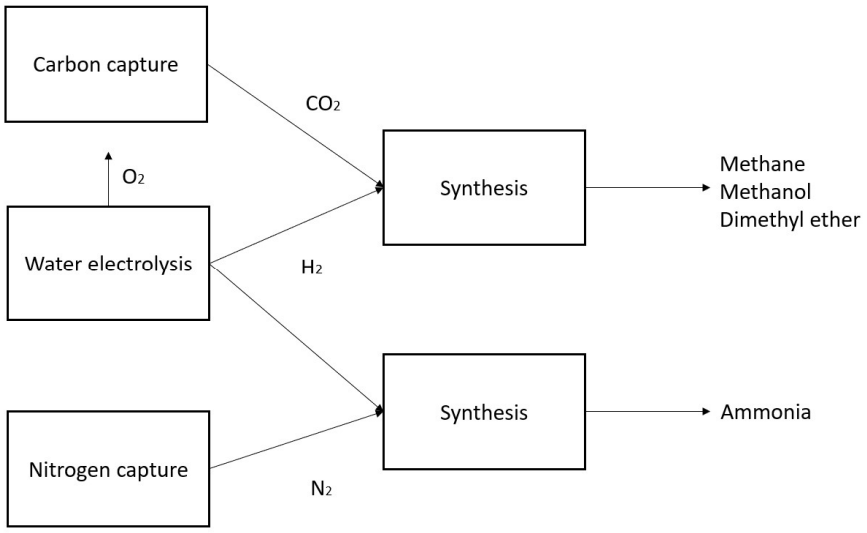

Figure 1 Principle of power-to-gas processes (adapted from LUT 2018). To avoid confusion, it should be noted that for example methanol can also be a power-to-liquid product depending on the production process.

2.1 Synthetic fuels

Methane can be produced from CO_2 and H_2 through Sabatier reaction (1) (Bassano et al. 2019).

$$4H_2 + CO_2 \rightarrow CH_4 + 2H_2O \qquad \Delta H\text{=-165 kJ/mol} \qquad (1)$$

Methanation can be done biologically using archaea or catalytically using a synthetic catalyst. The fundamentals of the methanation process are described more thoroughly in chapter 3. The produced synthetic natural gas can be utilized like conventional natural gas. This makes methane an attractive fuel since the infrastructure for natural gas already exists and the technology for using SNG is ready and available. Besides transportation fuel, SNG can also be used as feedstock to industry, for heating and it can be converted to electricity in combined cycle plants. (Lehner et al. 2014)

Methanol can be produced via catalytic hydrogenation of CO_2 (2).

$$CO_2 + 3H_2 \rightarrow CH_3OH + H_2O \qquad \Delta H\text{=-49.9 kJ/mol} \qquad (2)$$

The methanol synthesis requires energy input and a selective catalyst. Modern processes use $Cu/ZnO/Al_2O_3$ based catalyst with the operating conditions of 200–300 °C and 50–100 bar. Recently, other catalysts, zeolite membrane reactors and photocatalytic CO_2 conversion into

methanol have been studied on smaller scale. (Pearson et al. 2012) Even though methanol has been produced by catalytic hydrogenation of CO_2 industrially already in 1920s, nowadays it is usually produced from fossil based sources or biogas (Pearson et al. 2012; Verhelst et al. 2019). However, the technology is utilized in Iceland (Harp et al. 2015; Carbon Recycling International 2020). One advantage of methanol is that it is liquid in standard temperature and pressure (Verhelst et al. 2019). This is a good attribute when thinking about the practicality of its usage as fuel. Methanol has been used in fuel blends, but also pure methanol can be applied (Bromberg & Cheng 2010; Verhelst et al. 2019). Using high level blends and methanol as fuels means that hardware changes to engines are required (Verhelst et al. 2019). This makes methanol less desirable for a proximate future fuel transition.

Dimethyl ether (DME) can be produced via methanol dehydration (3). The synthesis method can be either indirect which means that DME is produced from separately produced methanol or direct which means that DME is produced from syngas. (Kansha et al. 2015)

$$2CH_3OH \leftrightarrow CH_3OCH_3 + H_2O \qquad \Delta H\text{=-23.4 kJ/mol} \qquad (3)$$

According to Kansha et al. (2015), many DME production processes (direct and indirect synthesis routes) use a reactant recycle stream. The product is distilled from the stream and this is a very energy intensive step. To reduce the energy consumption, catalysts that give higher conversion for the product and thus decrease the recycle stream have been researched. Alternative distillation methods have also been researched to lower the energy consumption of the process. The conventional indirect processes using catalyst have temperature range of 258–400 °C and pressures up to 18 bar (Yaripour et al. 2009). As a transport fuel DME is compatible with liquefied petroleum gas infrastructure with minor modifications. The engine would not need any modifications. DME would require new storage and fuel delivery systems and twice the tank size of a conventional diesel tank. There are some issues with viscosity that have led to leakages. However, DME is a promising alternative fuel that can also be used for heating and cooking. (Semelsberger et al. 2006)

Ammonia can be produced using Haber-Bosch process (4).

$$N_2(g) + 3H_2(g) \leftrightarrow 2NH_3(g) \qquad \Delta H\text{=-46.35 kJ/mol} \qquad (4)$$

Haber-Bosch is known to be a very energy intensive and thus expensive process due to the industrial operating conditions (300–550 °C, 100–300 bar). A single pass has low (10–15 %) conversion rate so the production plant needs to have several catalytic beds. The yield is increased by cooling the gas after each catalytic bed. Ammonia is separated from the cooled gas stream and unreacted gases are fed to the next catalytic bed. The catalyst is iron based. Ammonia can be used as fuel in high temperature or alkaline fuel cells. (Giddey et al. 2013) Since it hasn't been utilized as a fuel in conventional transport engines, currently it can't be seen as a feasible option.

It should be noted that the first product option of P2G process is hydrogen which has been considered a possible transport fuel for years. However, the infrastructure and technology for using hydrogen as a fuel is not mature and economically feasible enough for a fast, widely spread transition (Pearson et al. 2012). The option of hydrogen as a fuel in the future should not be excluded, but due to its issues it doesn't seem like a feasible solution in the proximate future.

In this thesis different synthetic fuels were compared from the viewpoint of their feasibility as transportation fuel. Liquefied natural gas (LNG) is already used as fuel in maritime transportation. Therefore, methane (synthetic natural gas, SNG) was chosen for closer examination.

2.2 Methane as a fuel

As mentioned previously, synthetic methane as a fuel can be used like natural gas. Because of this, the main requirements for the product are decided based on the fuel requirements of natural gas engines.

Methane is not suitable for all engine types. It has high octane number (up to 130), which means that it has high autoignition resistance (Fu et al. 2017; Senthamaraikkannan et al. 2014). Methane mixes easily with air, and it can be used in spark ignition engines. The ignition timing must be changed when converting diesel engine to be used with natural gas. This is because methane's flame speed is different than that of gasoline or diesel. Dual-fuel engines can use natural gas and diesel. When using natural gas, diesel is still used by injecting it to the mixture of air and natural gas. Methane's high autoignition resistance means that methane alone will not autoignite in the engine operating conditions. Because of

that, diesel is added so that autoignition can happen in the mixture. (Senthamaraikkannan et al. 2014) Besides dual-fuel engines, there are also engines that can run with natural gas only. According to Senthamaraikkannan et al. (2014) dual-fuel is the most common engine solution for natural gas vehicles on road transport, because the conversion from diesel engine to dual-fuel engine is relatively easy.

According to Gasum (2020a), LNG can be used as a fuel in all ship types. Wärtsilä has also reported collaboration with cruise ship companies that use LNG as a fuel (Orange 2019). Bunkering is possible shore-to-ship, truck-to-ship, and ship-to-ship (Gasum 2020a). This means that the infrastructure for using LNG and, thus, SNG already is available also for marine transport.

Wärtsilä has several marine engines that can use natural gas as fuel, such as 31 DF and 31 SG. 31 DF is a dual-fuel engine and 31 SG is a pure gas engine. The pure gas engine has a spark plug instead of a liquid fuel injection, so that it can be run with only gas as fuel. The engine is expected to be ready for use in 2021. (Wärtsilä 2019a) The dual fuel engine on the other hand is already available and utilized. The advantage of pure gas engine is that there is 15 % emission reduction compared to dual-fuel engine since no conventional liquid fuel is required. (Wärtsilä 2019a; Wärtsilä 2019b) The fuel gas requirements for both engines are similar (Table I).

Table I Fuel gas requirements for Wärtsilä 31DF and 31SG engines (Wärtsilä 2019a; Wärtsilä 2019b). Methane number refers to the methane content of the fuel. * Higher hydrogen content can be considered project specifically. ** Formation of condensation must be prevented in the operating conditions.

Property	Limit
Methane number	70
Methane content, min.	70 vol-%
Hydrogen content *, max.	3 vol-%
Hydrogen sulphide content, max.	0.05 vol-%
Liquid phase water and hydrocarbon condensate before engine **, max.	Not allowed
Oil content	0.01 mg/m^{3}N
Ammonia content, max.	25 mg/m^{3}N
Chlorine + fluoride content, max.	50 mg/m^{3}N
Particles or solids content in engine inlet, max.	50 mg/m^{3}N
Particles or solids size in engine inlet, max.	5 µm
Gas inlet temperature	0–60 °C

As can be seen, the gas does not have to be pure methane. Minimum methane content is 70 % and some impurities are allowed. In natural gas there are quite many impurities, but synthetic natural gas consists mostly of methane. When transitioning to renewables, SNG can be mixed with LNG. The suitable fuel composition for Wärtsilä's dual-fuel and pure gas engines can be estimated using Wärtsilä's methane number calculator (Wärtsilä 2020a). According to the calculator results, even pure methane can be used in the engines. So, using SNG with higher methane concentration is very good. The product does not have to be pure methane when using it as a fuel. But, the purity of the product also depends on the impurity limits. Hydrogen, carbon monoxide, carbon dioxide and water, which are the main impurities of SNG, have low allowed limits, if allowed at all. This must be kept in mind when adjusting the product purity.

2.2.1 Methane market potential

The market potential of renewables is currently growing. The Paris agreement calls for new regulations, emission targets and strategies. For example, each member state of the European Union has agreed to the target of 20 % renewables in each member state's energy production

(European Commission 2020a). The new regulations and strategies support the idea of P2G and SNG as a fuel from renewable sources. This means that the potential of P2G and methane fuel is expected to grow when transitioning to renewable fuels intensifies.

In Asia, the primary energy consumption is increasing (Herbes & Friege 2017). The price of fossil natural gas is expected to grow as the consumption especially in China and India increases. The possibly increasing oil price will also influence the price of imported natural gas to EU area, because its price is oil-indexed in gas import contracts. Most EU countries rely on imported natural gas (European Commission 2020b). This means that SNG production could also support EU's self-sufficiency. On the other hand, renewables are trending in Asia, particularly in China, India and Japan (Herbes & Friege 2017). This would suggest that there is market potential for SNG also in Asia.

There are various ways to support the producing of renewables on top of the regulatory measures and renewable energy targets. These are e.g. feed in tariff, tax reductions, support schemes and certificates that help the growth in value (Herbes & Friege 2017). Process design, sizing, control strategy and system integration affect the efficiency, reliability and economics of production. Electricity purchase and gas selling strategies along with operation strategy also affect the cost of production. (Gorre et al. 2019)

There are also unpredictable factors that can affect the market potential and investment in SNG production negatively. Unexpected crises can lead to economic depression or financial instability. One example of this is the global outbreak of COVID-19 disease in 2020 which is predicted to cause instability for both industry and consumers. During financial instability, investments can be considered too risky and thus, they are postponed. However, due to the unpredictability, risks like this cannot be included in this thesis.

Gorre et al. (2019) have estimated SNG prices for 2030 and 2050 to be 75 €/MWh and 125 €/MWh, respectively. They have studied different operating strategies and electricity supply concepts and how they affect the production costs in P2G process. When estimating the costs, they also estimated efficiency improvements for 2050. According to their results, SNG production with P2G process will be viable in 2030 and more so in 2050. Peters et al. (2019) reported SNG cost to be 3.51–3.88 €/kg for optimized P2G processes. They also point out that the interest for P2G processes and SNG use as a fuel is expected to increase by 2050.

For comparison, the price of natural gas in Finland in June 2020 was 1.13 €/kg and 1.45 €/kg for biogas, tax included. These prices were for road transport. (Gasum 2020b) For maritime market Gasum reported that the LNG price index in June was 15.58 €/MWh and for 10 % liquefied biogas (LBG) blend 18.58 €/MWh. The price index was for gas that has been liquefied at Gasum's plant in Risavika, Norway. (Gasum 2020c)

2.3 Carbon capture

Carbon dioxide (CO_2) is emitted from combustion of fossil fuels, chemical processes, such as cement manufacturing, iron and steel industry, gas processing, oil refining and exhaust emissions (Wilcox 2012). The main CO_2 sources for carbon capture are flue gas, syngas and air. The available carbon capture technologies are pre-combustion capture, post-combustion capture, oxyfuel combustion and direct air capture. After capture, CO_2 is compressed, stored and transported. Transport can be done via pipeline and with ship or rail transport (Wilcox 2012).

2.3.1 Post-combustion capture

In post-combustion capture CO_2 is captured from flue gas. The CO_2 concentration is 4–14 % in flue gas, depending on the combusted fuel (Olajire 2010; Wilcox et al. 2017). Flue gas composition from utility and industrial boilers is approximately 70 % N_2, 20 % CO_2 and H_2O and the impurities are SO_2, NO_x, Hg and ash particulate matter. Post-combustion technologies can be divided into four groups: absorption based, adsorption based, membrane based and algae based technologies. Out of these, absorption and adsorption based technologies are the most mature ones. (Horn & Zbacnik 2015)

Absorption based methods use either amine or ammonia based solvents. First the impurities are removed from flue gas using air control system. The cleaned flue gas is fed to scrubber where it is cooled and possible traces of sulfur impurities are removed. Then the CO_2 is absorbed using solvent. The CO_2 rich solvent mixture is then fed to heat exchanger. The solvent is steam-stripped, and CO_2 is separated from the solvent. The separated CO_2 is ready for compression and transport or storage and the regenerated solvent is re-used in the process. (Horn & Zbacnik 2015)

Suitable amine based solvents are monoethanolamine (MEA), diethylamine (DEA), methyldiethanolamine (MDEA), piperazine (PIPA) and 2-amino-2-methylpropanol (AMP). They react strongly and quickly with CO_2 and they release CO_2 during solvent regeneration. They can remove large amounts of CO_2 from flue gas in low pressure (4.5 bar). With amine solvents approximately 85–90 % of CO_2 can be removed. (Horn & Zbacnik 2015)

Ammonia based solvents are less expensive than amine solvents. They also have lower reaction heat and require less energy for regeneration. Ammonia can simultaneously absorb multiple pollutants (CO_2, SO_2, NO_x, and Hg). Their challenge, however, is ammonia slip. Ammonia slip means that ammonia is released into the flue gas stream during absorption. Ammonia slip requires control and it has been successfully executed on pilot scale by chilling the solvent. (Horn & Zbacnik 2015) This is not very efficient, because the energy costs increase with chilling. Ammonia is more volatile than amines and because of this, slip doesn't occur with amine based solvents (Horn & Zbacnik 2015).

In adsorption based capture, sorbents adsorb CO_2 onto their surface. The sorbents are regenerated by changing temperature or pressure which causes CO_2 to be released. Adsorption can be either physical or chemical. The challenges of adsorption based carbon capture are sorbent fouling and degradation over time. Solid sorbents are more difficult to handle than liquid sorbents, but their advantage is having lower energy requirements for heating. (Horn & Zbacnik 2015)

In membrane based capture, the porous membranes filter CO_2 from flue gas. The gas is either pushed or pulled through the membrane. The gas is pushed through by applying pressure to one side of the membrane. The gas is pulled through the membrane by creating a vacuum to the other side of the membrane. The selectivity and permeability of the membrane affect the required membrane surface area. Currently bench scale research is done to improve selectivity. The challenges of membrane capture are fouling of membrane and scaling up. (Horn & Zbacnik 2015)

Algae based capture is still in development stage. The idea is that the algae in algae ponds metabolize CO_2 to grow. However, algae do not take in CO_2 very quickly. Because of this, extremely large ponds would be required for industrial scale. (Horn & Zbacnik 2015) More research is required to find out if the scale up could be done in an easier and more feasible way.

2.3.2 Pre-combustion capture

In pre-combustion capture, CO_2 is captured from e.g. power generation processes. Integrated gasification combined cycles (IGCC) and natural gas combined cycles (NGCC) are technologies that are used for power generation from coal and natural gas. First step of the process is generating syngas which is composed of CO and H_2 by reacting a fuel with oxygen (partial oxidation), air or steam (steam reforming) or both with oxygen and steam (auto-thermal reforming). The second step is water-gas shift (5) using a catalytic reactor. (Jansen et al. 2015)

$$CO + H_2O \leftrightarrow CO_2 + H_2 \qquad \Delta H = -41 \text{ kJ/mol} \qquad (5)$$

CO_2 formed in water-gas shift is then separated from hydrogen using physical or chemical absorption and then the CO_2 is compressed. The hydrogen rich fuel is then used in the combined cycle power generation. (Jansen et al. 2015)

Pre-combustion capture technology is mature and utilized industrially for CO_2 separation, but for CO_2 capture and storage purposes it is just becoming commercial (Bellona 2020; IPCC 2005). According to Jansen et al. (2015) there are not NGCC plants that capture CO_2 for storage with this technology, but in IGCC plants there are pilot scale capture units. There are also some issues with efficiency and high costs (Jansen et al. 2015; Olajire 2010). These issues make pre-combustion capture less desirable, although e.g. Olajire (2010) stresses the potential of pre-combustion capture. Because of the aforementioned issues, the current research and development of pre-combustion capture is focused on reducing energy losses on each step of the process (Olajire 2010).

2.3.3 Oxyfuel combustion capture

In oxyfuel combustion the fuel is combusted in close to pure oxygen instead of air. This results in high, over 80 %, CO_2 concentration in the flue gases. Due to the high CO_2 concentration in the source, only purification is needed after combustion. There are no NO_x emissions so the volume of gas that is desulfurized is smaller than in post-combustion capture. The separation processes used in oxygen production from air and CO_2 capture are mainly physical. There are no additional reagent or solvent costs required. The disadvantage

of oxyfuel combustion is mostly the costs related to large quantity oxygen production. (Olajire 2010) This problem might be possible to tackle in a P2G process by using the by-product oxygen from electrolysis in the combustion process.

According to Olajire (2010) there are some pilot scale plants in operation using oxyfuel combustion for CO_2 capture. In the future it should be possible to also retrofit oxyfuel combustion capture to older facilities. This increases the future potential of the technology.

2.3.4 Direct air capture

In direct air capture (DAC) the CO_2 is captured from air. The CO_2 concentration in air is dilute (0.04 %) and this proposes some challenges to product purity demands (Wilcox et al. 2017). The advantage is that the location of the capture unit is not dependent on e.g. power plant location because the raw material air is available everywhere. So, the capture unit can be placed in a location where the P2G process line would fit the best.

There are two main routes for DAC: high temperature and low temperature capture. High temperature capture with aqueous solution is based on two main cycles which can happen simultaneously. The first cycle is absorption with sodium hydroxide (NaOH) while using fans or natural air flow (6). This happens in ambient temperature and pressure. (Fasihi et al. 2019)

$$2NaOH + CO_2 \rightarrow Na_2CO_3 + H_2O \quad (6)$$

After absorption follows regeneration cycle. First sodium carbonate (Na_2CO_3) is mixed with calcium hydroxide ($Ca(OH)_2$) in causticiser unit (7). Regenerated NaOH is recycled to absorption cycle. Calcium carbonate ($CaCO_3$) is heated to 900 °C causing CO_2 to release (8). CO_2 is then collected for purification. Calcium oxide (CaO) is then mixed with water in slaker and regenerated to $Ca(OH)_2$ (9). (Fasihi et al. 2019)

$$Na_2CO_3 + Ca(OH)_2 \rightarrow 2NaOH + CaCO_3 \quad (7)$$

$$CaCO_3 + heat \rightarrow CaO + CO_2 \quad (8)$$

$$CaO + H_2O \rightarrow Ca(OH)_2 \quad (9)$$

Low temperature capture is based on adsorption and desorption (regeneration) using solid sorbent. The capture is done in a single unit. First ambient air goes through the system

naturally or with the aid of fans. Then CO_2 is chemically adsorbed to filter. CO_2 depleted air goes through the filter and leaves the system. The adsorption step is ready when the sorbent is fully saturated with CO_2. After this the fans (if used) are switched off and the inlet valve is closed. The remaining air is let out by vacuuming or inserting steam into the system. Regeneration is done by heating. (Fasihi et al. 2019) The exact temperature depends on the sorbent, but temperature range 70–100 °C seems to be commonly used (Fasihi et al. 2019; Gutknecht et al. 2018). After regeneration, CO_2 is purified and compressed, and the sorbents are used again. Typically, the sorbents are amine-based compounds. (Fasihi et al. 2019)

Low temperature capture is used commercially for example by Climeworks (Gutknecht et al. 2018). There are still some issues with the product purity and efficiency (Wilcox et al. 2017). Another method for separating CO_2 from air is cryogenic distillation (Wilcox 2012). However, it requires a lot of energy, so it does not seem like an efficient option in this case when the goal is to separate just CO_2.

2.3.5 Comparison of carbon capture technologies

The discussed carbon capture technologies are summarized in Table II.

Table II Summary of carbon capture technologies. HT=high temperature, LT=low temperature. [1] Olajire 2010; [2] Wilcox et al. 2017; [3] Horn & Zbacnik 2015; [4] Jansen et al. 2015; [5] Gutknecht et al. 2018; [6] Fasihi et al. 2019, [7] Ghaib & Ben-Fares 2018

Technology		CO_2 source and approximate concentration	Maturity	Disadvantages	Advantages
Post-combustion	Absorption with amines	Flue gas, 4–14 % [1][2]	Mature [3]	More expensive than ammonia solvents, require higher reaction heat [3]	Most mature technology, solvent reacts strongly and quickly, lower pressure, no slip, 85–90 % CO_2 removed [3]
	Absorption with ammonia		Pilot scale [3]	Ammonia slip, slip control [3]	Lower solvent cost, simultaneous absorption of pollutants, lower retention heat and regeneration energy [3]
	Adsorption		Pilot scale [3]	Sorbent fouling and degradation over time, solids more difficult to handle than solvents [3]	Solid sorbents have lower energy requirements for heating than liquid solvents [3]
	Membrane		R&D [3]	Scale up, membrane fouling [3]	No regeneration step, low capital costs [7], simpler separation process
	Algae		R&D [3]	Scale up [3], captured CO_2 can't be utilized in P2G process, algae utilization: not clear what it could be used for	Algae uses the captured CO_2 as nutrient, CO_2 captured and stored simultaneously [3]
Pre-combustion	IGCC	Syngas, after water-gas shift 15–60 % [4]	Pilot scale [4]	Costs, efficiency [1][4]	Flexibility: co-production of H_2 and power possible [4]
	NGCC		R&D [4]		
Oxyfuel combustion		Flue gas, 80 % [1]	Pilot scale [1]	Costs related to O_2 production, complications with combustion with pure O_2 [1]	After combustion only purification is needed, no NO_x emissions, no additional reagent/solvent costs because mainly physical separation processes are used [1]
Direct air capture	HT aqueous solution	Air, 0.04 % [2]	Commercial [5]	Product purity targets challenging to achieve [2], energy intensive [6]	Location independent [2]
	LT solid sorbent				

Post-combustion capture using absorption with amines is the most mature technology for carbon capture and storage. Currently it seems the best option for a P2G process. However, the other technologies have a lot of potential. Some of them are already on pilot scale and utilized commercially, so their utilization may be possible on industrial scale in the close future. According to Bellona (2020) retrofitting is possible for post- and pre-combustion capture, but it is easier for post-combustion. Oxyfuel combustion also has retrofitting potential (Olajire 2010). These technologies are designed for cases when fossil fuels are used. The trend towards transitioning from fossil fuels to renewables can alter the applicability of these technologies. Based on the retrofitting potential, it should also be possible to utilize these capture technologies with biomass. Direct air capture has the advantage of raw material availability, but depending on the required product quantity and quality, its applicability may not yet be that good for all processes.

Emission trading affects the cost of captured CO_2. There are over 20 different emission trading systems (ETS) in force globally. The allowance for European Union's trading system (EU-ETS) was 17.37 €/tCO_2 in 2018 (converted from USD with the exchange rate of 19.3.2020). (ICAP 2019) Lehner et al. (2014) have reported carbon capture costs on the range of 25 to 60 €/t of CO_2. The capture costs depend on the capture technology used.

2.4 Electrolysis

Hydrogen can be produced through water electrolysis. In power-to-x applications it is desirable to use renewably sourced electricity, such as solar, wind or hydro power in hydrogen production process. The available technologies are polymer electrolyte membrane - also called proton exchange member - (PEM) electrolyser, alkaline water electrolyser (AWE) and electrolysis with solid oxide electrolyser cell (SOEC). An alternative technology for hydrogen production by electrolysis is microbial electrolysis cell (MEC). However, it is currently under development and not yet commercially available (Shiva Kumar & Himabindu 2019). Because of this, it is not presented more thoroughly in this thesis.

2.4.1 Alkaline water electrolysis

In alkaline water electrolysis a direct current (DC) is applied to maintain the energy balance. Electrons transfer from negative DC terminal to the cathode. On the cathode the electrons

and protons form hydrogen. Hydroxide anions transfer through the electrolyte to the anode surface where they lose electrons. The electrons then return to positive terminal of DC power source. (Zeng & Zhang 2010; Santos et al. 2013)

The reactions occurring on the anode (10) and cathode (11) are as follows (Shiva Kumar & Himabindu 2019; Santos et al. 2013):

$$2OH^- \rightarrow H_2O + \frac{1}{2}O_2 + 2e^- \quad (10)$$

$$2H_2O + 2e^- \rightarrow H_2 + 2OH^- \quad (11)$$

To avoid recombination of H_2 and O_2, the electrodes are separated with a gas-tight membrane. The membrane should have high ionic conductivity. (Ursúa et al. 2012) Nickel is known to be a good material for anode in alkaline systems (Kim et al. 2015).

The electrolyte in commercial applications is typically either potassium hydroxide (KOH) or sodium hydroxide (NaOH) as 30 % and 1 M solutions, respectively. (Nikolic et al. 2010; Zeng & Zhang 2010, LeRoy 1983). KOH is preferred due to its non-corrosiveness (Zeng & Zhang 2010; LeRoy 1983).

The overall efficiency of alkaline water electrolysis is typically below 40 %. The energy consumption is 4.5-5 kWh/m^3 of H_2 but there are studies about ways to lower the energy consumption. (Nikolic at al. 2010) However, the efficiency of the electrolysis cells can be 70–75 % in larger units and 80–85 % in smaller units (Santos et al. 2013). With AWE >99.9 % purity can be reached for hydrogen and >99 % for by-product oxygen (Santos et al. 2013; Schmidt et al. 2017).

A typical operating temperature range is 70–90 °C but also higher (up to 250 °C) temperature is possible (Allebrod et al. 2014; Lehner et al. 2014; Zeng & Zhang 2010). A typical pressure for AWE is up to 30 bar but also studies with higher pressures have been executed (Schmidt et al. 2017).

2.4.2 PEM electrolysis

In PEM electrolysis the water splits to oxygen, protons and electrons on the anode side (12). The protons then travel to the cathode side via the membrane and the electrons go through

external power circuit. On the cathode side the protons and electrons re-combine and hydrogen is formed (13). (Shiva Kumar & Himabindu 2019)

$$H_2O \rightarrow 2H^+ + \frac{1}{2}O_2 + 2e^- \quad (12)$$

$$2H^+ + 2e^- \rightarrow H_2 \quad (13)$$

In PEM electrolysis instead of liquid, the electrolyte is a solid, thin (50–250 μm), proton conducting membrane. Perfluorinated membranes are used and the most commonly used material is Nafion. PEM can be operated in low pressure (1–10 bar) and high pressure (10–150 bar) applications. The temperature is usually below 100 °C in low pressure conditions (Grigoriev et al. 2011). Typically, the PEM electrolysers are operated in the temperature range of 60–80 °C and pressure range of 30–60 bar. (Lehner et al. 2014) In high pressure conditions temperatures over 100 °C are possible. Hydrogen purity of >99.98 % has been reported possible to reach with PEM. (Grigoriev et al. 2006) Purity of by-product oxygen is >99 % (Schmidt et al. 2017). According to Grigoriev et al. (2011), over 70 % conversion efficiency is possible. The energy consumption of PEM is 4.2-6.6 kWh/m^3 of H_2 (Schmidt et al. 2017).

2.4.3 Solid oxide electrolyser cell

Solid oxide electrolyser cells operate in high temperatures. The reported operating temperature range varies, but a range of 500–1000 °C can be concluded from the papers by Shiva Kumar & Himabindu (2019) and Smith (2019). Higher temperature means that water is as gas and thus the electrical demand is reduced because it is compensated with thermal energy. In SOEC the water stream is reduced to hydrogen and oxygen ions at the cathode (also called hydrogen electrode). (Pandiyan et al. 2019) This stream is then oxidized to oxygen gas at the anode (also called air or oxygen electrode) (Pandiyan et al. 2019; Nechache et al. 2014). The occurring reactions on the cathode and anode are presented in equations (14) and (15), respectively (Nechache et al. 2014).

$$2H_2O + 4e^- \rightarrow 2H_2 + 2O^{2-} \quad (14)$$

$$2O^{2-} \rightarrow O_2 + 4e^- \quad (15)$$

The most commonly used electrolyte material is yttria-stabilized zirconia (YSZ). Strontium-doped lanthanum manganite (LSM)-YSZ composite is often used as anodic material. It has good catalytic properties at the operating temperature range, good electrolytic conductivity and it is very stable and has desirable thermal expansion behaviour. Other possible alternatives for LSM-YSZ composite are Sr-doped $LaCoO_3$ and $LaFeO_3$ and mixed ionic-electronic conducting electrodes e.g. lanthanum strontium cobalt ferrite. The most commonly used cathode material is nickel-yttria-stabilized zirconia (Ni-YSZ). It has a porous cermet structure which gives it good electrocatalytic properties as the electrons, oxygen ions and gas can percolate through the material. Another alternative material which is gaining interest is nickel-scandia-stabilized zirconia (Ni-ScSZ). (Nechache et al. 2014)

A typical SOEC energy consumption is 3.1 kWh/m^3 of H_2 (Udagawa et al. 2007). Wang et al. (2019) have reported SOEC efficiency of 94 %. According to Lehner et al. (2014) SOEC are typically operated in atmospheric pressure. Studies on possible operating pressures have been reported up to 100 bar but up to 25–30 bar seems to be a more commonly recognized pressure range with the typical experimental operating conditions being 1–10 bar (Thomsen et al. 2009; Jensen et al. 2010; Lehner et al. 2014; Bernadet et al. 2015). Hydrogen purity of 99.9 % can be assumed (Schmidt et al. 2017).

2.4.4 Comparison of the main electrolysis technologies

The main information of the available technologies AWE, PEM and SOEC is summarized in Table III.

Table III Summary of available technologies for hydrogen production through water electrolysis. [1] Santos et al. 2013; [2] Schmidt et al. 2017; [3] Lehner et al. 2014; [4] Petipas et al. 2017; [5] Grigoriev et al. 2006; [6] Grigoriev et al. 2011; [7] Shiva Kumar & Himabindu 2019; [8] Smith 2019; [9] Bernadet et al. 2015; [10] Udagawa et al. 2007; [11] Wang et al. 2019; [12] Bertuccioli et al. 2014

Technology	H_2 purity, %	O_2 purity, %	Typical operating temperature, °C	Operating pressure, bar	Energy consumption, kWh/m^3 of H_2	Efficiency, %	Maturity of technology
AWE	>99.9 [1]	>99 [2]	70–90 [3]	<30 [2]	4.5–5 [4]	70–75 [1]	Mature [3][4]
PEM	>99.98 [5]	>99 [2]	60–80 [3]	30-60 [3]	4.2–6.6 [2]	>70 [6]	Commercial [3][4]
SOEC	99.9 [2]	-	500–1000 [7][8]	<30 [3][9]	3.1 [10]	94 [12]	R&D [4][11][12]

Alkaline water electrolysis is currently the most mature and affordable technology (Lehner et al. 2014; Petipas et al. 2017). It is used industrially and available on MW scale (Lehner et al. 2014). Commercial PEM electrolysers are available, but they are more expensive and used mostly in smaller scale applications. (Lehner et al. 2014; Petipas et al. 2017) SOEC is used on laboratory scale and not yet commercially available for large scale applications (Bertuccioli et al. 2014; Petipas et al. 2017; Wang et al. 2019). However, it is seen as a promising technology due to its high electric efficiency (>97 %) (Kim et al. 2012; Schmidt et al. 2017). According to Schmidt et al. (2017) experts expect increased preference for PEM and SOEC over AWE in 2030s.

The main challenge in producing hydrogen through electrolysis economically is its high energy consumption. One way to increase the economic feasibility is to sell the by-produced pure oxygen. It could be utilized in and sold to e.g. pulp and paper industry, chemical and petroleum industry, medical industry, and power plants utilizing oxyfuel technology (Kato et al. 2005; Lehner et al. 2014; Air Products 2015). If selling oxygen, the balance between by-produced oxygen and oxygen demand is important (Kato et al. 2005).

Kayfeci et al. (2019) have reported that the cost of hydrogen produced through electrolysis using wind power is 5.45–5.58 €/kg. Buchholz et al. (2014) have reported that electrolysis can be around 78 % of the total costs of P2G methanation process.

3 Methanation

There are two possible production routes for methanation: biological and catalytic methanation. Both routes are based on the Sabatier reaction (1). Biological methanation is currently used on pilot plant scale, whereas catalytic methanation is used on commercial scale (Lecker et al. 2017; Götz et al. 2016).

3.1 Biological methanation

Methanogenic archaea are the catalyst in biological methanation. They can consume an equimolar amount of four times of hydrogen to carbon dioxide. The archaea can generate biomethane of natural gas quality. Biological methanation happens in anaerobic conditions.

(Voelklein et al. 2019) The operating temperature is typically 20–70 °C in ambient pressure, but pressure range 1–10 bar can be used (Götz et al. 2016).

Hydrogen solubilisation is the bottleneck of biological methanation process (Götz et al. 2014; Voelklein et al. 2019). Solubilisation is needed to make H_2 available for micro-organisms on a cellular level (Voelklein et al. 2019). CO_2 dissolves more easily in aqueous solutions and because of this, hydrogen solubilisation to the fermentation liquid is the limiting step (Götz et al. 2014; Voelklein et al. 2019). Mass transfer rate, pressure, solubility (Henry constant), temperature and hydrogen partial pressure affect how much of the hydrogen gets in the solution (Voelklein et al. 2019).

The advantage of biological methanation is moderate operating temperature and pressure. The disadvantage of biological methanation is its lower mass transfer, slow kinetics and low flexibility of the system (Ghaib & Ben-Fares 2018; Götz et al. 2016). According to Götz et al. (2014), it is possible to integrate biological methanation to biogas plants and wastewater treatment plants.

Biological methanation process can be either in-situ or ex-situ system. In-situ system means that the methanation is done within a biogas digester. In ex-situ system the methanation happens in an adjacent external reactor. (Voelklein et al. 2019; Lecker et al. 2017; Götz et al. 2016)

3.1.1 In-situ system

In-situ production is a batch process. Organic substrate and hydrogen are fed to digester. There are substrate degradation steps which include hydrolysis, acidogenesis, acetogenesis and methanation. (Lecker et al. 2017; Voelklein et al. 2019) In anaerobic digestion the polysaccharides, proteins and fat in the biomass are decomposed by extracellular enzymes. This produces substances such as sugar, amino acids, glycerine and fatty acids. In acidogenesis these monomers or dimers are converted to volatile fatty acids (VFA) such as propionate, butyrate and alcohol by the primary fermenting bacteria. In acetogenesis these metabolic products are degraded to acetic acid, hydrogen and carbon dioxide by the secondary fermenting bacteria (16). (Lecker et al. 2017) CO_2 and H_2 can also be metabolized by homoacetogens using the Wood-Ljungdahl pathway (17) (Lecker et al. 2017; Voelklein et al. 2019). After this, the methanation reaction occurs when methane is produced by the

methane producing archaea through acetoclastic methanogenesis pathway (18) (Lecker et al. 2017; Voelklein et al. 2019; Lehner et al. 2014). Hydrogenotrophic methanogenesis reaction pathway follows the Sabatier reaction (1) (Lehner et al. 2014).

$$CH_3CH_2COOH + 2H_2O \rightarrow CH_3COOH + CO_2 + H_2 \quad (16)$$

$$4H_2 + 2CO_2 \rightarrow CH_3COOH + 2H_2O \quad (17)$$

$$CH_3COOH \rightarrow CH_4 + CO_2 \quad (18)$$

In-situ system can utilise biogas digesters of biogas plants. Lecker et al. (2017) conclude that every biogas plant has a significant population of hydrogenotrophic methanogens that can metabolize the injected hydrogen. Using biogas digesters of biogas plants means that the required investment for methanation is low. However, if the CO_2 source is the biogas produced at the plant, the CO_2 production rate limits the methanation process. (Götz et al. 2014)

3.1.2 Ex-situ system

Ex-situ process can be batch or continuous. Carbon dioxide, hydrogen, nutrients and archaea are required in the synthesis. The initial stages of anaerobic digestion – hydrolysis and acidogenesis – are not present, so the reactor stability and performance depend only on the input of the required components. (Voelklein et al. 2019) The pure input gases are converted to methane by methanogen cultures. The occurring methanogenesis reaction follows the Sabatier reaction (1) (Sveinbjörnsson & Münster 2017). The supply of hydrogen to the micro-organisms is the rate limiting step in ex-situ system (Götz et al. 2016). When compared to in-situ process, the advantage is that the CO_2 source is not limited in ex-situ process. The reactor design and process conditions can also be more easily adjusted to fit the methanation process. (Götz et al. 2014)

The most common reactor concept is continuous stirred tank reactor (CSTR), but also fixed bed, trickle bed and membrane reactors have been studied as possible reactor concepts (Götz et al. 2016). When using CSTR reactor, the hydrogen solubilisation can be made easier by increasing the stirrer frequency. This improves hydrogen mass transfer. (Götz et al. 2014)

The process efficiency can be studied using methane formation rate (MFR). Operating conditions, such as pressure, temperature and pH affect MFR. Also, the reactor type and the micro-organisms used affect it. (Götz et al. 2014)

3.1.3 Archaea for methanation

The consortia that is used in biological methanation is mainly methanogenic archaea of the order of *Methanomicrobiales* (Gunnigle et al. 2013; Agneessens et al. 2018). All the methanogen orders are summarized in Table IV. Further specifications, such as size and specific growth rate, of some genera are given by e.g. Rusmanis et al (2019). Methanogens are anaerobic archaea. They can utilise hydrogen, carbon dioxide and acetate as substrates. Most of them can convert hydrogen and carbon dioxide to methane, but only a few can convert acetate to methane. (Guneratnam et al. 2017) Typically, hydrogenotrophic methanogens are preferred over homoacetogens because they produce methane more efficiently. When using homoacetogens, hydrogen should be injected to increase the production efficiency. (Agneessens et al. 2018)

Table IV Methanogen orders and their properties.

Order	Genera	pH	Temperature, °C	Ref.
Methanosarcinales	*Methanosarcinacea*, *Methanosaetaceae*	4.0–10.0	1–70	Angelidaki et al. 2011
Methanomicrobiales	*Methanoculeus*, *Methanogenium*	6.1–8.0	15–60	Angelidaki et al. 2011
Methanobacteriales	*Methanothermacaeae*, *Methanobacteriaceae*	5.0–8.8 [1]	20–88	Topçuoglu & Holden 2019; [1] Angelidaki et al. 2011
Methanococcales	*Methanocaldococcus*, *Methanotorris*	4.5–9.2 [1]	20–88	Topçuoglu & Holden 2019; [1] Angelidaki et al. 2011
Methanopyrales	*Methanopyrus*	5.5–7 [1]	84–110	Topçuoglu & Holden 2019; [1] Angelidaki et al. 2011
Methanocellales	*Methanocellaceae*	6.5–7.8	25–40	Sakai et al. 2008

Microbes of the genus of *Methanosaeta* can convert only acetate to methane, but those of the genus of *Methanosarcina* can convert acetate, hydrogen and carbon dioxide to methane. The methanogens typically grow in temperatures of 35–70 °C. (Guneratnam et al. 2017) For *Methanosarcina barkeri*, the optimal growth temperature is 37 °C (Gunnigle et al. 2013) The optimal pH for anaerobic digestion is 7.7–8.2 but the operation pH of the liquid methanogenic culture depends on the methanogens that are used (Guneratnam et al. 2017).

The *Methanosarcina* species use enzymes called hydrogenases to catalyst the oxidation of hydrogen. Methanogenic archaea have at least five types of hydrogenases. (Mand et al. 2018) *Methanosarcina* species can use four different reaction pathways to produce methane with hydrogenases and according to recent study by Mand et al. (2018) they appear to use all the pathways. The pathways they mention are CO_2 reduction, methyl reduction, methylotrophic and aceticlastic pathways. They studied *M. barkeri* with different kinds of hydrogenase mutations to characterise the biochemical and molecular properties. The *M. barkeri* were grown in 37 °C using pressure of 50 kPa and 300 kPa over ambient pressure. The substrates they used were methanol, sodium acetate or a combination of methanol and hydrogen. The mutations affected growth rate and preferred pathways, but all studied *Methanosarcina* were able to produce methane.

The *M. barkeri* are methanogens with cytochromes. Cytochromes allow the utilisation of acetic acid and carbon (C_1) compounds in addition to the utilisation of hydrogen, carbon dioxide and acetate as substrates. Non-cytochromes cannot utilise acetic acid or carbon (C_1) compounds. Another *Methanosarcina* that can be used in biological methanation is *Methanosarcina acetivorans*. (Mand et al. 2018)

According to Alitalo et al. (2015), methanogens require sulfur supply. Most methanogens can utilise sufides but not sulfates. They also need nitrogen as a nutrient. Ammonium (NH_4^+) is suitable for all methanogens, but most species can utilise also other nitrogen compounds as nutrients. Alitalo et al. (2015) used ammonium carbamate ($NH_4CO_2NH_2$) and sodium sulfide (Na_2S) as nutrients in biological methanation with a fixed bed reactor. They also used a mixture of wood ash and water as nutrient solution. According to them, the wood ash contained nutrients, that were suitable for methanogens and it was an inexpensive nutrient option. The wood ash reportedly contained Ca, K, Mg, P, Cu, Fe, Mn and Zn.

Because the methanogens need sulfur as nutrient, possible sulfur impurities for example in the captured carbon dioxide are not an issue. Since the methanogens require anaerobic conditions, it is assumed that oxygen impurities in hydrogen produced via electrolysis can damage the culture.

3.2 Catalytic methanation

Catalytic CO_2 methanation itself is not a very new concept. The Sabatier reaction was discovered in 1902 and the currently utilized CO_2 methanation technologies are based on processes developed in 1970s (Rönsch et al. 2016; Koytsoumpa & Karellas 2018). P2G methanation was also studied already in 1980s but it did not gain wide interest until the past decade. (Rönsch et al. 2016)

During catalytic CO_2 methanation through the Sabatier reaction, also reverse water gas shift (19) and CO methanation (20) reactions can take place (Koytsoumpa & Karellas 2018).

$$CO_2 + H_2 \leftrightarrow CO + H_2O \qquad \Delta H=+41 \text{ kJ/mol} \qquad (19)$$

$$CO + 3H_2 \leftrightarrow CH_4 + H_2O \qquad \Delta H=-206 \text{ kJ/mol} \qquad (20)$$

3.2.1 Catalytic methanation reactors

Catalytic methanation is mostly run using fixed-bed reactors. However, there are also other steady state reactor concepts that have been studied and some of them have been used on pilot or commercial scale. (Götz et al. 2016; Rönsch et al. 2016) According to Götz et al. (2016) fluidized bed reactors among with fixed bed reactors are established technologies. Three-phase reactors and structured reactors, such as honeycomb and multichannel reactors, are in development phase (Götz et al. 2016; Rönsch et al. 2016).

In adiabatic fixed bed reactors, the methane conversion is limited in high temperatures. Because of this, in commercial processes there are several reactors in series. The reactors have interstage cooling and recycle streams. In fluidized bed reactors the catalyst particles are fluidized by gaseous reactants. This allows a more effective heat removal as the fluidized solids mix in the gas uniformly. The conditions in the reactor are nearly isothermal. This enables the use of a single reactor and a simpler reactor design. Fluidized bed reactors are suitable for large scale production. The disadvantages of fluidized bed reactors are the issues

with catalyst deactivation due to attrition and bubbling, which can lead to incomplete conversion. In three-phase methanation the solid catalyst powder is suspended in an inert liquid, for example dibenzyltoluene. Three-phase methanation is flexible because the reaction kinetics and hydrodynamics of the reactor are not limiting factors. The catalyst can be replaced during the operation and the liquid phase's high heat capacity makes it easier to handle fluctuations and downtime. The mass transfer of the liquid side and gas velocity are limiting factors in three-phase methanation. Lower mass transfer can reduce the effectiveness of the reaction rate. (Götz et al. 2014)

The main difference between the reactor types is their temperature profile. There are three types of temperature profiles present in these reactors: adiabatic, isothermal and polytropic. (Rönsch et al. 2016) Adiabatic fixed bed reactors have high reaction rate and there is a possibility to produce steam at high temperature (Götz et al. 2014; Rönsch et al. 2016). The reactor exit temperature is high because the hot spot is close to the outlet. The process set up is also complex. In isothermal reactors, such as fluidized bed and three-phase reactors, the operating temperature is moderate. This makes the process and reactor simpler than with adiabatic reactors. The downside is that the moderate temperature results in limited reaction rates. In fluidized bed reactors there is also higher catalyst consumption because of catalyst attrition in the reactor. Polytropic reactors are for example cooled fixed bed reactors and structured reactors, such as microchannel and honeycomb reactors. The hot spot in the reactors is close to the inlet which results in moderate outlet temperature. The moderate hot spot temperature also increases the reaction rate and the conversion rate is higher due to the lower outlet temperature. The polytropic reactors combine the advantages of isothermal and adiabatic reactors. However, they are also the most expensive option. (Rönsch et al. 2016)

It has been studied that the methane yield increases with decreasing temperature and increasing pressure. However, it is not economical to have very high operation pressure and a low temperature would require a highly active catalyst. Because of this, compromises must be made when designing catalytic methanation process. (Ghaib & Ben-Fares 2018) It should also be noted that the catalyst must endure the operating temperatures. According to Rönsch et al. (2016) the methanation catalysts can't endure temperatures above 550–700 °C. Good temperature control is required to prevent the catalyst from fouling or sintering (Götz et al. 2016). Temperature control is also important since the methanation reaction is exothermic (Ghaib & Ben-Fares 2018). Typical operating temperature range in catalytic methanation is

250–550 °C with the pressure range of 1–100 bar (Götz et al. 2016). The optimal operating pressure is 30 bar because it helps reaching a high methane yield (Peters et al. 2019; Koytsoumpa & Karellas 2018). It is also known that in catalytic CO_2 methanation the pressure should be at least 10 bar or more to reach a good CO_2 conversion (Peters et al. 2019). In their study, Peters et al. (2019) stated that both CO_2 conversion and CH_4 yield increase as the pressure is increased. They reported 94 % CO_2 conversion in 10 bar and 400 °C, and 97 % conversion in 30 bar. CH_4 yield increased from 84.7 % at 1 bar and 400 °C to 95 % and above at 30 bar.

The H_2:CO_2 feed ratio should be stoichiometrically 4:1 and it's considered optimal, but also ratios above 4:1 can be used. However, when H_2 is added excessively, there is also higher amount of H_2 in the product gas. (Peters et al. 2019)

3.2.2 Catalysts

When choosing the catalysts, there are three compounds to consider: active compounds, supports and promoters. The active compounds work as catalysts for the reaction whereas supports and promoters are used to modify catalyst properties. The most suitable catalyst depends on the process conditions. Currently the most common catalyst in methanation process is Ni/Al_2O_3 (Rönsch et al. 2016; Ghaib & Ben-Fares 2018). According to Miguel et al. (2018), a typical methanation catalyst lifetime is from five to ten years.

Nickel (Ni) is the most selective methanation catalyst. It has high activity and its price is comparably low. In commercial applications, nickel is the most applied active compound. (Rönsch et al. 2016; Ghaib & Ben-Fares 2018) However, it has a tendency to oxidize which is a disadvantage because toxic nickel carbonyl can be formed (Ghaib & Ben-Fares 2018).

Besides nickel, other possible active compounds for methanation catalyst are ruthenium (Ru), cobalt (Co), iron (Fe) and molybdenum (Mo). Ruthenium is the most active metal for methanation, but it is also significantly more expensive than nickel and has lower selectivity than nickel. Ruthenium is considered especially suitable for low temperature methanation, but its price poses a problem (Rönsch et al. 2016; Frontera et al. 2017). According to Duyar et al. (2015) supported ruthenium catalyst is suitable for microchannel reactors because it has a high activity per gram of catalyst. Cobalt has similar methanation activity as nickel, but it is also more expensive. Iron has high reactivity but lower selectivity towards methane.

Molybdenum has lower methanation activity and it has higher selectivity towards C_{2+} hydrocarbons, which is a disadvantage. However, out of these metals it has the highest known sulfur tolerance. (Rönsch et al. 2016) It can be an advantage especially if using fossil based fuels for the process. In P2G methanation there should be no large quantities of sulfur in the input gases, but some impurities are possible if the CO_2 has been captured from flue gas.

Supports are metal oxides that have large surface area. They influence the activity of the active compound by enlarging the catalyst area. Al_2O_3 (alumina), SiO_2 (silica) and TiO_2 (titania) are common supports for methanation catalysts. (Rönsch et al. 2016) CeO_2 has also been studied as a support for nickel catalyst. Ni/CeO_2 had high stability, high methane selectivity and high CO_2 conversion in laboratory tests. The catalyst was tested using different structures and it was stated that the catalyst structure can affect the methanation performance. (Ratchahat et al. 2018) Currently Al_2O_3 is the most common support due to its low price. It can also disperse the metal species finely which is an advantage. (Ghaib & Ben-Fares 2018)

Promoters are used for enhancing the catalyst performance. They modify the surface basicity which results in lower activation energy. (Ghaib & Ben-Fares 2018) MgO can increase the carbon resistance and thermal stability of Ni/Al_2O_3 catalysts (Rönsch et al. 2016). On the other hand, CeO_2 improves the selectivity and activity of Al_2O_3 supported catalyst (Ghaib & Ben-Fares 2018). Many alternative promoters have been studied. For example, Liang et al. (2019) studied various promoters with Ni/Al_2O_3 catalysts. They concluded that cerium (Ce) doped catalyst shoved superior activity and better stability for methanation reaction.

Before the catalysts can be applied, they must be reduced. The reduction time and temperature depend on the active metal and support used. Nickel based catalysts do not require separate activation steps in addition to the reduction. Their reduction is done in atmospheric hydrogen with the temperature range of 300–600 °C. (Rönsch et al. 2016) Rönsch et al. (2016) have described the possible reduction conditions of Ni/Al_2O_3 catalyst in more detail.

Catalyst poisoning means chemical deactivation of the catalyst. For nickel based methanation catalysts the most important compound to avoid is sulfur. Chemisorption of sulfur can occur for example if there is hydrogen sulfide (H_2S) or thiophenes present in the

feed gas. If nickel sulfide (NiS) is formed (21), nickel loses its activity for the methanation reaction. Other impurities that can cause issues with nickel catalysts are ammonia, chlorine compounds, tars, alkalis and particles. (Rönsch et al. 2016) Bartholomew (2001) also mentions arsenic (As) as poison to nickel catalysts.

$$H_2S(g) + NiO(s) \leftrightarrow NiS(s) + H_2O(g) \quad (21)$$

Bartholomew et al. (1979) studied sulfur poisoning of nickel catalysts with 10 ppm H_2S. The catalysts were completely deactivated in two to three days. The sulfur concentration and effect of temperature were further studied by Erekson & Bartholomew (1983). They concluded that even 0.2 ppm H_2S caused some catalyst deactivation during CO methanation. Temperature and CO concentration also affected the deactivation rate. Bartholomew (2001) reports that even 15–100 ppb H_2S causes some activity loss of nickel catalyst which proves that nickel catalyst's sulfur tolerance is very low.

Another chemical deactivation that can occur during methanation is vapor-solid reactions. Nickel carbonyls can form when the temperature is below 230 °C and there is CO present (22). Because of this, contact between CO and catalyst must be avoided during start up and shutdown phases. (Rönsch et al. 2016)

$$Ni(s) + 4CO(g) \leftrightarrow Ni(CO)_4(g) \quad (22)$$

Some commercial methanation catalysts are presented in Table V.

Table V Commercial methanation catalysts and their properties. [1] Weiss & Schwinghammer 2012; [2] Haldor Topsøe 2020b; [3] Haldor Topsøe 2020e, [4] Haldor Topsøe 2020c; [5] Haldor Topsøe 2020d; [6] Johnson Matthey 2020

Name	Producer	Shape	Dimensions, mm	Temperature, °C	Active compound	Lifetime, years	Density, kg/m^3	Ref.
G1-81 Rings	Lurgi	Ring	7x7x3	230–480	55 w-% Ni	4–5	820	[1]
G1-81 Tablets	Lurgi	Tablet	5x5	230–650	55 w-% Ni	3	1050	[1]
G1-86HT	Lurgi	Ring	7x7x3	230–650	45 w-% Ni	3	900	[1]
MCR-8	Haldor Topsoe	Cylinder	4.5x4.5	”medium to high”	Ni	-	-	[2]
		7-hole cylinder	11x6, holes 2 mm					
PK-7R	Haldor Topsoe	Ring	-	”low”	-	-	-	[3]
MCR-2	Haldor Topsoe	Cylinder	-	”medium to high”	-	-	-	[4]
MCR-2X	Haldor Topsoe	Cylinder	-	”high”	-	-	-	[5]
CRG	Johnson Matthey	-	-	-	Ni	-	-	[6]

3.3 Kinetics

The kinetics of catalytic methanation have been studied and there are reported results that have been announced suitable for modelling, simulation and design of industrial CO_2 methanation reactors and processes. There are various reported reaction mechanisms. Miguel et al. (2018) studied CO_2 methanation kinetics and they included formyl intermediate, formate intermediate and carbon intermediate mechanisms in their studies. They reported that the kinetics for the formyl intermediate mechanism had a good fit with the formyl intermediate mechanism model. Marocco et al. (2018) also realised the fit for formyl species formation and declared it as rate determining step. The formyl intermediate mechanism means that adsorbed CO formed during CO_2 methanation is hydrogenated and thus forms formyl species (Marocco et al. 2018). Miguel et al. (2018) have reported in detail the intermediate mechanisms step by step.

Marocco et al. (2018) considered Sabatier and reverse water gas shift reactions in their research. However, they reported that the methane yield was similar also when only Sabatier reaction was considered. They proved this by applying the kinetic parameters of both cases in simulations. The kinetic parameters were estimated using experimental data and varying temperature, flow rates and H_2:CO_2 ratio.

Xu & Froment (1989) studied CO_2 methanation kinetics in detail and also included water gas shift and CO methanation reactions in their study. Their estimates are still considered fitting, even though the study is not that recent. For example, Peters et al. (2019) used their estimates when simulating methanation processes.

The kinetic parameters and experiment conditions are presented in Table VI.

Table VI The kinetic parameters and experiment conditions for CO_2 methanation.

	Miguel et al. 2018	Marocco et al. 2018	Xu & Froment 1989
Catalyst	Industrial Ni-based catalyst	Ni/Al hydrotalcite derived catalyst	$Ni/MgAl_2O_4$
Temperature range	250–350 °C	270–390 °C	300–500°C
Pressure	atmospheric	atmospheric	30 bar
Activation energy	118.7 kJ/mol	69.2 kJ/mol	243.9 kJ/mol
Hydroxyl enthalpy of adsorption	61.6 kJ/mol	61.2 kJ/mol	-
A, pre-exponential factor	0.8936 mol/$g_{catalyst}$ h	$4.4 \cdot 10^5$ 1/bar ^{½}	$1.02 \cdot 10^{15}$ kmol bar ^{½} /$kg_{catalyst}$ h

3.4 Commercial processes

3.4.1 Commercial catalytic processes

Commercial catalytic methanation processes are mostly based on CO methanation, but they can be used also for CO_2 methanation (Rönsch et al. 2016). Many of the commercial processes are designed for using primarily syngas from e.g. coal plants as the feed gas for methanation. Because of this, sulfur removal is applied before the gas is fed to the methanation reactors. This step can be adapted to P2G process if the captured CO_2 contains sulfur impurities. Commercial catalytic methanation processes are summarized in Table VII.

Table VII Commercial catalytic methanation processes. [1] Koytsoumpa & Karellas 2018, [2] Lehner et al. 2014, [3] Weiss & Schwinghammer 2012, [4] Johnson Matthey 2020, [5] Haldor Topsøe 2020a, [6] Romano & Ruggeri 2015

	Reactor concept	Catalyst	Temperature, °C	Pressure, bar	CH_4 in SNG
BASF high temperature methanation by Lurgi/Air Liquide	3 adiabatic fixed bed reactors in series [1]	G1–86HT; G1-85 (Nickel based) [2]	280–650 [1]	>18 [2]	85–95 mol-% [3]
Linde	Isothermal fixed bed reactor [1]	-	300–750 [2]	20 [2]	-
HICOM by Davy Technologies/Johnson Matthey	3 fixed bed reactors [1]	CRG-S2S, CRG-S2C (Nickel based [4])	250–700 [1]	25–70 [2]	-
TREMP by Haldor Topsøe	3-4 adiabatic fixed bed reactors in series [1]	MCR-2X, MCR-2, MCR-8 (Nickel based), PK-7R [5]	300–700 [1]	30 [2]	-
Vesta by Amec Foster Wheeler and Clariant	2-3 adiabatic fixed bed reactors in series [6]	Nickel based catalyst by Clariant [6]	<560 [1]	-	99.3 % [6]
Comflux by Engler-Bunte Institut and Thyssengas	Fluidized bed reactor [1]	-	400–500 [2]	20–60 [2]	-

The Vesta process is novel; a pilot plant using Vesta was started-up in 2014. The process is originally designed to use syngas as CO and CO_2 source. The syngas can be used after it has been purified of sulfur in an acid gas removal unit. The operating conditions, number of reactors and the feed gas source can however be adjusted. The catalyst used in the process is nickel based and it is produced by Clariant exclusively for Amec Foster Wheeler. (Romano & Ruggeri 2015)

BASF high temperature methanation by Lurgi and Air Liquide is also designed for using syngas as the feed in methanation (Figure 2). Before the methanation reactors, the H_2S content in the syngas is reduced from 0.1 ppm to 30 ppb in a deep desulfuriser unit. They use their own nickel based methanation catalysts. (Weiss & Schwinghammer 2012)

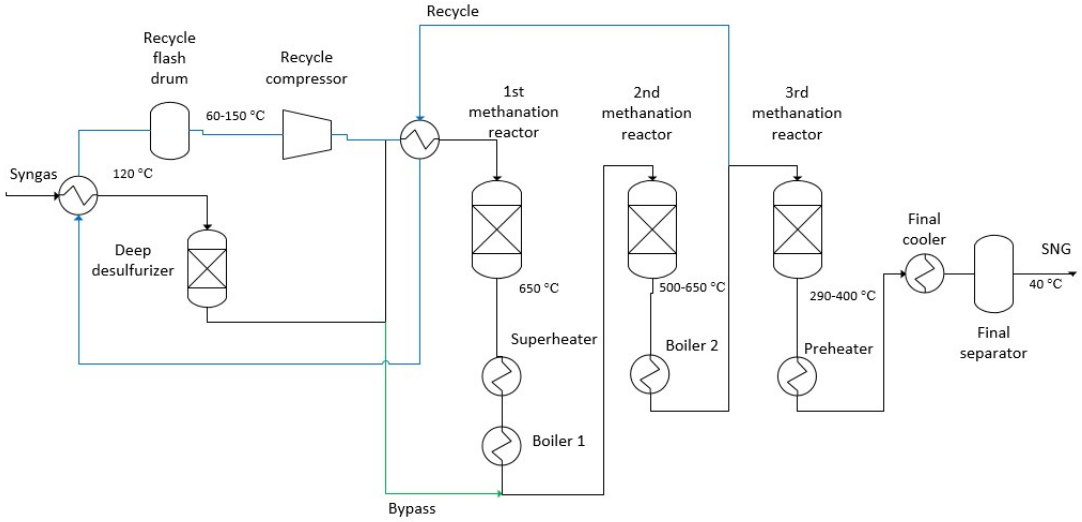

Figure 2 BASF high temperature methanation. Recycle ratio is 70–85 %. Bypass ratio is 10–60 %. The CH_4 content in the reactor outlets: 1st reactor 60–70%, 2nd reactor 70–85 % and 3rd reactor 85–90 %. (Adapted from Weiss & Schwinghammer 2012)

The catalysts used in the TREMP process are produced by Haldor Topsøe (Haldor Topsøe 2020a). The active compound in MCR-8 catalyst is nickel (Haldor Topsøe 2020b). The other, more expensive, catalysts MCR-2 and MCR-2X are used for e.g. improved sulfur tolerance or higher conversion (Haldor Topsøe 2020c; 2020d).

The Comflux process was operated on pilot scale in 1980s, but the technology has been used again in various experiments since 2004 and on pilot scale since 2009 (Lehner et al. 2014; Götz et al. 2014; Koytsoumpa & Karellas 2018).

There is also an interesting process currently under research on laboratory scale: ESME process by the Energy research Centre of the Netherlands (ECN). The process feed is from biomass gasification. Because of this, various purification steps are needed before methanation in two reactors. Nickel catalyst is used in the process. The inlet temperature is 340 °C and operating temperature is 6 bar. The concept is focused on reforming hydrocarbons, such as benzene or toluene, in the feed gas, and converting them to methane in a pre-reformer unit. (Almansa et al. 2015) However, the methane content in the SNG product is only 39 vol-% which is very low compared to the commercial catalytic methanation processes.

3.4.2 Commercially potential biological processes

Biological methanation is not technologically as mature as catalytic methanation. There are some promising pre-commercial processes on pilot scale (Table VIII).

In ex-situ biological methanation CSTR is the mostly used reactor concept. The existing process designs are mostly continuous operations, but also batch processes are used in smaller scale. (Guneratnam et al. 2017)

Table VIII Potential biological methanation processes on pilot scale.

	Reactor concept	Methanogen culture	Temperature, °C	Pressure, bar	CH_4 in SNG	Ref.
St1 and Q Power	Ex-situ [1]	Grown from swamp samples [2]	52.3–54.8 [1]	-	>95 % [1]	[1] Alitalo & Aura 2013; [2] St1 2019
MicrobEnergy and Audi	Ex-situ	-	40	5	>95 %	Sveinbjörnsson & Münster 2017
Electrochea	Ex-situ	Selectively evolved in laboratory	63	9	98 %	Sveinbjörnsson & Münster 2017

In Finland, St1 and Q Power had a biological methanation pilot plant in the end of 2019. The process was ex-situ and the microbe culture was collected from swamp samples. The CO_2 was taken from St1's ethanol production line located at the same plant. (St1 2019)

MicrobEnergy and Audi have built an ex-situ methanation process in Allendorf, Germany. The CO_2 source is biogas from attached biogas plant. (Sveinbjörnsson & Münster 2017)

Electrochaea's biological ex-situ methanation process in Avedøre, Denmark, is part of BioCat Project. The process is located at a wastewater treatment plant which provides biogas as a CO_2 source. (Electrochaea 2020; Sveinbjörnsson & Münster 2017) The methanogenic archaea used in the process have been selectively evolved in laboratory (BioCat Project 2020). The archaea are said to be very tolerant of H_2S and O_2 impurities in the feed gas. The process is now at a pre-commercial demonstration stage (Electrochaea 2020).

In May 2020 Wärtsilä and Vantaa Energy Ltd. announced a co-operation project on biological methane production. They intend to continue development towards a pilot plant operating on commercial scale. (Wärtsilä 2020b)

3.5 Impurity removal

It is assumed that the CO_2 used in the process has been captured from flue gas. Since the main impurities of flue gas are SO_2 and NO_x, the captured CO_2 can contain traces of these impurities. CO_2 can be purified with activated carbon when the gas contains lower amounts of SO_x (Shah et al. 2011). Because of this, activated carbon method is suitable for P2G processes. Another option would be to remove SO_x with sodium hydroxide (NaOH).

In the activated carbon method, the SO_2 and NO_x are first oxidized in an activated carbon bed (23–24). The activated carbon catalyses the oxidation. The gas is passed over the activated carbon bed. After the bed has been saturated with SO_x and NO_x, it must be regenerated. Regeneration is done by washing the bed with water. Water reacts with the formed SO_3 and NO_2, resulting in sulfuric and nitric acid (25–26). (Shah et al. 2011)

$$SO_2 + \frac{1}{2}O_2 \rightarrow SO_3 \quad (23)$$

$$NO + \frac{1}{2}O_2 \rightarrow NO_2 \quad (24)$$

$$SO_3 + H_2O \rightarrow H_2SO_4 \quad (25)$$

$$3NO_2 + H_2O \rightarrow 2HNO_3 + NO \quad (26)$$

At least two activated carbon beds are needed; the other one is regenerated while the other one is used for oxidation. The carbon beds can be dried with a regeneration gas, such as nitrogen, by passing the gas through the beds. The activated carbon process can be operated in 20 °C. The performance is said to increase at elevated pressure. (Shah et al. 2011) The process is described in Figure *3*. It is assumed that the formed sulfuric and nitric acid are dilute and low in quantity. Because of this, they are not considered suitable for selling as by-products for additional profit.

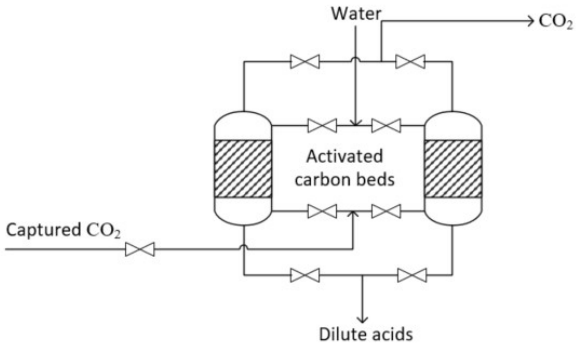

Figure 3 CO_2 purification in activated carbon beds (adapted from Shah et al. 2011).

It is assumed that the hydrogen purity after electrolysis is 99.9 %. This level of purity is possible to reach with both alkaline water electrolysis (AWE) and polymer electrolyte membrane (PEM) (see Table III). The impurity in the produced hydrogen is oxygen. In 99.9 % H_2, there is 1000 ppm of O_2. The oxygen level should be lowered to avoid the poisoning of catalyst or methanogens.

The oxygen can be removed with catalytic recombination reaction (27) which is also known as deoxo process. The reaction can be catalysed with e.g. supported palladium catalyst in a packed bed reactor. (Sandeep et al. 2014) The reaction should occur in 25 °C and 1 bar (Ortloff et al. 2014).

$$H_2(g) + \frac{1}{2}O_2(g) \rightarrow H_2O(g) \qquad \Delta H = -244.5 \text{ kJ/mol} \qquad (27)$$

An example of a possible process flow diagram of side-by-side hydrogen purification with deoxo and carbon dioxide purification with activated carbon beds is given in Figure 4. In the diagram, the purified H_2 and CO_2 streams are mixed and then dried in e.g. zeolite bed before feeding them to the methanation process.

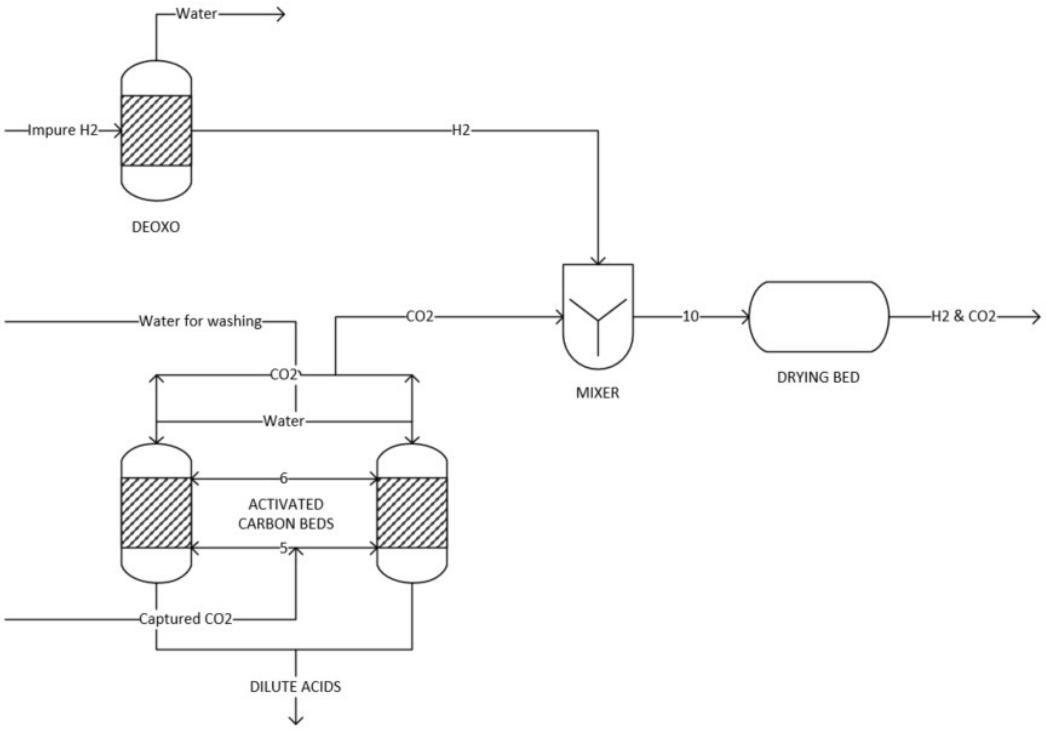

Figure 4 An example of process flow diagram for side-by-side hydrogen and carbon dioxide purification.

4 Parameters for techno-economic analysis

In the techno-economic analysis both technological and economic feasibility are studied. The main factors affecting technological feasibility are the readiness for industrial scale production, consumption of raw materials and energy, utilities, product yield and purity. The technological feasibility is analysed by modelling the processes using simulation software.

The parameters for economic analysis include investment and operating costs, revenues and thus the cost-effectiveness of the process. Raw material prices, consumables, the cost of electricity and other utilities affect the costs. The costs also depend on the location of the plant. Profitability and break-even point of the investment can be analysed with net present value (NPV) analysis (Sinnot & Towler 2009).

For example, raw material prices and competitive product selling price can vary. Because of this, the parameters for economic analysis need to be analysed more closely. For this, uncertainty factors need to be studied.

A common way to assess the uncertainty factors is to conduct a sensitivity analysis. Monte-Carlo analysis is another method that can be used. (Sinnot & Towler 2009) However, it requires building a model for the exact case and thus, it is too time consuming to be used in this thesis. Threshold analysis can be used for studying pre-set upper and lower limits for e.g. raw material price.

According to Sinnot & Towler (2009), there is a simplified statistical analysis method based on setting a most likely value (ML), upper value (H) and lower value (L). Mean value ($\bar{x}$) and standard deviation (S_x) can be estimated using these values with equations (28) and (29). The total mean value and standard deviation of the project are calculated by combining the calculated values for each parameter. Examples of combination of the values for project ISBL and OSBL costs are shown in equations (30) and (31). When combining the values for ISBL and OSBL, the mean values and standard deviations should be increased by 10 % to include engineering costs. With this method there is 98 % confidence that the costs are less than $\bar{x}+2.05S_x$. (Sinnot & Towler 2009)

$$\bar{x} = \frac{H+2ML}{4} \tag{28}$$

In which $\bar{x}$ mean value, €;

H upper value, €;

ML most likely value, €;

L lower value, €.

$$S_x = \frac{H-L}{2.65} \tag{29}$$

In which S_x standard deviation, €.

$$\bar{x}_{total} = 1.1\bar{x}_{ISBL} + 1.1\bar{x}_{OSBL} \tag{30}$$

In which $\bar{x}_{ISBL}$ mean value for ISBL, €;

$\bar{x}_{OSBL}$ mean value for OSBL, €.

$$S_{x,total} = \sqrt{(1.1S_{x,ISBL})^2 + (1.1S_{x,OSBL})^2} \quad (31)$$

In which $S_{x,ISBL}$ standard deviation for ISBL, €;

$S_{x,OSBL}$ standard deviation for OSBL, €.

The upper and lower values can be estimated using the ranges of variation given by Sinnot & Towler (2009). The values are given in Table IX.

Table IX Range of variation from base value for some process parameters (Sinnot & Towler 2009).

Parameter	Range of variation from base value
Sales price	± 20 %
Feed cost	-10% to +30 %
Fixed costs	-20 % to +100 %
ISBL capital investment	-20 % to +50 %
OSBL capital investment	-20 % to +50 %

5 Process design

In this applied part of the thesis, CO_2 methanation processes for producing SNG and biogas are designed. Process simulation and economic analysis are described in the following chapters.

5.1 Production capacity estimation

A feasible production capacity can be estimated based on available renewable electricity. This will determine the capacity of electrolysis and hydrogen production. The maximum amount of produced hydrogen is then a limiting factor for the methane production.

In the end of 2019, the total wind power capacity in Finland was 2284 MW. By the end of February 2020 there were reported upcoming projects to build more wind power plants. The total planned capacity increase is 18500 MW. (Finnish Wind Power Association 2020) Finland's strategy is to increase wind power production to 8 TWh by 2030 (Energiateollisuus 2020). In 2019 Finland's wind electricity production was 5.9 TWh (Finnish Wind Power Association 2020).

Nieminen et al. (2019) estimated that 30 MW capacity would be suitable for electrolysis unit powered by wind electricity in Finland. Finland's constructed and planned wind power capacities have both increased since then, which means that the electrolysis capacity estimation could also be increased. Thus, 40 MW capacity is proposed. This means that the maximum capacity of the electrolysis unit in the methanation process is 40 MW.

Lehner et al. (2014) have stated that on MW scale P2G plants catalytic methanation is the preferred methane production method. They also note that the available CO_2 sources need to be considered on MW scale production.

In catalytic methanation the H_2 to CO_2 ratio in the feed gas is the stoichiometric ratio of 4:1. In biological methanation also H_2 to CO_2 ratio of 4:1.064 can be used (Lecker et al. 2017). This is due to CO_2 losses, because according to Lecker et al. (2017) 6.4 % of added CO_2 is utilised by the methanogens for cell growth and not for methane production.

To calculate the hydrogen production, commercial electrolysers are used for reference. McPhy has a 4 MW module of McLyzer 800-30, which can produce 800 Nm^3/h of hydrogen.

The modules can be added as needed to reach the desired capacity. (McPhy 2020) Thyssenkrupp reports a similar production rate. With 5 MW module the production rate is 1000 Nm^3/h of hydrogen and 4000 Nm^3/h of hydrogen with 20 MW module (Thyssenkrupp 2020). All these modules produce 200 Nm^3/h of hydrogen per 1 MW in theory. So, with the capacity of 40 MW, the estimated hydrogen production is 8000 Nm^3/h.

With 8000 Nm^3/h of hydrogen in the feed, 2000 Nm^3/h of carbon dioxide is needed to reach the ratio of 4:1. The mass and mole flows for the feed are given in Table X.

Table X Hydrogen and carbon dioxide feed streams with the estimated capacity of 40 MW and H_2 to CO_2 ratio 4:1.

	Nm^3/h	kg/h	kmol/h
H_2	8000	656	325.4
CO_2	2000	3684	83.7

5.2 Initial information for process design

Wärtsilä's methane number calculator is used for setting the product quality limits. The calculator results show that the maximum H_2 content in a suitable fuel is 3 mol-% and the maximum CO_2 content is 6 mol-%. The methane content would then be 91 mol-%. These are set as the product's impurity limits. Higher or lower methane content and lower impurity levels are also suitable for Wärtsilä's gas and dual-fuel engines (Wärtsilä 2020a).

The reactors in the catalytic methanation process are adiabatic fixed bed reactors. The catalyst is Ni/Al_2O_3, which is the most commonly used methanation catalyst. The process should be operated continuously.

As mentioned previously, the optimal operating pressure is 30 bar and typical temperature range is 250–550 °C in catalytic CO_2 methanation. Based on this, the initial operating pressure was chosen to be 30 bar. The reactor inlet was chosen to be 250 °C because most of the commercial Ni/Al_2O_3 catalysts are activated near this temperature. The number of reactors will be defined based on how many reactors are needed to reach the required purity limits for SNG. It is known that several reactors are required, because the reaction is not run to equilibrium in the first reactor. This is to avoid the temperature increasing over the

catalyst's temperature limits. If the reaction would be run to equilibrium in the first reactor, the temperature would damage the catalyst and the product would not meet the purity targets. Water is formed during the reaction, and excess water needs to be removed before entering the gas stream to another reactor. This is done to allow the remaining hydrogen and carbon dioxide to react and thus meet the pre-set impurity limits.

The biological methanation process was chosen to be continuous ex-situ process. The operating conditions depend on the microbes used in the process. It was decided that commercially used archaea would be reasonable to use in this process. However, there was not much data available on the commercially used methanation archaea. It was discovered that the most specific information available was about the archaea patented by Electrochaea. Because of this, the archaea patented by Electrochaea was chosen as the reference archaea for biological methanation.

The archaea Electrochaea has patented for biological methanation is *Methanothermobacter thermautotrophicus* strain UC 120910 (Rusmanis et al. 2019). The patented archaea should be operated with pH range of 6.5–7.5 and temperature range 55–69 °C. The cell culture density is reported to be at least 6 $g_{\text{dry mass of cells}}/L_{\text{culture}}$ in stationary phase. (Mets 2012) The operating pressure range is 4–9 bar (Rusmanis et al. 2019). The operating temperature was chosen to be 60 °C and pressure 6 bar in the process designed in this thesis.

Cultivation of the archaea can be conducted in CSTR in 60 °C, atmospheric pressure and pH 6.85. The pH should be controlled with NH_4OH solution. H_2:CO_2 mixture with ratio 4:1 should be spurted to the reactor intermittently. Nutrients and medium solution should also be fed to the reactor. The duplication time of *M. thermautotrophicus* is 103 hours and exponential growth takes 30 days. (Mets 2012) The cultivation unit was designed based on this information.

The products can be either compressed or liquefied. These steps are not included in the design. It is assumed that the further processing of the product can be done in collaboration with local natural gas and biogas supplier. In Finland Gasum is the local supplier. The maximum pressure for the gas transfer pipeline is 54 bar in Finland, but also much lower pressures can be applied depending on the project (Neste Jacobs & Gasum 2015; Nevalainen 2020). Thus, both SNG and biogas can be transferred for further processing in the designed process outlet pressures.

According to the most recent information, captured CO_2 should be purified as a part of the capture process rather than separately (Laari 2020). Because of this, only deoxo process was included in the applied part of this thesis.

The initial information for process design and simulation is summarised in Table XI.

Table XI Initial information for process design and simulation.

	Catalytic methanation	Biological methanation
Capacity	40 MW	
H_2:CO_2 feed ratio	4:1	
H_2 feed	325.4 kmol/h	
CO_2 feed	83.7 kmol/h	
Product impurity limits	3 % H_2; 6 % CO_2	
Process concept	Continuous	
Catalyst/Archaea	Ni/Al_2O_3	*Methanothermobacter thermautotrophicus* strain UC 120910
Pressure, bar	30	6
Temperature in reactor, °C	250	60
Reactor type	Fixed-bed reactor	CSTR

6 Simulation

The processes were simulated using Aspen Plus simulation software. In this chapter it is explained how the models for catalytic and biological methanation processes and deoxo process were built. The complete stream tables for catalytic and biological simulation models are given in Appendix 1.

6.1 Simulation of catalytic methanation process

6.1.1 Property method selection

The property method in Aspen Plus defines how the results are calculated. Aspen's Methods assistant recommends using equation of state (EOS) based property methods, e.g. SRK, PENG-ROB, PC-SAFT or CPA for gas processing.

Soave-Redlich-Kwong (SRK) and Peng-Robinson (PENG-ROB) are cubic equation of state methods. They can be used for systems with hydrocarbons and light gases, e.g. CO_2 and H2. They can be used in gas processing, petrochemical and refinery applications.

The simulation was run using SRK, PENG-ROB and CPA property methods. The results were quite similar with all these methods. Peng-Robinson gave results that were between the results of SRK and CPA. Since the results with Peng-Robinson were average, it was chosen as the most suitable property method.

The Peng-Robinson equation of state is presented in equations (32–36) (Nasri & Housam 2009; U.S. Geological Survey 2006).

$$P = \frac{RT}{V-b} - \frac{a}{V(V+b)+b(V-b)} \quad (32)$$

In which

$$b = 0.07780\frac{RT_c}{P_c} \quad (33)$$

$$a = 0.45724\frac{(RT_c)^2}{p_c}\left[1 + m(1-\sqrt{T_r})\right]^2 \quad (34)$$

$$T_r = \frac{T}{T_c} \quad (35)$$

$$m = 0.37464 + 1.54226\omega - 0.26992\omega^2 \quad (36)$$

T_c critical temperature, K;

p_c critical pressure, bar;

R ideal gas constant, J/mol K;

ω acentric factor for the species, -.

6.1.2 Description of the catalytic process model

The simulation flowsheet and process flow diagram are presented in Figure 5 and Figure 6. The stream table for the process is in Table XII and equipment list is given in Table XIII.

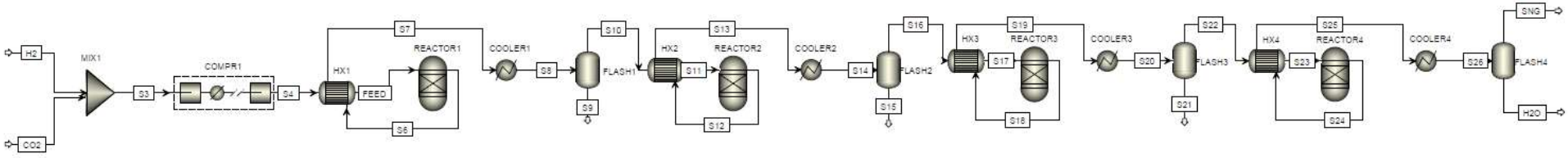

Figure 5 Simulation flowsheet of catalytic methanation process.

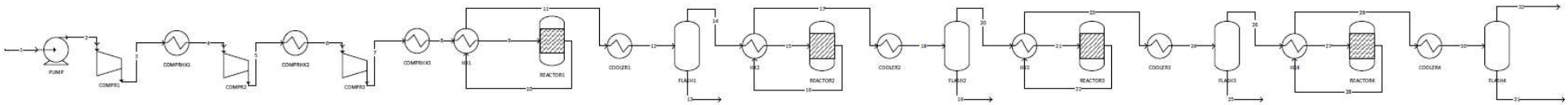

Figure 6 Process flow diagram of catalytic methanation process.

Table XII Stream table for catalytic methanation process. The stream numbers refer to the process flow diagram (Figure 6). The table continues on page 55.

Stream	Stream name in Aspen	Stream composition	Temperature, °C	Pressure, bar	Phase	Mass flow, kg/h	Mole flow, kmol/h	Mole fractions
1		H_2; CO_2	25	1	Gas	4270.9	406.9	0.797 H_2; 0.2 CO_2; 0.001 H_2O
2	S3	H_2; CO_2	25	1	Gas	4270.9	406.9	0.797 H_2; 0.2 CO_2; 0.001 H_2O
3		H_2; CO_2	167	3	Gas	4270.9	406.9	0.797 H_2; 0.2 CO_2; 0.001 H_2O
4		H_2; CO_2	90	3	Gas	4270.9	406.9	0.797 H_2; 0.2 CO_2; 0.001 H_2O
5		H_2; CO_2	263	9,7	Gas	4270.9	406.9	0.797 H_2; 0.2 CO_2; 0.001 H_2O
6		H_2; CO_2	90	9,7	Gas	4270.9	406.9	0.797 H_2; 0.2 CO_2; 0.001 H_2O
7		H_2; CO_2	263	30	Gas	4270.9	406.9	0.797 H_2; 0.2 CO_2; 0.001 H_2O
8	S4	H_2; CO_2	150	30	Gas	4270.9	406.9	0.797 H_2; 0.2 CO_2; 0.001 H_2O
9	FEED	H_2; CO_2	250	30	Gas	4270.9	406.9	0.797 H_2; 0.2 CO_2; 0.001 H_2O
10	S6	CH_4; H_2O; H_2; CO_2	350	30	Gas	4270.9	248.1	0.32 CH_4; 0.64 H_2O; 0.011 CO_2; 0.028 H_2
11	S7	CH_4; H_2O; H_2; CO_2	225	30	Gas	4270.9	248.1	0.32 CH_4; 0.64 H_2O; 0.011 CO_2; 0.028 H_2
12	S8	CH_4; H_2O; H_2; CO_2	180	30	Gas	4270.9	248.1	0.32 CH_4; 0.64 H_2O; 0.011 CO_2; 0.028 H_2
13	S9	H_2O	180	30	Liquid	1963.0	109.0	0.999 H_2O; 0.00056 CH_4; 0.00005 CO_2; 0.00001 H_2
14	S10	CH_4; H_2O; H_2; CO_2	180	30	Gas	2308.0	139.1	0.57 CH_4; 0.36 H_2O; 0.019 CO_2; 0.049 H_2
15	S11	CH_4; H_2O; H_2; CO_2	250	30	Gas	2308.0	139.1	0.57 CH_4; 0.36 H_2O; 0.019 CO_2; 0.049 H_2
16	S12	CH_4; H_2O; H_2; CO_2	350	30	Gas	2308.0	137.4	0.584 CH_4; 0.38 H_2O; 0.024 H_2; 0.012 CO_2
17	S13	CH_4; H_2O; H_2; CO_2	285	30	Gas	2308.0	137.4	0.584 CH_4; 0.38 H_2O; 0.024 H_2; 0.012 CO_2
18	S14	CH_4; H_2O; H_2; CO_2	180	30	Gas	2308.0	137.4	0.584 CH_4; 0.38 H_2O; 0.024 H_2; 0.012 CO_2
19	S15	H_2O	180	30	Liquid	66.3	3.7	0.999 H_2O; 0.00059 CH_4; 0.00003 CO_2; 0.000006 H_2
20	S16	CH_4; H_2O; H_2; CO_2	180	30	Gas	2241.7	133.7	0.60 CH_4; 0.36 H_2O; 0.025 H_2; 0.013 CO_2
21	S17	CH_4; H_2O; H_2; CO_2	250	30	Gas	2241.7	133.7	0.60 CH_4; 0.36 H_2O; 0.025 H_2; 0.013 CO_2

Table XII Stream table for catalytic methanation process. The stream numbers refer to the process flow diagram (Figure 6). (continued)

Stream	Stream name in Aspen	Stream composition	Temperature, °C	Pressure, bar	Phase	Mass flow, kg/h	Mole flow, kmol/h	Mole fractions
22	S18	CH_4; H_2O; H_2; CO_2	350	30	Gas	2241.7	133.6	0.60 CH_4; 0.36 H_2O; 0.025 H_2; 0.013 CO_2
23	S19	CH_4; H_2O; H_2; CO_2	285	30	Gas	2241.7	133.6	0.60 CH_4; 0.36 H_2O; 0.025 H_2; 0.013 CO_2
24	S20	CH_4; H_2O; H_2; CO_2	180	30	Gas	2241.7	133.6	0.60 CH_4; 0.36 H_2O; 0.025 H_2; 0.013 CO_2
25	S21	H_2O	180	30	Liquid	2.6	0.1	0.999 H_2O; 0.00058 CH_4; 0.000006 H_2; 0.00003 CO_2
26	S22	CH_4; H_2O; H_2; CO_2	180	30	Gas	2239.1	133.5	0.60 CH_4; 0.36 H_2O; 0.024 H_2; 0.013 CO_2
27	S23	CH_4; H_2O; H_2; CO_2	250	30	Gas	2239.1	133.5	0.60 CH_4; 0.36 H_2O; 0.024 H_2; 0.013 CO_2
28	S24	CH_4; H_2O; H_2; CO_2	340	30	Gas	2239.1	133.3	0.60 CH_4; 0.36 H_2O; 0.021 H_2; 0.012 CO_2
29	S25	CH_4; H_2O; H_2; CO_2	274	30	Gas	2239.1	133.3	0.60 CH_4; 0.36 H_2O; 0.021 H_2; 0.012 CO_2
30	S26	CH_4; H_2O; H_2; CO_2	140	30	Gas	2239.1	133.3	0.60 CH_4; 0.36 H_2O; 0.021 H_2; 0.012 CO_2
31	H2O	H_2O	140	30	Liquid	639.2	35.5	0.9996 H_2O; 0.00038 CH_4; 0.000003 H_2; 0.00002 CO_2
32	SNG	Synthetic natural gas	140	30	Gas	1599.9	97.8	0.82 CH_4; 0.13 H_2O; 0.028 H_2; 0.016 CO_2

Table XIII Equipment list of the main equipment of catalytic methanation process. Sizing of equipment was not provided in the simulation results. The reactor volumes were calculated by hand as described in chapter 7.2. Stainless steel 316 was chosen as material based on its austenitic properties.

Equipment	Equipment type	Material	Volume, m^3
REACTOR1	Fixed-bed reactor	Stainless steel 316	0.5
REACTOR2	Fixed-bed reactor	Stainless steel 316	0.5
REACTOR3	Fixed-bed reactor	Stainless steel 316	0.5
REACTOR4	Fixed-bed reactor	Stainless steel 316	0.5
FLASH1	Liquid-vapor separator	Stainless steel 316	-
FLASH2	Liquid-vapor separator	Stainless steel 316	-
FLASH3	Liquid-vapor separator	Stainless steel 316	-
FLASH4	Liquid-vapor separator	Stainless steel 316	-
COMPR1	Isentropic multi-stage compressor	Stainless steel 316	-
HX1	Shell and tube heat exchanger	Stainless steel 316	-
HX2	Shell and tube heat exchanger	Stainless steel 316	-
HX3	Shell and tube heat exchanger	Stainless steel 316	-
HX4	Shell and tube heat exchanger	Stainless steel 316	-
COOLER1	Shell and tube heat exchanger	Stainless steel 316	-
COOLER2	Shell and tube heat exchanger	Stainless steel 316	-
COOLER3	Shell and tube heat exchanger	Stainless steel 316	-
COOLER4	Shell and tube heat exchanger	Stainless steel 316	-

Hydrogen and carbon dioxide are mixed and the mixed stream conditions are 1 bar and 25 °C. The pressure is increased to 30 bar in three stage compression with interstage cooling. The compressed stream (stream 8) is heated to 250 °C in heat exchanger HX1. The heated stream is fed to REACTOR1. The outlet stream (stream 10, 350 °C) of the reactor is fed to HX1 and used for heating. The stream is pre-cooled in HX1 and further cooled down to 180 °C in COOLER1. Excess water is separated from the stream with FLASH1 (180 °C, 30 bar). The gas stream (stream 14) is fed to HX2 for heating the stream to 250 °C and then it is fed to REACTOR2. REACTOR2 outlet stream (350 °C) is used for heating stream 14 in HX2. The reactor outlet stream is pre-cooled in HX2 and further cooled down to 180 °C in COOLER2. Excess water is separated in FLASH2 (180 °C, 30 bar). The gas stream (stream 20) is fed to HX3 for heating the stream to 250 °C. Then the stream is fed to REACTOR3. The reactor outlet stream (350 °C) is used for heating stream 20 in HX3. After

pre-cooling the reactor outlet stream in HX3, the stream is further cooled down to 180 °C in COOLER3. Excess water is removed in FLASH3 (180 °C, 30 bar). The gas stream (stream 26) is heated to 250 °C in HX4 and then fed to REACTOR4. The reactor outlet stream (340 °C) is used for heating stream 26 in HX4. The stream is further cooled to 140 °C in COOLER4. Water is removed in FLASH4 (140 °C, 30 bar). The product stream (stream 32) consists of synthetic natural gas and it is ready for further processing, such as drying and then liquefaction or compression.

The reactor type used in the simulation was RGibbs. Multistage compression was simulated with MCompr block. Two-stream heat exchangers were simulated using HeatX and coolers were simulated using Heater blocks. The flash separators were simulated with Flash2 blocks.

6.1.3 Heat integration

Heat integration was included in the process design. The streams that require cooling or heating are listed in Table XIV and the heat exchangers utilised in the heat integration are summarized in Table XV. From this table it can be seen that the reactor outlets (350 °C) can be used for heating the reactor feed streams (250 °C). When the reactor outlet streams are used for heating the colder streams, the hot outlet streams are already pre-cooled before entering the coolers used for cooling the streams to the target temperature of 180 °C. This also lowers the cooling utility consumption.

Table XIV Stream table for heat integration.

Stream	Type	Supply temperature, °C	Target temperature, °C
Reactor 1 feed	cold	150	250
Reactor 1 outlet	hot	350	180
Reactor 2 feed	cold	180	250
Reactor 2 outlet	hot	350	180
Reactor 3 feed	cold	180	250
Reactor 3 outlet	hot	350	180
Reactor 4 feed	cold	180	250
Reactor 4 outlet	hot	340	140

Table XV Summary of heat exchangers utilised in heat integration. The heat transfer area was provided in the simulation results.

Heat exchanger	Heat exchanger type	Heat transfer area, m^2
HX1	Shell and tube	4.97
HX2	Shell and tube	1.34
HX3	Shell and tube	1.30
HX4	Shell and tube	1.44

The target of heat integration is to lower the utility consumption of the process. The designed heat integration meets this target. No outside heating utility is required for heating the streams when the process is operated continuously. The cooling requires a cooling utility, such as water.

6.2 Simulation of biological methanation process

6.2.1 Property method selection

The model was run with the suggested property methods SRK, PENG-ROB and CPA. Peng-Robinson was deemed most suitable also for this model.

6.2.2 Description of the biological process model

The simulation flowsheet and process flow diagram are presented in Figure 7 and Figure 8. Cultivation unit was not included in the simulation. The stream table for the process flow diagram is given in Table XVI and equipment list in Table XVII.

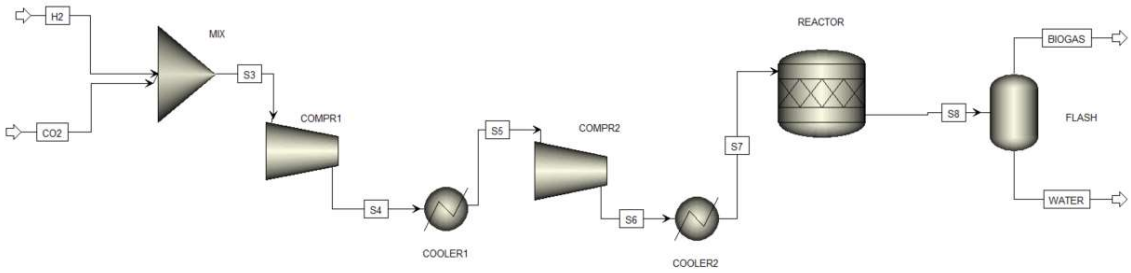

Figure 7 Simulation flowsheet of biological methanation process.

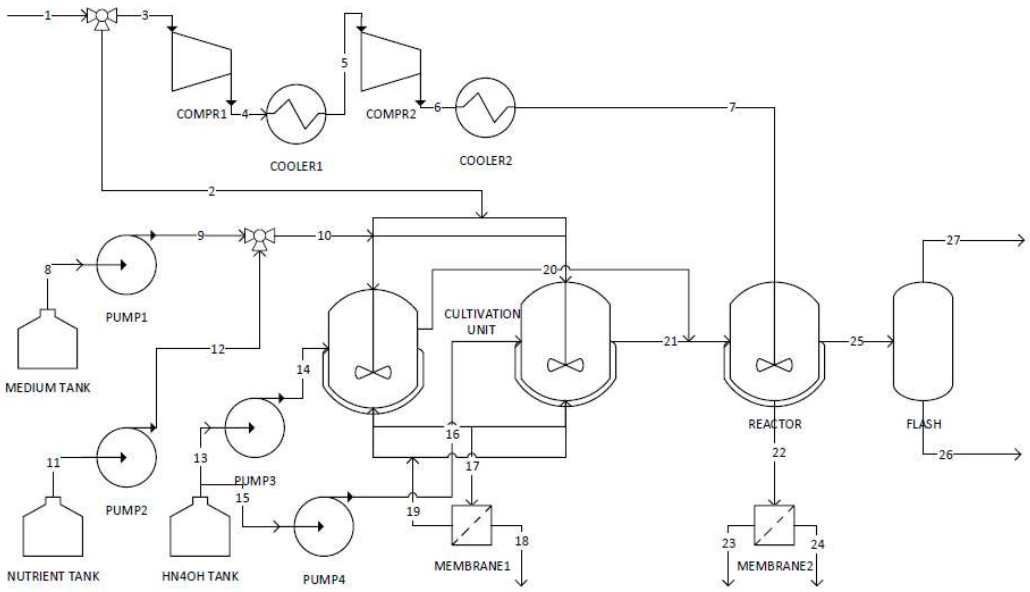

Figure 8 Process flow diagram of biological methanation process.

Table XVI Stream table for biological methanation process. The stream numbers refer to the process flow diagram (Figure 8). The table continues on page 60.

Stream	Stream name in Aspen	Composition	Temperature, °C	Pressure, bar	Phase	Mass flow, kg/h	Mole flow, kmol/h	Mole fractions
1		H_2; CO_2	25	1	Gas	4218	405	0.8 H_2; 0.2 CO_2
2		H_2; CO_2	25	1	Gas	4218	405	0.8 H_2; 0.2 CO_2
3	S3	H_2; CO_2	25	1	Gas	4218	405	0.8 H_2; 0.2 CO_2
4	S4	H_2; CO_2	165	3	Gas	4218	405	0.8 H_2; 0.2 CO_2
5	S5	H_2; CO_2	50	3	Gas	4218	405	0.8 H_2; 0.2 CO_2
6	S6	H_2; CO_2	141	6	Gas	4218	405	0.8 H_2; 0.2 CO_2
7	S7	H_2; CO_2	60	6	Gas	4218	405	0.8 H_2; 0.2 CO_2
8		Medium solution	60	1	Liquid			
9		Medium solution	60	1	Liquid			
10		Medium solution and nutrients	25	1	Liquid			
11		Nutrients	25	1	Liquid			
12		Nutrients	25	1	Liquid			
13		HN_4OH	25	1	Liquid			
14		HN_4OH	25	1	Liquid			
15		HN_4OH	25	1	Liquid			
16		HN_4OH	25	1	Liquid			
17		Diluted medium solution	60	1	Liquid			

Table XVI Stream table for biological methanation process. The stream numbers refer to the process flow diagram (Figure 8). (continued)

Stream	Stream name in Aspen	Composition	Temperature, °C	Pressure, bar	Phase	Mass flow, kg/h	Mole flow, kmol/h	Mole fractions
18		Diluted medium solution	60	1	Liquid			
19		Biomass	60	1	Liquid			
20		Biomass	60	1	Liquid			
21		Biomass	60	1	Liquid			
22		Diluted water solution	60	6	Liquid			
23		Inactive biomass	60	6	Liquid			
24		Diluted water solution	60	6	Liquid			
25	S8	CH_4; H_2; CO_2; H_2O	60	6	Gas	4218	245	0.33 CH_4; 0.017 H_2; 0.004 CO_2; 0.65 H_2O
26	WATER	H_2O; CH_4; CO_2; H_2	60	6	Liquid	2859	159	0.989 H_2O; 0.01 CH_4; 0.0005 CO_2; 0.00002 H_2
27	BIOGAS	Biogas	60	6	Gas	1359	86	0.907 CH_4; 0.049 H_2; 0.011 CO_2; 0.033 H_2O

Table XVII Equipment list of the main equipment of biological methanation process. The sizing of flash separator was provided in the simulation results. Stainless steel 316 was chosen as material based on its austenitic properties.

Equipment name	Equipment type	Material	Volume, m^3
REACTOR	CSTR	Stainless steel 316	42.5
FLASH	Liquid-vapor separator	Stainless steel 316	2.4
COMPR1	Isentropic compressor	Stainless steel 316	-
COMPR2	Isentropic compressor	Stainless steel 316	-
COOLER1	Shell-and tube heat exchanger	Stainless steel 316	-
COOLER2	Shell-and tube heat exchanger	Stainless steel 316	-

The cultivation unit consists of two CSTRs (60 °C, 1 bar). Nutrients and medium solution are fed to the tanks that have the archaea inside. HN_4OH is used for pH control (pH 6.85). Hydrogen and carbon dioxide mixture with stoichiometric ratio 4:1 is spurted to the cultivation CSTRs intermittently. For this, a small part of the H_2:CO_2 mixture is separated

to stream 2 from stream 1. Excess water and medium solution must be removed from the cultivation unit (stream 17). Because some biomass may also transfer during the removal, the biomass is separated from the diluted medium solution with MEMBRANE1 and recycled to the cultivation unit. Biomass from both cultivation units is fed to REACTOR. H_2 and CO_2 mixture is compressed in two stages with interstage cooling to 6 bar and then fed to REACTOR. The reactor operates in 60 °C and 6 bar. Water is formed in the methanation reaction. Excess water and deactivated biomass are removed in stream 22. MEMBRANE2 separates the water solution and deactivated biomass. The gas stream from the reactor (stream 25) is fed to FLASH (60 °C, 6 bar) to separate gas phase water from the product biogas (stream 27).

The reactor type used in the simulation was RStoic. Rstoic was used to find out the required hydrogen conversion. It was discovered that the hydrogen conversion required to reach the product impurity limits would have to be 99.3 %. However, Mets (2012) reported maximum hydrogen conversion of 98.7 % for *M. thermautotrophicus*. This means that the impurity levels cannot be met in the designed process. The biogas requires further purification with e.g. pressure swing adsorption or catalytic methanation before it can meet the product impurity limits. After purification the biogas can be liquefied or compressed. The results given in this thesis are for the feasible conversion of 98.7 %.

The compressors were simulated with Aspen block Compr. The coolers were simulated with Heater blocks and flash separator with Flash2 block.

6.3 Simulation of deoxo process

The deoxo process was simulated to find out how much hydrogen would be consumed in the oxygen separation process. The result was used when adjusting the feed flows of the designed methanation processes. Peng-Robinson was set as the property method also in this simulation. The simulation flowsheet of the process is in Figure 9 and stream table in Table XVIII.

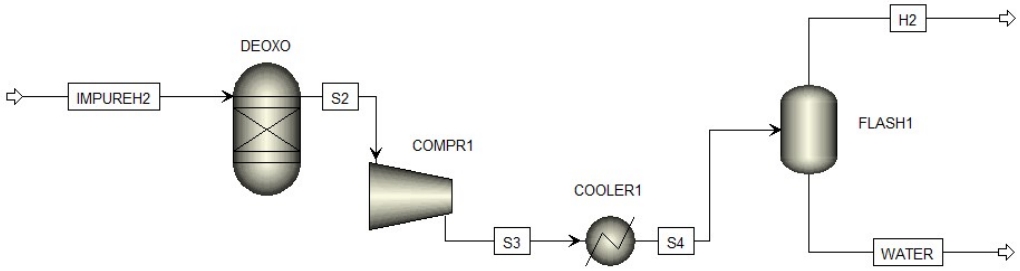

Figure 9 Simulation flowsheet of deoxo process.

The deoxo reactor was modelled using RGibbs reactor type. The compressor was simulated with Compr block, cooler with Heater block and flash separator with Flash2 block. The impure hydrogen stream (IMPUREH2) is fed to the reactor DEOXO in 25 °C and 1 bar. After the deoxo reaction the gas stream is compressed to 10 bar and cooled to 15 °C. The formed water is separated from the hydrogen gas in FLASH1. Purified hydrogen (stream H2) is in 15 °C and 10 bar.

Table XVIII Stream table for deoxo process. The stream names refer to the simulation flowsheet (Figure 9).

Stream name	Temperature, °C	Pressure, bar	Mass flow, kg/h	Mole flow, kmol/h	Mole fractions
IMPUREH2	25	1	666	325.4	0.999 H_2; 0.001 O_2
S2	25	1	666	325.1	0.998 H_2; 0.002 H_2O
S3	409	10	666	325.1	0.998 H_2; 0.002 H_2O
S4	15	10	666	325.1	0.998 H_2; 0.002 H_2O
WATER	15	10	662	0.20	1 H_2O
H2	15	10	4	324.9	0.999 H_2; 0.001 H_2O

It should be noted that in reality the compression should be executed with multi-stage compression with interstage cooling. Compression in one stage is possible in Aspen Plus,

but in reality, the outlet temperature of COMPR1 would be too hot to be feasible. This should be taken in account in more detailed process design if deoxo is required.

6.4 Basis of cost estimation

The cost estimation for purification step and catalytic and biological process options was based on the simulation results. Aspen Economic Evaluation gives estimates for the major equipment costs and utility costs. These estimates were used in the cost estimation calculations. To get the results for the adiabatic reactor costs and deoxo reactor cost, reactor dimensions were added to the models by hand. The basis of the sizing calculations is given in chapter 7.

The investment cost for the biogas purification process was assumed to be 1 M€ and this cost was added to the major equipment costs.

The fixed capital cost includes inside battery limits (ISBL) investment, off-site (outside battery limits, OSBL) investment, engineering and construction costs and contingency charges. According to Sinnot & Towler (2009), ISBL costs can be calculated with equation (37).

$$C_{ISBL} = \sum C_e \cdot 3.3 \quad (37)$$

In which C_{ISBL} ISBL cost, €;

C_e equipment cost, €.

An initial estimate for OSBL costs is 40 % of ISBL costs. Engineering and construction costs are estimated to be 30 % of the sum of ISBL and OSBL costs. Contingency is typically 10 % of the sum of ISBL and OSBL costs. However, if the technology is uncertain, the contingency charges can be assumed bigger, up to 50 %. (Sinnot & Towler 2009) Because P2X is a new field of technology, the contingency charges are estimated to be 20 % in this thesis. The total fixed capital cost can be calculated with equation (38) (Sinnot & Towler 2009).

$$C_{FC} = \sum C_e \cdot \{ISBL(1 + OS)(1 + D\&E + X)\} \quad (38)$$

In which C_{FC} total fixed capital cost , €;

ISBL	cost factor for ISBL cost, -;
OS	cost factor for OSBL cost, -;
D&E	cost factor for design and engineering costs, -;
X	cost factor for contingency charges, -.

Raw material costs were calculated with the prices 60 €/t for CO2 and 5.52 €/kg for hydrogen as presented in chapters 2.3 and 2.4. The product selling price was set to 1.45 €/kg as presented in chapter 2.2. This reference price was reported for biogas, but it was used for both SNG and biogas, since both products are renewables. When reporting the price as €/MWh, the assumed heat value of methane is 50 MJ/kg (World nuclear Association 2018).

The Ni/Al_2O_3 catalyst cost was calculated for the reference catalyst which contains 45 w-% of Ni. Production costs of 30 % were added to the raw material prices. Raw material prices were 12.37 €/kg for nickel and 284 €/t for Al_2O_3 (Business Insider 2020; Focus Economics 2020). The calculated cost for the catalyst was 7.4 €/kg.

The archaea used in the designed biological methanation process is *Methanothermobacter thermautotrophicus* strain UC 120910 which is the patented archaea used by Electrochaea. It was assumed that the strain could be used with licence payment to the patent owner. The licencing cost of the methanation microbes was assumed to be 5 % of the investment on a yearly basis. The equipment cost for cultivation unit and membrane for methanation reactor outlet was assumed (Table XIX). The total assumed cost was added to the equipment cost of the biological process.

Table XIX Assumed equipment costs for cultivation unit.

Equipment	Amount	Assumed cost per equipment, k€
Cultivation reactor	2	40
Pump	4	3
Membrane	2	20
Storage tank	3	1.5
Total cost, k€	64.5	

The cost for Pd/Al_2O_3 catalyst used in deoxo process was determined with the same principle as the cost for Ni/Al_2O_3 catalyst. The Pd/Al_2O_3 catalyst contains 0.5 % of Pd (Sandeep et al.

2014). The price of palladium was 62047 €/kg (Money Metals Exchange 2020). The production costs were assumed 30 %. The calculated cost for the catalyst was 404 €/kg. Catalyst lifetime was assumed to be three years.

Sensitivity analysis was conducted for the price of hydrogen and product selling price. The initially assumed price for hydrogen was quite high, so the upper limit (120 %) for hydrogen price was set to the initial price. The effect of the hydrogen price decreasing was studied using revenue with initial price of 1.45 €/kg for the products. The effect of the product selling price increasing or decreasing was studied using hydrogen raw material costs with price of 4.42 €/kg for hydrogen. The values used in the analysis are given in Table XX.

Table XX Hydrogen and product prices for sensitivity analysis. The price of hydrogen was varied from 30 % to 120 % of the base value and the product price from 80 % to 160 % from the base value.

	H_2, €/kg	Product, €/kg
30 %	1.32	
40 %	1.77	
50 %	2.21	
60 %	2.65	
70 %	3.09	
80 %	3.53	1.16
90 %	3.97	1.31
100 %	4.42	1.45
110 %	4.97	1.60
120 %	5.52	1.74
130 %		1.89
140 %		2.03
150 %		2.18
160 %		2.32

Interest of 8 % and operating time of 8000 h/a were assumed. Project lifetime was set to 20 years. The project profitability was analysed with net present value (NPV) analysis. The break-even point of the projects can be found with this analysis. The break-even point shows when the investment has paid itself and starts making profit. The NPV analysis was conducted using Excel template by Sinnot & Towler (2009). The filled templates are in Appendix 2.

7 Sizing

7.1 Deoxo unit

The deoxo unit can be sized based on pressure drop of the reactor bed and superficial gas velocity. The pressure drop can be solved with Ergun formula (39-41) (Guo & Li 2014).

$$\frac{\Delta p_b}{H_b} = f_m \frac{\rho v^2}{d_p}\left(\frac{1-\varepsilon_b}{\varepsilon_b}\right) \quad (39)$$

In which $$f_m = a_E + b_E\left(\frac{1-\varepsilon_b}{R_e}\right) \quad (40)$$

$$R_e = \frac{d_p \rho v}{\mu} \quad (41)$$

Δp_b pressure drop, Pa;

f_m modified coefficient of friction, -;

ρ fluid density, kg/m^3;

v superficial linear velocity, m/s;

d_p diameter of the catalyst particle, m;

ε_b bed voidage, -;

H_b bed height, m;

R_e Reynolds number, -;

μ viscosity of the fluid, Pa s;

a, b coefficient, values proposed by Ergun a=1.75 and b=150.

The assumptions that were used in the calculations to reach a realistic pressure drop are given in Table XXI. To calculate the pressure drop, elevated reactor pressure (10 bar) and temperature (60 °C) were assumed. The calculated pressure drop was 121 kPa (1.21 bar).

Table XXI Assumptions for pressure drop calculation. The calculated pressure drop was 121 kPa.

Parameter	Value
Bed height, m	2
Catalyst particle diameter, m	0.005
Bed voidage, -	0.3
Superficial linear velocity, m/s	10

When flowrate and superficial gas velocity are known, the required cross-sectional area of reactor can be calculated with equation (42). The feed flowrate used in the calculation was 2.24 m^3/s.

$$v = \frac{Q}{A} \tag{42}$$

In which Q feed flowrate, m^3/s;

A cross-sectional area of reactor, m^2.

The reactor diameter was calculated from the cross-sectional area of reactor and the reactor was assumed to be cylindrical. The catalyst volume was calculated from the bed voidage with equation (43). The catalyst density (0.5 % Pd and 99.5 % Al_2O_3) was calculated to be 3990 kg/m^3 based on the densities of Al_2O_3 and Pd.

$$V_{catalyst} = (1 - \varepsilon_b) \cdot V_{reactor} \tag{43}$$

In which $V_{catalyst}$ catalyst volume, m^3.

$V_{reactor}$ reactor volume, m^3.

7.2 Fixed bed reactors

The catalytic methanation reactors are adiabatic fixed bed reactors. The required catalyst bed volume for each reactor can be calculated with space-time yield (STY). Türks et al. (2017) have reported STY of 1.7 $L_{product}/mL_{catalyst}$ h for CO_2 methanation using a commercial Ni/Al_2O_3 catalyst at 350 °C reactor temperature. The catalyst activated at 250 °C. Because the experiment conditions were similar to the process conditions used in this thesis, the STY value can be used as a reference value in this thesis. The reference catalyst used in the sizing calculations is G1-86HT by Lurgi (see Table V for specifications).

STY can be calculated with equation (44) (Türks et al. 2017; Hagen 2015). Because the STY is known, the required catalyst volume can be calculated with this equation.

$$\mathrm{STY} = \frac{\mathrm{V_{product}}}{\mathrm{V_{catalyst}}} \tag{44}$$

In which STY space-time yield, $dm^3_{product}/cm^3_{catalyst}$ h;

$V_{product}$ product flowrate, dm^3/h;

$V_{catalyst}$ catalyst volume, cm^3.

The reactor volume can be calculated from the required catalyst volume. The reactors were assumed to be cylinders. The reactor height can be calculated through geometry when the catalyst volume is known (45). It was assumed that the height to diameter ratio is 1:4 and the catalyst volume to reactor volume ratio 1:5. The reasonability of the sizing was ensured by calculating the velocity of gas in the reactors with equation (42).

$$\mathrm{h} = \sqrt[3]{\frac{320 \cdot \mathrm{V_{catalyst}}}{\pi}} \tag{45}$$

In which h reactor height, m.

7.3 CSTR

The reactors used in the biological methanation process are continuous stirred tank reactors (CSTR). Inkeri et al. (2018) have modelled biological ex-situ methanation in CSTR based on available experimental data of biological methanation pilot plants. Reference GHSV value was calculated based on the values presented by them with equation (46). With reactor size of 8 m^3 and total gas inflow of 350 m^3/h, the GHSV is approximately 44 h^{-1}.

$$\mathrm{GHSV} = \frac{\mathrm{V_{feed}}}{\mathrm{V_{reactor}}} \tag{46}$$

In which GHSV gas hourly space velocity, h^{-1};

V_{feed} flowrate of feed, m^3/h.

The required minimum volume of the CSTR was calculated with equation (46) with GHSV of 44 h^{-1} and 1870 m^3/h feed flowrate.

8 Results and discussion

8.1 Product purity

It was discovered that the catalytic process requires four reactors to meet the product purity targets. The methane content in SNG was 82.15 mol-%. The hydrogen content was 2.84 mol-% and carbon dioxide content 1.62 mol-%. The rest (13.38 mol-%) was water, which means that the product would have to be dried to remove gas phase water before e.g. liquefaction. The hydrogen and carbon dioxide contents are within the impurity limits, which means that besides drying, no additional purification steps are needed.

The biological process was not able to meet the product purity targets. The required hydrogen conversion to reach the targets would be 99.3 %. However, the maximum hydrogen conversion of the methanation archaea used in the process is 98.7 %. With the conversion of 98.7 %, the biogas contained 90.71 mol-% methane, 4.87 mol-% hydrogen, 1.13 mol-% carbon dioxide and 3.29 mol-% water. The hydrogen content exceeds the maximum limit of 3 mol-% which means that the produced biogas should be further purified. The purification could be done with e.g. pressure swing adsorption or catalytic methanation unit.

8.2 Equipment sizing

The results for the deoxo reactor sizing are given in Table XXII.

Table XXII Results for deoxo reactor sizing.

Cross-sectional area, m^2	0.22
Diameter, m	0.53
Height, m	2
Reactor volume, m^3	0.45
Catalyst volume, m^3	0.31
Catalyst mass, kg	1252

The results for the required amount of catalyst in each reactor in the catalytic methanation process calculated with STY value of 1.7 $L_{product}$/mLcatalyst h are in Table XXIII. The reactor sizing based on the catalyst amount for each reactor is given in Table XXIV. The

assumed height to diameter ratio of 1:4 would give diameter of 0.5 m. To ensure better flow in the tube reactors, the diameter was changed to 0.4 m.

Table XXIII Required amount of catalyst in each reactor. STY=1.7 $L_{product}$/mLcatalyst h.

Reactor	Product flowrate, m^3/h	Catalyst volume, m^3	Catalyst mass, kg
1	135.7	0.08	71.8
2	137.1	0.08	72.6
3	137.1	0.08	72.6
4	137.3	0.08	72.7

Table XXIV The calculated reactor sizing based on the catalyst volumes.

Reactor	Height, m	Diameter, m	Area, m^2	Volume, m^3	Flowrate, m^3/s	Velocity of gas, m/s
1	2.01	0.4	0.13	0.26	0.17	1.32
2	2.02	0.4	0.13	0.26	0.05	0.43
3	2.02	0.4	0.13	0.26	0.05	0.42
4	2.02	0.4	0.13	0.26	0.05	0.42

Because the catalyst amount and reactor sizing were very similar for each reactor, the final sizing was adjusted so that all the reactors are the same size. The catalyst amount was rounded up to 73 kg. The calculated reactor height was doubled to make sure that operating the reactors is possible since the previously calculated height was just the theoretical minimum height requirement. The final sizing is given in Table XXV.

Table XXV Final sizing of fixed bed reactors in catalytic methanation process.

Catalyst volume, m^3	0.08
Catalyst mass, kg	73.0
Reactor height, m	4.0
Reactor diameter, m	0.4
Cross-sectional area, m^2	0.13
Reactor volume, m^3	0.50

The size of the CSTR reactor in biological methanation process was calculated to be 42.5 m^3.

8.3 Cost estimation

It should be noted that location factors and equipment material factors are not considered in the cost estimation results. The default material for equipment in Aspen Plus is carbon steel

but stainless steel 316 is preferable as a material to avoid corrosion. The accuracy of the cost estimation can be considered ± 30 %.

8.3.1 Investment costs

The investment costs of both designed processes are given in Table XXVI. It can be seen that the total fixed capital cost of the biological methanation process is slightly lower than that of the catalytic methanation process. The equipment cost of deoxo process (2.5 M€) was added to the equipment costs of both processes. The equipment cost for cultivation unit (0.065 M€) and investment cost for purification unit (1.0 M€) were also added to the costs of biological methanation.

Table XXVI Investment costs of catalytic and biological methanation processes.

	Catalytic methanation with deoxo	Biological methanation with deoxo	Catalytic methanation without deoxo	Biological methanation without deoxo
Equipment cost, M€	5.4	4.9	2.9	2.5
ISBL, M€	17.8	16.3	9.7	8.1
OSBL, M€	7.1	6.5	3.9	3.2
Engineering costs, M€	7.5	6.8	4.1	3.4
Contingency charges, M€	5.0	4.6	2.7	2.3
Total fixed capital cost, M€	37.4	34.1	20.3	17.0

8.3.2 Variable costs and revenue

The variable costs and revenue of catalytic and biological processes are given in Table XXVII. The production rate of the catalytic process is 12799 t/a, and that of the biological process is 10875 t/a. The variable costs of catalytic methanation are slightly higher. On the other hand, also the revenue of catalytic methanation is higher due to larger production rate.

Table XXVII Variable costs and revenue of the processes.

	Catalytic methanation	Biological methanation
H_2 cost, M€/a	29.0	29.0
CO_2 cost, M€/a	1.7	1.7
Methanation catalyst or archaea, M€/a	0.001	0.4
Deoxo catalyst, M€/a	0.17	0.17
Utilities, M€/a	1.9	0.6
Total variable costs, M€/a	32.8	31.9
Revenue, M€/a	18.6	15.8

The variable costs of both processes are roughly twice as much as the revenues. This means that the processes cannot be profitable with the initial raw material or product selling prices.

The deoxo process increases both the fixed capital costs and variable costs of the methanation processes. If possible, it might be more cost-effective to insert impure hydrogen in the catalytic methanation process. This would mean that the methanation catalyst's lifetime would be shorter, but on the other hand, the methanation catalyst's cost is much lower than that of Pd/Al_2O_3. Further research is required to find out the most feasible option. However, the methanation archaea is anaerobic and is likely to be damaged if impure hydrogen is used in the biological methanation process. This means that including the deoxo process in biological methanation seems preferable.

8.3.3 Sensitivity analysis

The revenue and hydrogen cost per year were calculated with the varied prices presented in Table XX. The results are given in Table XXVIII.

Table XXVIII Hydrogen cost and revenue of the processes per year for varied hydrogen price and product selling prices.

	H_2, M€/a	SNG, M€/a	Biogas, M€/a
30 %	6,9		
40 %	9,3		
50 %	11,6		
60 %	13.9		
70 %	16.2		
80 %	18.5	14.8	
90 %	20.8	16.7	14.0
100 %	23.2	18.6	15.6
110 %	26.1	20.4	17.1
120 %	29.0	22.3	18.7
130 %		24.1	20.2
140 %		26.0	21.8
150 %			23.3
160 %			24.9

Sensitivity analysis shows that the price of hydrogen should be below 3.53 €/kg when the selling price of SNG is 1.45 €/kg (Figure 10). When the price of hydrogen is 4.42 €/kg, the selling price of SNG should be above 1.8 €/kg (Figure 11).

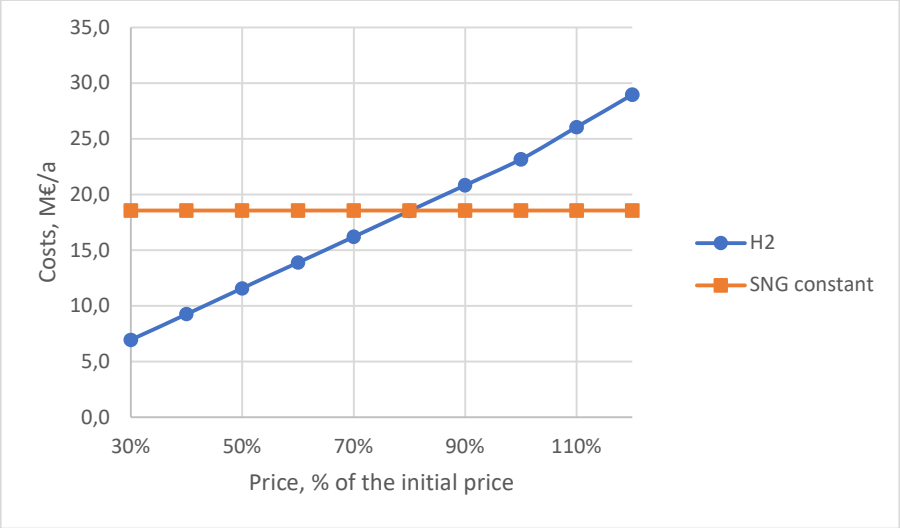

Figure 10 Sensitivity analysis for the price of hydrogen for annual total costs of the catalytic methanation process. Hydrogen price at 100 % is 4.42 €/kg.

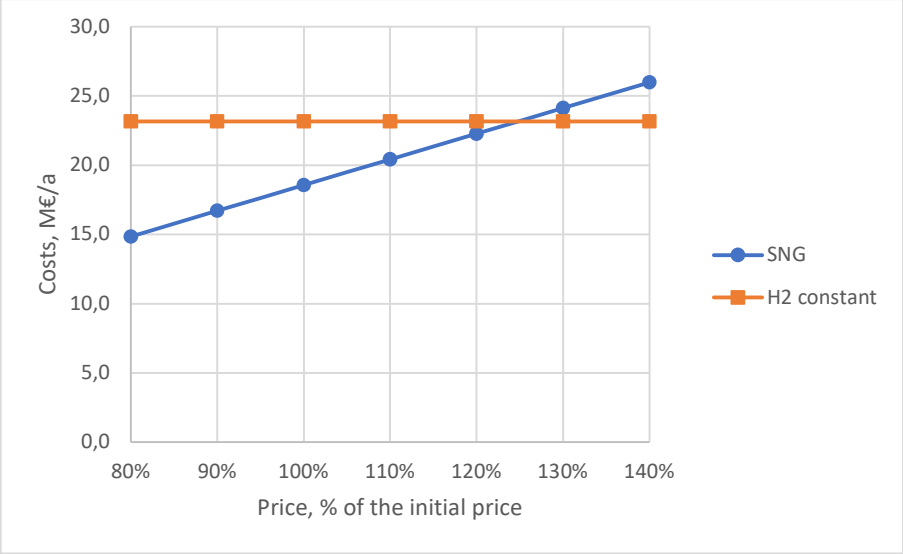

Figure 11 Sensitivity analysis for the selling price of SNG for annual total costs. SNG price at 100 % is 1.45 €/kg.

When the selling price of biogas is 1.45 €/kg, the price of hydrogen should be below 3.0 €/kg (Figure 12). When the price of hydrogen is 4.42 €/kg, the selling price of biogas should be above 2.18 €/kg (Figure 13).

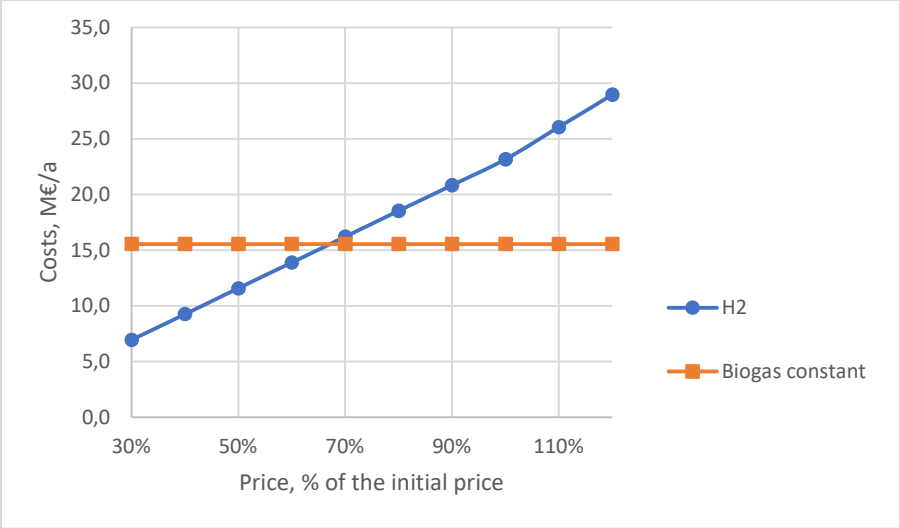

Figure 12 Sensitivity analysis for the price of hydrogen for annual total costs of the biological methanation process. Hydrogen price at 100 % is 4.42 €/kg.

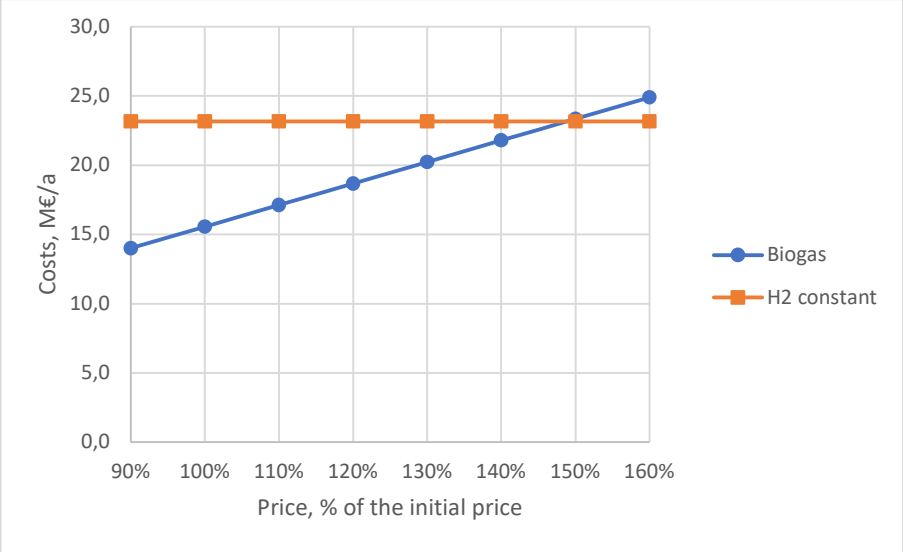

Figure 13 Sensitivity analysis for the selling price of biogas for annual total costs. Biogas price at 100 % is 1.45 €/kg.

8.3.4 Statistical analysis based on most likely value

The mean values and standard deviations were calculated for the investment (Table XXIX), raw material costs (Table XXX) and sales price (Table XXXI) of the methanation processes.

Table XXIX The mean values and standard deviations for the investment costs of catalytic and biological methanation processes when deoxo process is included. With 98 % confidence the investment costs are less than 40.9 M€ for catalytic methanation and 37.3 M€ for biological methanation.

	Catalytic methanation	Biological methanation
$\bar{x}_{ISBL}$, M€	19.1	17.5
$\bar{x}_{OSBL}$, M€	7.7	7.0
$S_{x,ISBL}$, M€	4.7	4.3
$S_{x,OSBL}$, M€	1.9	1.7
$\bar{x}_{total}$, M€	29.5	26.9
$S_{x,total}$, M€	5.6	5.1
Costs less than, M€	40.9	37.3

Table XXX The mean values and standard deviations for the raw material costs of catalytic and biological methanation processes per year. With 98 % confidence the raw material costs are less than 41.2 M€/year for both processes.

	Catalytic methanation	Biological methanation
$\bar{x}_{H2}$, M€/year	30.4	30.4
$\bar{x}_{CO2}$, M€/year	1.8	1.8
$S_{x,H2}$, M€/year	4.4	4.4
$S_{x,CO2}$, M€/year	0.3	0.3
$\bar{x}_{total}$, M€/year	32.2	32.2
$S_{x,total}$, M€/year	4.4	4.4
Costs less than, M€/year	41.2	41.2

Table XXXI Mean value and standard deviation for product sales price. With 98 % confidence the sales price will not be more than 1.90 €/kg.

	Sales price
$\bar{x}$, €/kg	1.45
S_x, €/kg	0.22
Maximum sales price, €/kg	1.90

8.3.5 Profitability analysis

The net present value analysis showed that neither of the processes were profitable with the price of hydrogen and selling price of the product reported in literature (Figure 14 & Figure 15).

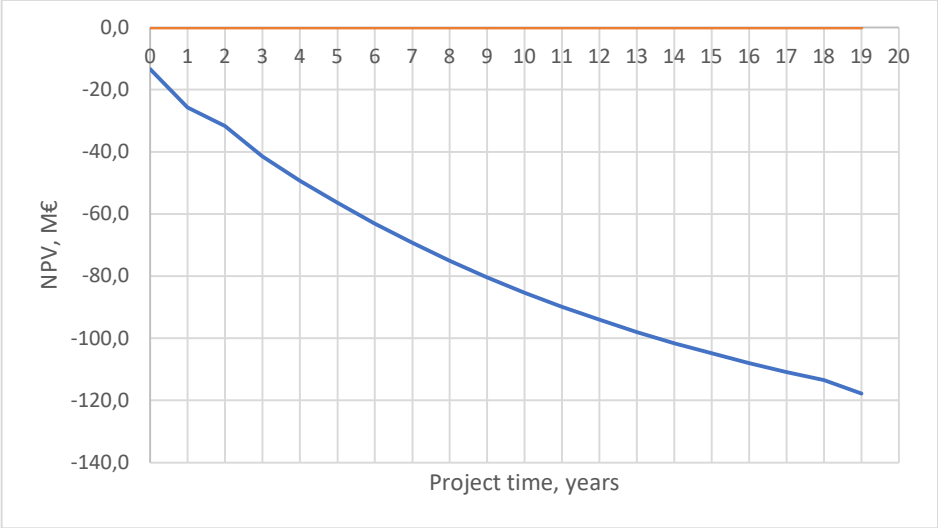

Figure 14 NPV analysis of catalytic methanation process deoxo process is included. SNG selling price was set to 1.45 €/kg (103.57 €/MWh) and hydrogen price to 4.42 €/kg. The interest rate was 8 % and the plant capacity 40 MW. The process is not profitable.

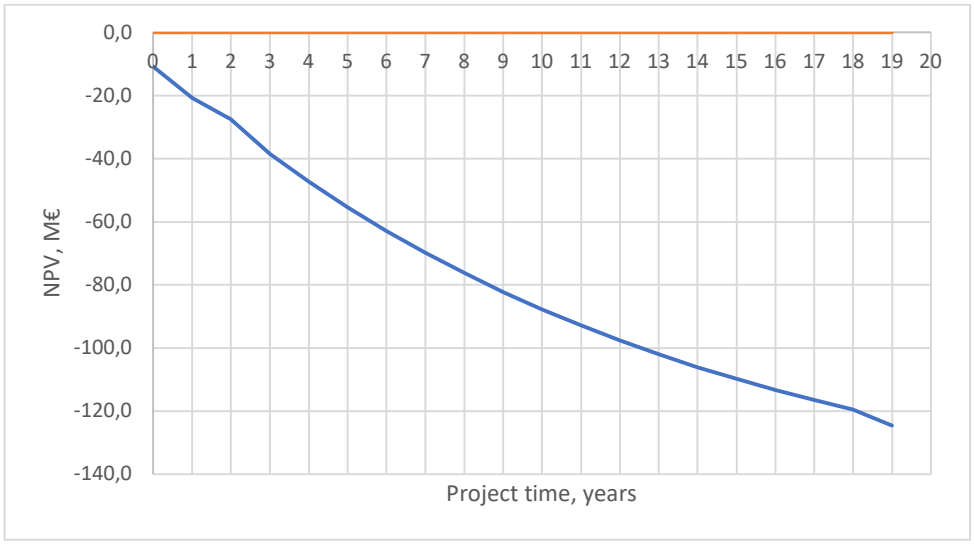

Figure 15 NPV analysis of biological methanation process deoxo process is included. Biogas selling price was set to 1.45 €/kg (103.57 €/MWh) and hydrogen price to 4.42 €/kg. The interest rate was 8 % and the plant capacity 40 MW. The process is not profitable.

To see how the processes could become profitable, the hydrogen price was lowered to 2 €/kg and product selling price was increased until the processes became profitable within the project lifetime. The product selling price was increased to 1.90 €/kg. The break-even point

of catalytic processes is at 16 years (Figure 16) and at 17.5 years for biological process (Figure 17).

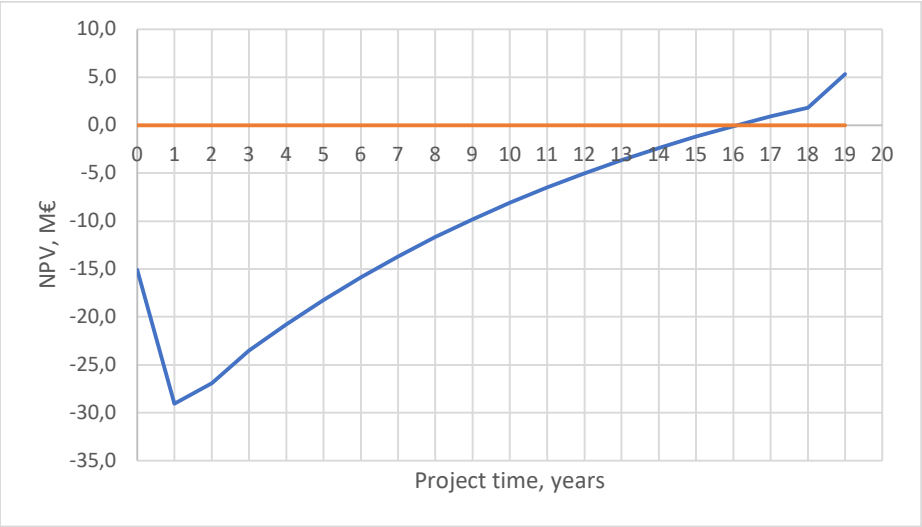

Figure 16 NPV analysis of catalytic methanation process when deoxo process is included. Hydrogen price was set to 2 €/kg and SNG price to 1.9 €/kg (135.71 €/MWh). The interest rate was 8 % and the plant capacity 40 MW. The break-even point is at 16 years.

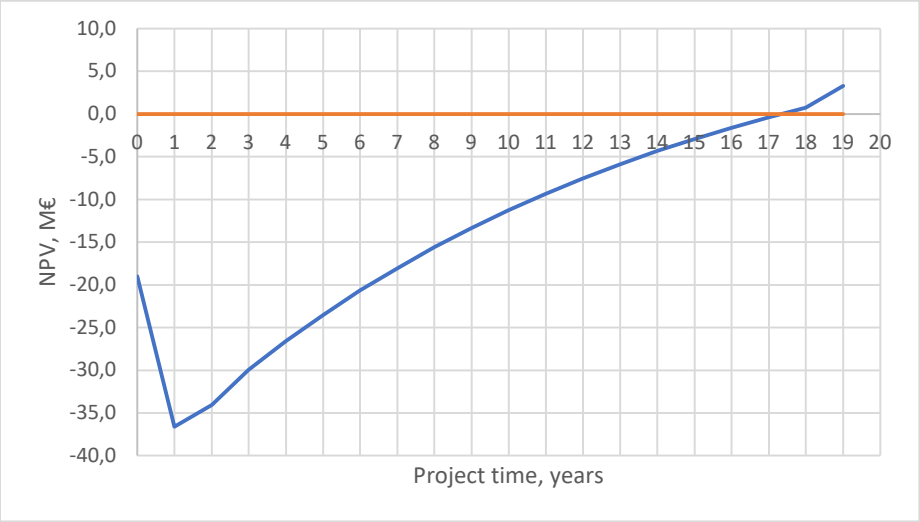

Figure 17 NPV analysis of biological methanation process deoxo process is included. Hydrogen price was set to 2 €/kg and biogas price to 1.9 €/kg (135.71 €/MWh). The interest rate was 8 % and the plant capacity 40 MW. The break-even point is at 17.5 years.

The analysis proved that the selling price should be close to 1.90 €/kg for the processes to be profitable. The price should be increased even more for the break-even point to come

earlier. The statistical analysis showed that the selling price will not likely increase to more than 1.90 €/kg. Thus, increasing the selling price to more than 1.90 €/kg seems unlikely. Because of this, the profitability analysis was conducted for both processes without the costs of deoxo process to see how excluding deoxo process would affect the profitability. In this case, the break-even point is at 9.5 years for the catalytic process (Figure 18) and at 8 years for the biological process (Figure 19).

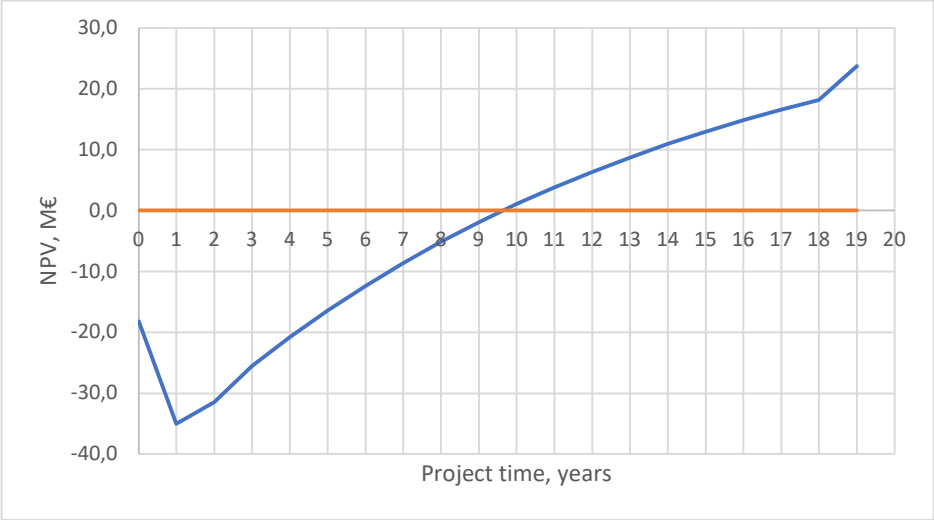

Figure 18 NPV analysis of catalytic methanation process without deoxo process. Hydrogen price was set to 2 €/kg and SNG price to 1.9 €/kg (135.71 €/MWh). The interest rate was 8 % and the plant capacity 40 MW. The break-even point is at 9.5 years.

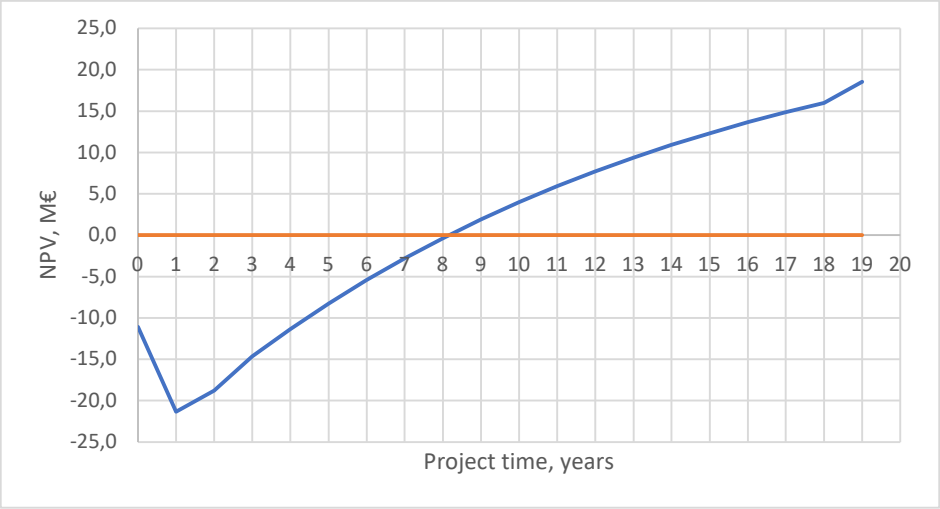

Figure 19 NPV analysis of biological methanation process without deoxo process. Hydrogen price was set to 2 €/kg and SNG price to 1.9 €/kg (135.71 €/MWh). The interest rate was 8 % and the plant capacity 40 MW. The break-even point is at 8 years.

9 Conclusions

The technology required to utilise SNG as transport fuel and the required infrastructure are already available. SNG also has various utilisation options besides as transport fuel, which means that the market for SNG is quite large. The other alternatives still require more research before they can be used efficiently as transport fuels as they are. Also, their infrastructure and technological readiness pose problems for a proximate future fuel transition. This is important because the need for fuel transition is quite urgent when considering climate change mitigation. Another factor in favour of methane is its low process complexity level. Because of this, methane production was chosen as the focus of this thesis.

Synthetic natural gas and biogas production processes based on P2X technology were studied. Catalytic and biological methanation processes were designed based on the literature research. Simulation models of both processes were created using Aspen Plus simulation software. Hydrogen purification with deoxo process was also studied and simulated.

The product purity targets were reached in catalytic methanation process. SNG still contains gas phase water, which means that the product should be dried before further processing, such as compression or liquefaction. The biological methanation process could not meet the purity targets. The produced biogas requires purification before it can be processed further and used as transport fuel.

The accuracy of the cost estimation results can be considered ± 30 %. The accuracy would increase with more detailed process design and detailed information on the equipment purchase costs and plant location. However, the results can be used for estimating the profitability of the processes and for comparing the process costs. The results showed that the total fixed and variable costs of catalytic methanation were slightly higher than those of biological methanation. On the other hand, also the revenue of the catalytic methanation process was higher. Hydrogen purification with deoxo process would increase the process costs considerably. Methanation archaea is intolerant of oxygen, so the purification step is likely required in biological methanation process. In catalytic methanation it might be possible to leave the purification step out of the process. In that case, the methanation catalyst

lifetime would decrease, but the total costs would still be lower than if the deoxo process was included. More research is required on the necessity of the deoxo process.

The profitability analysis and sensitivity analysis showed that the processes cannot be profitable with the reference hydrogen purchase price and product selling price. The hydrogen price should be lowered, or product price increased. For the product to be competitive, it would be preferable to try to lower the raw material costs. Statistical analysis showed that the sales price of the product will not increase over 1.90 €/kg (135.71 €/MWh) with 98 % confidence. Based on the net present value analysis results, both processes can become profitable when deoxo process is included within 20 years with product sales price of 1.90 €/kg (135.71 €/MWh) and hydrogen price of 2 €/kg. With these prices both processes are profitable within 10 years if deoxo process is not included. Sensitivity analysis showed that with the initial hydrogen price 4.42 €/kg, the selling price of SNG should be at least 1.80 €/kg (128.57 €/MWh) and biogas price 2.18 €/kg (155.71 €/MWh). The SNG price is within the limits of the analysed possible price increase, but the biogas price exceeds the limit. In conclusion, the profitability depends strongly on the selling price and raw material costs. SNG production will be profitable more likely than biogas production if the price of hydrogen is close to the initial reference price.

Biogas purification methods and the necessity of hydrogen purification with deoxo process are suggested for further research. Before detailed process design is possible, experimental results are required to see how they correlate to the simulation results to confirm the accuracy of the models. The models can be developed further by adding reaction kinetics to the models. This can also improve the accuracy of the models.

The results of this thesis can be considered as conceptual design and evaluation for both methanation processes.

References

Agneessens, L. M., Ottosen, L. D. M., Andersen, M., Berg Olesen, C., Feilberg, A. & Kofoed, M. V. W. 2018. Parameters affecting acetate concentrations during in-situ biological hydrogen methanation. Bioresource Technology. 258. Pp. 33-40.

Air Products. 2015. Safetygram 6. Web document. Accessed 13.3.2020. Available online: http://www.airproducts.com/~/media/Files/PDF/company/safetygram-6.pdf

Alitalo, A. & Aura, E. 2013. Means and methods for methane production. Maa- ja elintarviketalouden tutkimuskeskus. Patent. WO2013167806A1. 14 pp.

Alitalo, A., Niskanen, M. & Aura, E. 2015. Biocatalytic methanation of hydrogen and carbon dioxide in a fixed bed bioreactor. Bioresource technology. 196. Pp. 600-605.

Allebrod, F., Chatzichristodoulou, C. & Mogensen, M.B. 2014. Cobalt and molybdenum activated electrodes in foam based alkaline electrolysis cells at 150–250 °C and 40 bar. Journal of Power Sources. 255. Pp. 394-403.

Almansa, G. A., Rabou, L. P. L. M., van der Meijden, C. M. & van der Drift, A. 2015. ECN System for MEthanation (ESME). Conference paper. 23rd European Biomass Conference and Exhibition (EUBCE 2015). 1-4.6.2015. Vienna, Austria.

Angelidaki, I., Karakashev, D., Batstone, D. J., Plugge, C. M. & Stams, A. J. M. 2011. Biomethanation and its potential. Methods in enzymology. 494. Pp. 327-351.

Bartholomew, C., Weatherbee, G. & Jarvi, G. 1979. Sulfur poisoning of nickel methanation catalysts: I. in situ deactivation by H2S of nickel and nickel bimetallics. Journal of Catalysis. 60(2). Pp. 257-269.

Bartholomew, C. H. 2001. Mechanisms of catalyst deactivation. Applied Catalysis A: General. 212(1-2). Pp. 17-60.

Bassano, C., Deiana, P., Lietti, L. & Visconti, C. G. 2019. P2G movable modular plant operation on synthetic methane production from CO2 and hydrogen from renewables sources. Fuel. 253. Pp. 1071-1079.

Bellona. 2020. Capture of CO2. Web document. Accessed 5.3.2020. Available online: https://bellona.org/about-ccs/how-ccs/capture

Bernadet, L., Gousseau, G., Chatroux, A., Laurencin, J., Mauvy, F. & Reytier, M. 2015. Influence of pressure on solid oxide electrolysis cells investigated by experimental and modeling approach. International Journal of Hydrogen Energy. 40(38). Pp. 12918-12928.

Bertuccioli, L., Chan, A., Hart, D., Lehner, F., Madden, B. & Standen, E. 2014. Study on development of water electrolysis in the EU. Final report. E4tech Sàrl and Element Energy Ltd for the Fuel Cells and Hydrogen Joint Undertaking.

BioCat Project. 2020. Technology Components. Web document. Accessed 13.5.2020. Available online: http://biocat-project.com/about-the-project/technology-components/

Bromberg, L. & Cheng, W. K. 2010. Methanol as an alternative transportation fuel in the US: Options for sustainable and/or energy-secure transportation. Final report. Massachusetts Institute of Technology. Web document. Accessed 6.2.2020. Available online: https://afdc.energy.gov/files/pdfs/mit_methanol_white_paper.pdf

Brummelkamp, S. & Sardjoepersad, R. 2007. International trade to push up fuel oil consumption in shipping. CBS. 17.7.2007. Web document. Accessed 6.2.2020. Available online: https://www.cbs.nl/en-gb/news/2007/29/international-trade-to-push-up-fuel-oil-consumption-in-shipping

Buchholz, O., van Der Ham, A., Veneman, R., Brilman, D. & Kersten, S. 2014. Power-to-Gas: Storing Surplus Electrical Energy. A Design Study. Energy Procedia. 63(C). Pp. 7993-8009.

Business Insider. 2020. Nickel price. Web document. Accessed 23.8.2020. Available online: https://markets.businessinsider.com/commodities/nickel-price

Carbon Recycling International. 2020. Technology profile. Web document. Accessed 6.2.2020. Available online: https://static1.squarespace.com/static/56926c502399a318016c5ed8/t/5d6cf592a464e5000146f426/1567421842744/Carbon+Recycling+International+-+Technology+Profile+-+PDF+Document.pdf

Dautzenberg, F.M. 1989 Ten Guidelines for Catalyst Testing. In Characterization and Catalyst Development. ACS Symposium Series. American Chemical Society. Washington, DC, USA. Vol. 411. Pp. 99–119.

Duyar, M.S., Ramachandran, A., Wang, C. & Farrauto, R.J. 2015. Kinetics of CO2 methanation over Ru/γ-Al2O3 and implications for renewable energy storage applications. Journal of CO2 Utilization. 12. Pp. 27-33.

Electrochaea. 2020. Technology. Web document. Accessed 13.5.2020. Available online: http://www.electrochaea.com/technology/

Energiateollisuus. 2020. Tuulivoiman lisäämiseksi on potentiaalia. Web document. Accessed 24.4.2020. Available online: https://energia.fi/energiasta/energiantuotanto/sahkontuotanto/tuulivoima

Erekson, E. J., & Bartholomew, C. H. 1983. Sulfur poisoning of nickel methanation catalysts. Applied Catalysis. 5(3). Pp. 323–336.

European Commission. 2020a. 2020 Climate and energy package. Web document. Accessed 13.3.2020. Available online: https://ec.europa.eu/clima/policies/strategies/2020_en

European Commission. 2020b. Secure gas supplies. Published 31.7.2014. Updated 17.3.2020. Web document. Accessed 20.3.2020. Available online: https://ec.europa.eu/energy/topics/energy-security/secure-gas-supplies_en

Fasihi, M., Efimova, O. & Breyer, C. 2019. Techno-economic assessment of CO2 direct air capture plants. Journal of Cleaner Production. 224. Pp. 957-980.

Finnish Government. 2020. Carbon neutral Finland that protects biodiversity. Government programme. Web document. Accessed 3.9.2020. Available online: https://valtioneuvosto.fi/en/marin/government-programme/carbon-neutral-finland-that-protects-biodiversity

Finnish Wind Power Association. 2020. Web document. Accessed 24.4.2020. Available online: https://www.tuulivoimayhdistys.fi/en/wind-power-in-finland/wind-power-projects-in-finland/wind-power-projects-in-finland

Focus Economics. 2020. Alumina. Web document. Accessed 23.8.2020. Available online: https://www.focus-economics.com/commodities/base-metals/alumina

Frontera, P., Macario, A., Ferraro, M. & Antonucci, P. 2017. Supported catalysts for CO2 methanation: A review. Catalysts. 7(2):59. 28 pp.

Fu, J., Shu, J., Zhou, F., Liu, J., Xu, Z. & Zeng, D. 2017. Experimental investigation on the effects of compression ratio on in-cylinder combustion process and performance improvement of liquefied methane engine. Applied Thermal Engineering. 113. Pp. 1208-1218.

Gasum. 2020a. LNG is the cleanest alternative for marine fuel. Web document. Accessed 9.3.2020. Available online: https://www.gasum.com/en/for-businesses/sustainable-transport/LNG-for-marine/

Gasum. 2020b. Maa- ja biokaasun hinnat tankkausasemilla. Web document. Accessed 17.6.2020. Available online: https://www.gasum.com/yksityisille/tankkaa-kaasua/tankkaushinnat/

Gasum. 2020c. Maritime market update: Oil stocks continue building on low demand. 16.6.2020. Web document. Accessed 17.6.2020. Available online: https://www.gasum.com/en/About-gasum/for-the-media/News/2020/maritime-market-update-oil-stocks-continue-building-on-low-demand/

Ghaib, K. & Ben-Fares, F. 2018. Power-to-methane: A state-of-the-art review. Renewable and Sustainable Energy Reviews. 81. Pp. 433-446.

Giddey, S., Badwal, S.P.S. & Kulkarni, A. 2013. Review of electrochemical ammonia production technologies and materials. International Journal of Hydrogen Energy. 38. Pp. 14576-14594.

Gorre, J., Ortloff, F. & van Leeuwen, C. 2019. Production costs for synthetic methane in 2030 and 2050 of an optimized Power-to-Gas plant with intermediate hydrogen storage. Applied Energy. 253. P. 113594.

Grigoriev, S., Porembsky, V. & Fateev, V. 2006. Pure hydrogen production by PEM electrolysis for hydrogen energy. International Journal of Hydrogen Energy. 31(2). Pp. 171-175.

Grigoriev, S.A., Porembskiy, V.I., Korobtsev, S.V., Fateev, V.N., Auprêtre, F. & Millet, P. 2011. High-pressure PEM water electrolysis and corresponding safety issues. International Journal of Hydrogen Energy. 36(3). Pp. 2721-2728.

Guneratnam, A. J., Ahern, E., Fitzgerald, J. A., Jackson, S. A., Xia, A., Dobson, A. D. & Murphy, J. D. 2017. Study of the performance of a thermophilic biological methanation system. Bioresource Technology. 225. Pp. 308-315.

Gunnigle, E., Mccay, P., Fuszard, M., Botting, C. H., Abram, F. & O'Flaherty, V. 2013. A functional approach to uncover the low-temperature adaptation strategies of the archaeon Methanosarcina barkeri. Applied and environmental microbiology. 79(14). P. 4210.

Guo, X. & Li, Q. 2014. Fixed bed reactor design program development based on Java. Journal of Software. 9(5). Pp. 1263-1269.

Gutknecht, V., Snæbjörnsdóttir, S. Ó., Sigfússon, B., Aradóttir, E. S. & Charles, L. 2018. Creating a carbon dioxide removal solution by combining rapid mineralization of CO2 with direct air capture. Energy Procedia. 146. Pp. 129-134.

Götz, M., Koch, A. & Graf, F. 2014. State of the art and perspectives of CO 2 methanation process concepts for power-to-gas applications. International Gas Research Conference Proceedings, 1(January). Pp. 314-327.

Götz, M., Lefebvre, J., Mörs, F., Mcdaniel Koch, A., Graf, F., Bajohr, S., Reimert, R. & Kolb, T. 2016. Renewable Power-to-Gas: A technological and economic review. Renewable Energy. 85. Pp. 1371-1390.

Hagen, J. 2015. Industrial Catalysis: A Practical Approach, Third Edition. Wiley-VCH Verlag GmbH & Co. KGaA. Focus on Catalysts. 2015(7). Pp. 1-16.

Haldor Topsøe. 2020a. SNG Methanation. Web document. Accessed 13.5.2020. Available online: https://www.topsoe.com/processes/sng/methanation

Haldor Topsøe. 2020b. MCR-8. Web document. Accessed 13.5.2020. Available online: https://www.topsoe.com/products/catalysts/mcr-8?hsLang=en

Haldor Topsøe. 2020c. MCR-2. Web document. Accessed 13.5.2020. Available online: https://www.topsoe.com/products/catalysts/mcr-2?hsLang=en

Haldor Topsøe. 2020d. MCR-2X. Web document. Accessed 13.5.2020. Available online: https://www.topsoe.com/products/catalysts/mcr-2X

Haldor Topsøe. 2020e. PK-7R. Web document. Accessed 26.5.2020. Available online: https://www.topsoe.com/products/catalysts/pk-7r?hsLang=en

Harp, G., Tran, K-C, Sigurbjörnsson, Ó., Bergins, C., Buddenberg, T., Drach, I. & Koytsoumpa, E. I. 2015. Application of Power to Methanol Technology to Integrated Steelworks for

Profitability, Conversion Efficiency, and CO2 Reduction. Conference paper. 2nd European Steel Technology and Application Days, At Düsseldorf, Germany. 15.-19.7.2015.

Herbes, C. & Friege, C. (Eds.) 2017. Marketing Renewable Energy: Concepts, Business Models and Cases. Cham: Springer International Publishing.

Horn, J. & Zbacnik, R., 2015. Post-Combustion Carbon Capture Technologies. Chemical Engineering. 122(3). Pp. 70-73.

IEA. 2019. World Energy Outlook 2019. Web document. Accessed 7.2.2020. Available online: https://www.iea.org/reports/world-energy-outlook-2019

ICAP. 2019. Emissions Trading Worldwide: Status Report 2019. Berlin: ICAP

IPCC. 2005. Bert Metz, Ogunlade Davidson, Heleen de Coninck, Manuela Loos & Leo Meyer (Eds.) Cambridge University Press, UK. 431 pp.

Jansen, D., Gazzani, M., Manzolini, G., Dijk, E. v. & Carbo, M. 2015. Pre-combustion CO2 capture. International Journal of Greenhouse Gas Control. 40. Pp. 167-187.

Johnson Matthey. 2020. Methanation catalysts. Web document. Accessed 13.5.2020. Available online: https://matthey.com/en/products-and-services/chemical-processes/chemical-catalysts/methanation-catalysts

Kansha, Y., Ishizuka, M., Song, C. & Tsutsumi, A. 2015. Process intensification for dimethyl ether production by self-heat recuperation. Energy. 90. Pp. 122-127.

Kato, T., Kubota, M., Kobayashi, N. & Suzuoki, Y. 2005. Effective utilization of by-product oxygen from electrolysis hydrogen production. Energy. 30(14). Pp. 2580-2595.

Kayfeci, M., Keçebaş, A., & Bayat, M. 2019. Hydrogen production. Solar Hydrogen Production: Processes, Systems and Technologies. Pp. 45–83.

Kim, J., Lee, J., Yoo, C., Lee, K. & Lee, W. 2015. Low-cost and energy-efficient asymmetric nickel electrode for alkaline water electrolysis. International Journal of Hydrogen Energy. 40(34). Pp. 10720-10725.

Kim, S., Yu, J., Seo, D., Han, I. & Woo, S. 2012. Hydrogen production performance of 3-cell flat-tubular solid oxide electrolysis stack. International Journal of Hydrogen Energy. 37(1). Pp. 78-83.

Koytsoumpa, E. I. & Karellas, S. 2018. Equilibrium and kinetic aspects for catalytic methanation focusing on CO2 derived Substitute Natural Gas (SNG). Renewable and Sustainable Energy Reviews. 94. Pp. 536-550.

Laari, A. 2020. Personal communication. 17.8.2020. Docent, LUT University.

Lecker, B., Illi, L., Lemmer, A. & Oechsner, H. 2017. Biological hydrogen methanation – A review. Bioresource Technology. 245. Part A. Pp. 1220-1228.

Lehner, M., Tichler, R., Steinmüller, H. & Koppe, M. 2014. Power-to-Gas: Technology and Business Models. Springer. ISBN 978-3-319-03994-7.

LeRoy, R.L. 1983. Industrial water electrolysis: Present and future. International Journal of Hydrogen Energy. 8(6). Pp. 401-417.

Liang, C., Ye, Z., Dong, D., Zhang, S., Liu, Q., Chen, G., Li, C., Wang, Y. & Hu, X. 2019. Methanation of CO2: Impacts of modifying nickel catalysts with variable-valence additives on reaction mechanism. Fuel. 254. P. 115654.

LUT. 2018. Power-to-x (P2X) – Mitä se tarkoittaa ja miten se mullistaa energian- ja ruoantuotannon? LUT University. 14.11.2018. Web document. Accessed 7.2.2020. Available online: https://www.lut.fi/uutiset/-/asset_publisher/h33vOeufOQWn/content/power-to-x-p2x-%E2%80%93-mita-se-tarkoittaa-ja-miten-se-mullistaa-energian-ja-ruoantuotannon-

Mand, T., Kulkarni, G. & Metcalf, W. 2018. Genetic, biochemical, and molecular characterization of methanosarcina barkeri mutants lacking three distinct classes of hydrogenase. Journal of Bacteriology. 200(20).

Marocco, P., Morosanu, E.A., Giglio, E., Ferrero, D., Mebrahtu, C., Lanzini, A., Abate, S., Bensaid, S., Perathoner, S., Santarelli, M., Pirone, R. & Centi, G. 2018. CO2 methanation over Ni/Al hydrotalcite-derived catalyst: Experimental characterization and kinetic study. Fuel. 225. Pp. 230-242.

McPhy. 2020. New generation of pressurized alkaline electrolysis for large-scale platforms (multi-MW-GW). Web document. Accessed 11.5.2020. Available online: https://mcphy.com/en/our-products-and-solutions/electrolyzers/augmented-mclyzer/

Mets, Laurens. 2012. Methanothermobacter thermautotrophicus strain and variants thereof. Patent. WO/2012/094538.

Miguel, C., Mendes, A. & Madeira, L. 2018. Intrinsic kinetics of CO2 methanation over an industrial nickel-based catalyst. Journal of CO2 Utilization. 25. Pp. 128-136.

Money Metals Exchange. 2020. Palladium spot price history & current prices. Web document. Accessed 31.8.2020. Available online: https://www.moneymetals.com/precious-metals-charts/palladium-price

Nasri, Z. & Housam, B. 2009. Applications of the peng-robinson equation of state using MATLAB. Chemical Engineering Education. 43(2). Pp. 115-124.

Nechache, A., Cassir, M. & Ringuedé, A. 2014. Solid oxide electrolysis cell analysis by means of electrochemical impedance spectroscopy: A review. Journal of Power Sources. 258. Pp. 164-181.

Neste Jacobs & Gasum. 2015. Venäjältä Suomeen tuodun maakaasun toimitusketjun ympäristövaikutukset. Web document. Accessed 28.8.2020. Available online: https://www.gasum.com/globalassets/pdf-files/gasum-venajalta-suomeen-tuodun-maakaasun-toimitusketjun-ymparistovaikutukset-2015.pdf

Nevalainen, O. 2020. Personal communication. 14.8.2020. Product Manager, Gasum Oy.

Nieminen, H., Laari, A. & Koiranen, T. 2019. CO2 hydrogenation to methanol by a liquid-phase process with alcoholic solvents: A techno-economic analysis. Processes. 7(7). 24 pp.

Nikolic, V.M., Tasic, G.S., Maksic, A.D., Saponjic, D.P., Miulovic, S.M. & Marceta Kaninski, M.P. 2010. Raising efficiency of hydrogen generation from alkaline water electrolysis – energy saving.

Olajire, A. A. 2010. CO2 capture and separation technologies for end-of-pipe applications – A review. Energy. 35(6). Pp. 2610-2628.

Orange, R. 2019. Cruise ships herald the age of LNG fuel. In detail. Wärtsilä technical journal. (2)2019. Pp. 28-33.

Ortloff, F., Graf, F. & Kolb, T. 2014. Removal of Oxygen from Biogas via Catalytic Oxidation of Methane. Conference paper. IGRC 2014. Copenhagen.

Pandiyan, A., Uthayakumar, A., Subrayan, R., Cha, S.W. & Krishna Moorthy, S.B. 2019. Review of solid oxide electrolysis cells: a clean energy strategy for hydrogen generation. Nanomaterials and Energy. 8(1). Pp. 2-22.

Pearson, R.J., Eisaman, M., Turner, J., Edwards, P., Jiang, Z. Kuznetsov, V., Littau, K., Di Marco, L. & Taylor, S. R. G. 2012. Energy Storage via Carbon-Neutral Fuels Made from CO2, Water, and Renewable Energy. Proceedings of the IEEE. 100(2). Pp. 440-460.

Petipas, F. 2017. Thermal management of solid oxide electrolysis cell systems through air flow regulation. Chemical Engineering Transactions. 61. Pp. 1069-1074.

PwC. 2020. Megatrends: 5 global shifts changing the way we live and do business. Web document. Accessed 6.2.2020. Available online: https://www.pwc.co.uk/issues/megatrends.html

Peters, R., Baltruweit, M., Grube, T., Samsun, R. C. & Stolten, D. 2019. A techno economic analysis of the power to gas route. Journal of CO2 Utilization. 34. Pp. 616-634.

Ratchahat, S., Sudoh, M., Suzuki, Y., Kawasaki, W., Watanabe, R. & Fukuhara, C. 2018. Development of a powerful CO2 methanation process using a structured Ni/CeO2 catalyst. Journal of CO2 Utilization. 24. Pp. 210-219.

Romano, L. & Ruggeri, F. 2015. Methane from Syngas – Status of Amec Foster Wheeler VESTA Technology Development. Energy Procedia. 81. Pp. 249-254.

Rusmanis, D., O'Shea, R., Wall, D. M., & Murphy, J. D. 2019. Biological hydrogen methanation systems – an overview of design and efficiency. Bioengineered. 10(1). Pp. 604-634.

Rönsch, S., Schneider, J., Matthischke, S., Schlüter, M., Götz, M., Lefebvre, J., Prabhakaran, P. & Bajohr, S. 2016. Review on methanation – From fundamentals to current projects. Fuel. 166. Pp. 276-296.

Sakai, S., Imachi, H., Hanada, S., Ohashi, A., Harada, H., & Kamagata, Y. 2008. Methanocella paludicola gen. nov., sp. nov., a methane-producing archaeon, the first isolate of the lineage

'Rice Cluster I', and proposal of the new archaeal order Methanocellales ord. nov. International Journal of Systematic and Evolutionary Microbiology. 58. Pp. 929-936.

Sandeep, K., Bhattacharyya, R., Warghat, C., Bhanja, K. & Mohan, S. 2014. Experimental investigation on the kinetics of catalytic recombination of hydrogen with oxygen in air. International Journal of Hydrogen Energy. 39(31). Pp. 17906-17912.

Santos, D.M.F., Sequeira, C.A.C. & Figueiredo, J.L. 2013. Hydrogen Production by Alkaline Water Electrolysis. Quimica Nova. 36(8). Pp. 1176-1193.

Schmidt, O., Gambhir, A., Staffell, I., Hawkes, A., Nelson, J. & Few, S. 2017. Future cost and performance of water electrolysis: An expert elicitation study. International Journal of Hydrogen Energy. 42(52). Pp. 30470-30492.

Semelsberger, T. A., Borup, R. L. & Greene, H. L. 2006. Dimethyl ether (DME) as an alternative fuel. Journal of Power Sources. 156(2). Pp. 497-511.

Senthamaraikkannan, G., Chakrabarti, D. & Prasad, V. 2014. Chapter 13 - Transport Fuel – LNG and Methane. Future Energy. 2nd ed. Elsevier. Pp. 271-288.

Sinnott, R. & Towler, G. 2009. Chemical engineering design. 5th ed. Amsterdam: Elsevier. 1255 pp.

Smith, A. 31.1.2019. Solid Oxide Electrolysis Cells. Web document. Accessed 13.3.2020. Available online: https://www.energy.dtu.dk/english/Research/Electrolysis-Cells/Solid-Oxide-Electrolysis-Cells

Shah, M., Degenstein, N., Zanfir, M., Kumar, R., Bugayong, J. & Burgers, K. 2011. Near zero emissions oxy-combustion CO2 purification technology. Energy Procedia. 4. Pp. 988-995.

Shiva Kumar, S. and Himabindu, V. 2019. Hydrogen production by PEM water electrolysis – A review. Materials Science for Energy Technologies. 2(3). Pp. 442-454.

Solovjew-Wartiovaara, A. 2020. Tässä ne nyt ovat: 20-luvun tärkeimmät kehityskulut. Sitra. 31.12.2019. Web document. Accessed 6.2.2020. Available online: https://www.sitra.fi/uutiset/tassa-ne-nyt-ovat-20-luvun-tarkeimmat-kehityskulut/

St1. 2019. Q Power ja St1 pilotoivat synteettisen polttoaineen valmistusta biojalostamon hiilidioksidista. Web document. Accessed 14.5.2020. Available online: https://www.st1.fi/q-

power-ja-st1-pilotoivat-synteettisen-polttoaineen-valmistusta-biojalostamon-hiilidioksidista

Sveinbjörnsson, D. & Münster, E. 2017. WP1 Gas conditioning and grid operation. Upgrading of Biogas to Biomethane with the Addition of Hydrogen from Electrolysis. PlanEnergi. Web document. Accessed 13.5.2020. Available online: https://futuregas.dk/wp-content/uploads/2018/06/FutureGas-WP1-Deliverable-1.1.1.-Technologies-and-status-of-methanation-of-biogas-2017_Final.pdf

Thomsen, E.C., Coffey, G.W., Pederson, L.R. & Marina, O.A. 2009. Performance of lanthanum strontium manganite electrodes at high pressure. Journal of Power Sources. 191(2). Pp. 217-224.

Thyssenkrupp. 2020. Hydrogen from large-scale electrolysis. Web document. Accessed 11.5.2020. Available online: https://d13qmi8c46i38w.cloudfront.net/media/UCPthyssenkruppBAISUhdeChlorineEngineers/assets.files/products/water_electrolysis/thyssenkrupp_electrolytic_hydrogen_brochure.pdf

Topçuoglu, B. D. & Holden, J. F. 2019. Extremophiles: Hot Environments. Encyclopedia of Microbiology, 4th ed. Academic Press. ISBN 9780128117378. Pp. 263-269.

Türks, D. Mena, H. Armbruster, U. & Martin, A. 2017. Methanation of CO2 on Ni/Al2O3 in a Structured Fixed-Bed Reactor – A Scale-Up Study. Catalysts. 2017. 7(152). 15 pp.

Udagawa, J., Aguiar, P. & Brandon, N. 2007. Hydrogen production through steam electrolysis: Model-based steady state performance of a cathode-supported intermediate temperature solid oxide electrolysis cell. Journal of Power Sources. 166(1). Pp. 127-136.

UNFCC: United Nations Framework Convention on Climate Change. 2016. Report of the Conference of the Parties on its twenty-first session, held in Paris from 30 November to 13 December 2015. Part two: Action taken by the Conference of the Parties at its twenty-first session. FCCC/CP/2015/10/Add.1. 36 pp.

Ursua, A., Gandia, L.M. & Sanchis, P. 2012. Hydrogen Production from Water Electrolysis: Current Status and Future Trends. Proceedings of the IEEE. 100(2). Pp. 410-426.

U.S. Geological Survey. 2006. Peng-Robinson Equation of State. Web document. Accessed 17.7.2020. Available online: https://pubs.usgs.gov/of/2005/1451/equation.html

Verhelst, S., Turner, J. W. G., Sileghem, L. & Vancoillie, J. 2019. Methanol as a fuel for internal combustion engines. Progress in Energy and Combustion Science. 70. Pp. 43-88.

Voelklein, M., Rusmanis, D. & Murphy, J. 2019. Biological methanation: Strategies for in-situ and ex-situ upgrading in anaerobic digestion. Applied Energy. 235. Pp. 1061-1071.

Wang, L., Chen, M., Küngas, R., Lin, T., Diethelm, S., Maréchal, F. & Van herle, J. 2019. Power-to-fuels via solid-oxide electrolyzer: Operating window and techno-economics. Renewable and Sustainable Energy Reviews. 110. Pp. 174-187.

Weiss, M. & Schwinghammer, S. 2012. Lurgi advanced Mk Plus ™ coal gasifier technology applied for SNG production. Conference paper. Gasification Technologies Conference 28.-31.10.2012. Washington, DC. Web document. Accessed 13.5.2020. Available online: https://www.globalsyngas.org/uploads/eventLibrary/GTC-2012-5-3.pdf

Wilcox, J., 2012. Carbon Capture. New York, NY: Springer New York: Imprint: Springer.9781461422150.

Wilcox, J., Psarras, P. & Liguori, S. 2017. Assessment of reasonable opportunities for direct air capture. Environmental Research Letters. 12(6).

World Nuclear Association. 2018. Heat values of various fuels. Web document. Accessed 10.9.2020. Available online: https://www.world-nuclear.org/information-library/facts-and-figures/heat-values-of-various-fuels.aspx

Wärtsilä. 2020a. Wärtsilä methane number calculator. Web document. Accessed 2.7.2020. Available online: https://www.wartsila.com/marine/build/gas-solutions/methane-number-calculator

Wärtsilä. 2020b. Wärtsilä and Vantaa Energy Ltd. to cooperate on a carbon neutral synthetic biogas production project in Finland. Web document. Accessed 3.7.2020. Available online: https://www.wartsila.com/media/news/18-05-2020-wartsila-and-vantaa-energy-ltd-to-cooperate-on-a-carbon-neutral-synthetic-biogas-production-project-in-finland-2709538

Wärtsilä. 2019a. Wärtsilä 31 SG product guide. Web document. Accessed 10.3.2020. Available online: https://www.wartsila.com/docs/default-source/product-files/engines/wartsila-31sg-

product-guide.pdf?utm_source=engines&utm_medium=puregasengine&utm_term=w31sg&utm_content=product+guide&utm_campaign=msleadscoring

Wärtsilä 2019b. Wärtsilä 31 DF product guide. Web document. Accessed 10.3.2020. Available online: https://www.wartsila.com/docs/default-source/product-files/engines/df-engine/product-guide-o-e-w31df.pdf

Xu, J. & Froment, G. F. 1989. Methane steam reforming, methanation and water-gas shift: I. Intrinsic kinetics. AIChE Journal. 35(1). Pp. 88-96.

Yaripour, F., Mollavali, A., Jam, S. & Atashi, H. 2009. Catalytic Dehydration of Methanol to Dimethyl Ether Catalyzed by Aluminum Phosphate Catalysts. Energy & Fuels. 23(3-4). Pp. 1896-1900.

Zeng, K. & Zhang, D. 2010. Recent progress in alkaline water electrolysis for hydrogen production and applications. Progress in Energy and Combustion Science. 36(3). Pp. 307-326.

Appendix 1: Stream tables

Table A-I Stream table for catalytic methanation. Streams CO2 to S11. Table continues on the next page.

Stream Name	Units	CO2	FEED	H2	S3	S4	S6	S7	S8	S9	S10	S11
Description												
From			HX1		MIX1	COMPR1	REACTOR1	HX1	COOLER 1	FLASH1	FLASH1	HX2
To		MIX1	REACTOR1	MIX1	COMPR1	HX1	HX1	COOLER1	FLASH1		HX2	REACTOR2
Stream Class		CONVEN	CONVEN	CONVEN	CONVEN	CONVEN	CONVEN	CONVEN	CONVE N	CONVEN	CONVEN	CONVEN
Phase		Vapor Phase	Vapor Phase	Vapor Phase	Vapor Phase	Vapor Phase	Vapor Phase	Vapor Phase		Liquid Phase	Vapor Phase	Vapor Phase
Temperature	C	25	250	25	22.2772373	150	350	225.2828	180	180	180	250
Pressure	bar	10	30	1	1	30	30	30	30	30	30	30
Molar Vapor Fraction		1	1	1	1	1	1	1	0.560798	0	1	1
Molar Liquid Fraction		0	0	0	0	0	0	0	0.439202	1	0	0
Molar Solid Fraction		0	0	0	0	0	0	0	0	0	0	0
Mass Vapor Fraction		1	1	1	1	1	1	1	0.54039	0	1	1
Mass Liquid Fraction		0	0	0	0	0	0	0	0.45961	1	0	0
Mass Solid Fraction		0	0	0	0	0	0	0	0	0	0	0
Mole Flows	kmol/h	82	406.876	324.876	406.876	406.876	248.09	248.09	248.09	108.96	139.13	139.13
METHANE	kmol/h	0	0	0	0	0	79.39	79.39	79.39	0.06	79.33	79.33
WATER	kmol/h	0	0.451786	0.45178588	0.45178588	0.451786	159.24	159.24	159.24	108.89	50.34	50.34
CO2	kmol/h	82	82	0	82	82	2.61	2.61	2.61	0.00	2.60	2.60
H2	kmol/h	0	324.4242	324.424214	324.424214	324.4242	6.85	6.85	6.85	0.00	6.85	6.85
O2	kmol/h	0	0	0	0	0	7.5E-33	7.5E-33	7.5E-33	0	0	0

Table A-I Stream table for catalytic methanation. Streams CO2 to S11. (continued)

Stream Name	Units	CO2	FEED	H2	S3	S4	S6	S7	S8	S9	S10	S11
Mole Fractions												
METHANE		0	0	0	0	0	0.320	0.320	0.320	0.001	0.570	0.570
WATER		0	0.00111	0.00139064	0.00111038	0.00111	0.642	0.642	0.642	0.999	0.362	0.362
CO2		1	0.201536	0	0.2015356	0.201536	0.011	0.011	0.011	0.000	0.019	0.019
H2		0	0.797354	0.99860936	0.79735402	0.797354	0.028	0.028	0.028	0.000	0.049	0.049
O2		0	0	0	0	0	3.02E-35	3.02E-35	3.02E-35	0	0	0
Mass Flows	kg/h	3608.804	4270.943	662.139334	4270.94293	4270.943	4270.94	4270.94	4270.94	1962.97	2307.97	2307.97
METHANE	kg/h	0	0	0	0	0	1273.67	1273.67	1273.67	0.98	1272.70	1272.70
WATER	kg/h	0	8.139049	8.13904905	8.13904905	8.139049	2868.69	2868.69	2868.69	1961.77	906.92	906.92
CO2	kg/h	3608.804	3608.804	0	3608.8036	3608.804	114.76	114.76	114.76	0.22	114.54	114.54
H2	kg/h	0	654.0003	654.000285	654.000285	654.0003	13.82	13.82	13.82	0.00	13.82	13.82
O2	kg/h	0	0	0	0	0	2.4E-31	2.4E-31	2.4E-31	0	0	0
Mass Fractions												
METHANE		0	0	0	0	0	0.298	0.298	0.298	0.0005	0.551	0.551
WATER		0	0.001906	0.01229205	0.00190568	0.001906	0.672	0.672	0.672	0.999	0.393	0.393
CO2		1	0.844966	0	0.84496648	0.844966	0.027	0.027	0.027	0.0001	0.050	0.050
H2		0	0.153128	0.98770795	0.15312784	0.153128	0.003	0.003	0.003	1.35E-06	0.006	0.006
O2		0	0	0	0	0	5.62E-35	5.62E-35	5.62E-35	0	0	0
Volume Flow	l/min	3197.25	9924.57	134287.74	166578.65	8026.03	6926.66	5334.47	2818.20	39.57	2778.63	3272.01

Table A-II Stream table for catalytic methanation. Streams S12 to S22. Table continues on the next page.

Stream Name	Units	S12	S13	S14	S15	S16	S17	S18	S19	S20	S21	S22
Description												
From		REACTOR 2	HX2	COOLER 2	FLASH2	FLASH2	HX3	REACTOR 3	HX3	COOLER 3	FLASH3	FLASH3
To		HX2	COOLER2	FLASH2		HX3	REACTOR 3	HX3	COOLER3	FLASH3		HX4
Stream Class		CONVEN	CONVEN	CONVEN	CONVEN	CONVEN	CONVEN	CONVEN	CONVEN	CONVEN	CONVEN	CONVEN
Phase		Vapor Phase	Vapor Phase		Liquid Phase	Vapor Phase	Vapor Phase	Vapor Phase	Vapor Phase		Liquid Phase	Vapor Phase
Temperature	C	350	284.5123	180	180	180	250	350	284.9403	180	180	180
Pressure	bar	30	30	30	30	30	30	30	30	30	30	30
Molar Vapor Fraction		1	1	0.973214	0	1	1	1	1	0.998909	0	1
Molar Liquid Fraction		0	0	0.026786	1	0	0	0	0	0.001091	1	0
Molar Solid Fraction		0	0	0	0	0	0	0	0	0	0	0
Mass Vapor Fraction		1	1	0.971282	0	1	1	1	1	0.998829	0	1
Mass Liquid Fraction		0	0	0.028718	1	0	0	0	0	0.001171	1	0
Mass Solid Fraction		0	0	0	0	0	0	0	0	0	0	0
Mole Flows	kmol/h	137.36	137.36	137.36	3.68	133.68	133.68	133.61	133.61	133.61	0.15	133.46
METHANE	kmol/h	80.22	80.22	80.22	0.00	80.22	80.22	80.25	80.25	80.25	0.00	80.25
WATER	kmol/h	52.11	52.11	52.11	3.68	48.44	48.44	48.51	48.51	48.51	0.15	48.36
CO2	kmol/h	1.72	1.72	1.72	0.00	1.72	1.72	1.68	1.68	1.68	0.00	1.68

Table A-II Stream table for catalytic methanation. Streams S12 to S22. (continued)

Stream Name	Units	S12	S13	S14	S15	S16	S17	S18	S19	S20	S21	S22
H2	kmol/h	3.31	3.31	3.31	0.00	3.31	3.31	3.17	3.17	3.17	0.00	3.17
O2	kmol/h	2.01E-33	2.01E-33	2.01E-33	0	0	0	1.79E-33	1.79E-33	1.79E-33	0	0
Mole Fractions												
METHANE		0.584	0.584	0.584	0.001	0.600	0.600	0.601	0.601	0.601	0.001	0.601
WATER		0.379	0.379	0.379	0.999	0.362	0.362	0.363	0.363	0.363	0.999	0.362
CO2		0.012	0.012	0.012	0.000	0.013	0.013	0.013	0.013	0.013	0.000	0.013
H2		0.024	0.024	0.024	0.000	0.025	0.025	0.024	0.024	0.024	0.000	0.024
O2		1.46E-35	1.46E-35	1.46E-35	0	0	0	1.34E-35	1.34E-35	1.34E-35	0	0
Mass Flows	kg/h	2307.97	2307.97	2307.97	66.28	2241.69	2241.69	2241.69	2241.69	2241.69	2.63	2239.07
METHANE	kg/h	1286.91	1286.91	1286.91	0.03	1286.88	1286.88	1287.44	1287.44	1287.44	0.00	1287.44
WATER	kg/h	938.84	938.84	938.84	66.24	872.60	872.60	873.86	873.86	873.86	2.62	871.24
CO2	kg/h	75.55	75.55	75.55	0.01	75.55	75.55	74.00	74.00	74.00	0.00	74.00
H2	kg/h	6.67	6.67	6.67	0.00	6.67	6.67	6.39	6.39	6.39	0.00	6.39
O2	kg/h	6.43E-32	6.43E-32	6.43E-32	0	0	0	5.72E-32	5.72E-32	5.72E-32	0	0
Mass Fractions												
METHANE		0.558	0.558	0.558	0.0005	0.574	0.574	0.574	0.574	0.574	0.000525	0.575
WATER		0.407	0.407	0.407	0.999	0.389	0.389	0.390	0.390	0.390	0.999	0.389
CO2		0.033	0.033	0.033	7.63E-05	0.034	0.034	0.033	0.033	0.033	7.49E-05	0.033
H2		0.003	0.003	0.003	6.82E-07	0.003	0.003	0.003	0.003	0.003	6.54E-07	0.003
O2		2.79E-35	2.79E-35	2.79E-35	0	0	0	2.55E-35	2.55E-35	2.55E-35	0	0
Volume Flow	l/min	3898.65	3457.25	2665.89	1.34	2664.56	3139.86	3795.62	3369.82	2660.09	0.05	2660.04

Table A-III Stream table for catalytic methanation. Streams S22 to H2O. Table continues on the next page.

Stream Name	Units	S22	S23	S24	S25	S26	SNG	H2O
Description								
From		FLASH3	HX4	REACTOR4	HX4	COOLER4	FLASH4	FLASH4
To		HX4	REACTOR4	HX4	COOLER4	FLASH4		
Stream Class		CONVEN	CONVEN	CONVEN	CONVEN	CONVEN	CONVEN	CONVEN
Phase		Vapor Phase	Vapor Phase	Vapor Phase	Vapor Phase		Vapor Phase	Liquid Phase
Temperature	C	180	250	340	274.4365	140	140	140
Pressure	bar	30	30	30	30	30	30	30
Molar Vapor Fraction		1	1	1	1	0.73377	1	0
Molar Liquid Fraction		0	0	0	0	0.26623	0	1
Molar Solid Fraction		0	0	0	0	0	0	0
Mass Vapor Fraction		1	1	1	1	0.714532	1	0
Mass Liquid Fraction		0	0	0	0	0.285468	0	1
Mass Solid Fraction		0	0	0	0	0	0	0
Mole Flows	kmol/h	133.46	133.46	133.27	133.27	133.27	97.79	35.48
METHANE	kmol/h	80.25	80.25	80.35	80.35	80.35	80.33	0.01
WATER	kmol/h	48.36	48.36	48.55	48.55	48.55	13.09	35.47
CO2	kmol/h	1.68	1.68	1.59	1.59	1.59	1.58	0.00
H2	kmol/h	3.17	3.17	2.78	2.78	2.78	2.78	0.00
O2	kmol/h	0	0	5.1E-34	5.1E-34	5.1E-34	0	0
Mole Fractions								
METHANE		0.601	0.601	0.603	0.603	0.603	0.821	0.000
WATER		0.362	0.362	0.364	0.364	0.364	0.134	1.000
CO2		0.013	0.013	0.012	0.012	0.012	0.016	0.000

Table A-III Stream table for catalytic methanation. Streams S22 to H2O. (continued)

Stream Name	Units	S22	S23	S24	S25	S26	SNG	H2O
H2		0.024	0.024	0.021	0.021	0.021	0.028	0.000
O2		0	0	3.83E-36	3.83E-36	3.83E-36	0	0
Mass Flows	kg/h	2239.07	2239.07	2239.07	2239.07	2239.07	1599.89	639.18
METHANE	kg/h	1287.44	1287.44	1288.98	1288.98	1288.98	1288.76	0.22
WATER	kg/h	871.24	871.24	874.71	874.71	874.71	235.79	638.92
CO2	kg/h	74.00	74.00	69.76	69.76	69.76	69.72	0.04
H2	kg/h	6.39	6.39	5.61	5.61	5.61	5.61	0.00
O2		0	0	1.63E-32	1.63E-32	1.63E-32	0	0
Mass Fractions								
METHANE		0.575	0.575	0.576	0.576	0.576	0.806	0.000343
WATER		0.389	0.389	0.391	0.391	0.391	0.147	0.9996
CO2		0.033	0.033	0.031	0.031	0.031	0.044	6.1E-05
H2		0.003	0.003	0.003	0.003	0.003	0.004	3.49E-07
O2		0	0	7.29E-36	7.29E-36	7.29E-36	0	0
Volume Flow	l/min	2660.04	3134.62	3720.55	3291.27	1820.45	1808.26	12.19

Table A-IV Stream table for biological methanation. The table continues on the next page.

	Units	CO2	H2	S3	S4	S5	S6	S7	S8	WATER	BIOGAS
Description											
From				MIX	COMPR1	COOLER 1	COMPR2	COOLER 2	REACTOR	FLASH	FLASH
To		MIX	MIX	COMPR1	COOLER1	COMPR2	COOLER2	REACTOR	FLASH		
Stream Class		CONVEN	CONVEN	CONVEN	CONVEN	CONVEN	CONVEN	CONVEN	CONVEN	CONVEN	CONVEN
Phase		Vapor Phase	Vapor Phase	Vapor Phase	Vapor Phase	Vapor Phase	Vapor Phase	Vapor Phase		Liquid Phase	Vapor Phase
Temperature	C	25	25	25.00000048	165.4366769	50	140.6009597	60	60	60	60
Pressure	bar	10	1	1	3	3	6	6	6	6	6
Molar Vapor Fraction		1	1	1	1	1	1	1	0.352	0	1
Molar Liquid Fraction		0	0	0	0	0	0	0	0.648	1	0
Molar Solid Fraction		0	0	0	0	0	0	0	0	0	0
Mass Vapor Fraction		1	1	1	1	1	1	1	0.322	0	1
Mass Liquid Fraction		0	0	0	0	0	0	0	0.678	1	0
Mass Solid Fraction		0	0	0	0	0	0	0	0	0	0
Mole Flows	kmol/h	81	324	405	405	405	405	405	245.11	158.73	86.37
H2O	kmol/h	0	0	0	0	0	0	0	159.89	157.05	2.84
CH4	kmol/h	0	0	0	0	0	0	0	79.95	1.60	78.35
H2	kmol/h	0	324	324	324	324	324	324	4.21	0.003	4.21

Table A-IV Stream table for biological methanation. (continued)

	Units	CO2	H2	S3	S4	S5	S6	S7	S8	WATER	BIOGAS
O2	kmol/h	0	0	0	0	0	0	0	0	0	0
CO2	kmol/h	81	0	81	81	81	81	81	1.05	0.08	0.97
Mole Fractions											
H2O		0	0	0	0	0	0	0	0.652	0.989	0.033
CH4		0	0	0	0	0	0	0	0.326	0.010	0.907
H2		0	1	0.8	0.8	0.8	0.8	0.8	0.017	0.00002	0.049
O2		0	0	0	0	0	0	0	0	0	0
CO2		1	0	0.2	0.2	0.2	0.2	0.2	0.004	0.001	0.011
Mass Flows	kg/h	3564.79	653.15	4217.94	4217.94	4217.94	4217.94	4217.94	4217.94	2858.51	1359.43
H2O	kg/h	0	0	0	0	0	0	0	2880.54	2829.37	51.17
CH4	kg/h	0	0	0	0	0	0	0	1282.57	25.60	1256.98
H2	kg/h	0	653.15	653.15	653.15	653.15	653.15	653.15	8.49	0.01	8.48
O2	kg/h	0	0	0	0	0	0	0	0	0	0
CO2	kg/h	3564.79	0	3564.79	3564.79	3564.79	3564.79	3564.79	46.34	3.54	42.80
Mass Fractions											
H2O		0	0	0	0	0	0	0	0.683	0.990	0.038
CH4		0	0	0	0	0	0	0	0.304	0.009	0.925
H2		0	1	0.155	0.155	0.155	0.155	0.155	0.002	0.000002	0.006
O2		0	0	0	0	0	0	0	0	0	0
CO2		1	0	0.845	0.845	0.845	0.845	0.845	0.011	0.001	0.031
Volume Flow	l/min	3346.54	133861.54	167326.93	82047.47	60452.45	38700.70	31161.59	6696.10	50.37	6645.73

Appendix 2: Economic analysis templates

Figure A-1 Economic analysis of catalytic methanation when deoxo process is included, with hydrogen price of 4.42 €/kg and SNG selling price of 1.45 €/kg.

ECONOMIC ANALYSIS

Project Name
Project Number
Sheet 1

REV	DATE	BY	APVD	REV	DATE	BY	APVD

Owner's Name
Plant Location Finland
Case Description Methanation plant

Capital Cost Basis Year 2006
Units ○ English ◉ Metric
On Stream 8 000 hr/yr 333,33 day/yr

REVENUES AND PRODUCTION COSTS

	M€/yr
Main product (methane) revenue	18,5
Raw materials cost	30,7
Utilities cost	1,9
Consumables cost	0,00
VCOP	32,6
Salary and overheads	0,9
Maintenance	0,0
Interest	0,08
FCOP	1,0

CAPITAL COSTS

	M€
ISBL Capital Cost	17,8
OSBL Capital Cost	7,1
Engineering Costs	7,5
Contingency	5,0
Total Fixed Capital Cost	37,4
Working Capital	-8,544 year 4

Use suitable fractions/expressions

CONSTRUCTION SCHEDULE

Year	% FC	% WC	% FCOP	% VCOP
1	50,00 %	50,00 %		
2	50,00 %	50,00 %		
3			50,00 %	50,00 %
4			100,00 %	100,00 %
5			100,00 %	100,00 %
6			100,00 %	100,00 %
7+			100,00 %	100,00 %

Select percentages according to scheduling of construction, start-up and full operation

ECONOMIC ASSUMPTIONS

Cost of equity 8 %
Cost of debt 8 %
Cost of capital 8 %
Debt ratio
Tax rate 24 %
Depreciation method
Depreciation period 20 years

CASH FLOW ANALYSIS

All figures in €MM unless indicated

Project year	Cap Ex	Revenue	CCOP	Gr. Profit	Deprcn	Taxbl Inc	Tax Paid	Cash Flow	PV of CF	NPV
1	14,4	0,0	0,0	0,0	0,0	0,0	0,0	-14,4	-13,4	-13,4
2	14,4	0,0	0,0	0,0	0,0	0,0	0,0	-14,4	-12,4	-25,7
3	0,0	9,3	16,8	-7,5	0,0	-7,5	0,0	-7,5	-6,0	-31,7
4	0,0	18,5	33,6	-15,1	0,0	-15,1	-1,8	-13,3	-9,7	-41,5
5	0,0	18,5	33,6	-15,1	0,0	-15,1	-3,6	-11,5	-7,8	-49,3
6	0,0	18,5	33,6	-15,1	0,0	-15,1	-3,6	-11,5	-7,2	-56,5
7	0,0	18,5	33,6	-15,1	0,0	-15,1	-3,6	-11,5	-6,7	-63,2
8	0,0	18,5	33,6	-15,1	0,0	-15,1	-3,6	-11,5	-6,2	-69,3
9	0,0	18,5	33,6	-15,1	0,0	-15,1	-3,6	-11,5	-5,7	-75,1
10	0,0	18,5	33,6	-15,1	0,0	-15,1	-3,6	-11,5	-5,3	-80,4
11	0,0	18,5	33,6	-15,1	0,0	-15,1	-3,6	-11,5	-4,9	-85,3
12	0,0	18,5	33,6	-15,1	0,0	-15,1	-3,6	-11,5	-4,5	-89,8
13	0,0	18,5	33,6	-15,1	0,0	-15,1	-3,6	-11,5	-4,2	-94,0
14	0,0	18,5	33,6	-15,1	0,0	-15,1	-3,6	-11,5	-3,9	-97,9
15	0,0	18,5	33,6	-15,1	0,0	-15,1	-3,6	-11,5	-3,6	-101,6
16	0,0	18,5	33,6	-15,1	0,0	-15,1	-3,6	-11,5	-3,3	-104,9
17	0,0	18,5	33,6	-15,1	0,0	-15,1	-3,6	-11,5	-3,1	-108,0
18	0,0	18,5	33,6	-15,1	0,0	-15,1	-3,6	-11,5	-2,9	-110,9
19	0,0	18,5	33,6	-15,1	0,0	-15,1	-3,6	-11,5	-2,7	-113,5
20	8,5	18,5	33,6	-15,1	0,0	-15,1	-3,6	-20,0	-4,3	-117,8

ECONOMIC ANALYSIS

Average cash flow -12,5 €MM/yr
Simple pay-back period -2,3082797 yrs
Return on investment (10 yrs) -39,15 %
Return on investment (15 yrs) -43,51 %

NPV			IRR	
10 years	-80,4	€MM	10 years	#LUKU!
15 years	-101,6	€MM	15 years	#LUKU!
20 years	-117,8	€MM	20 years	#LUKU!
NPV to yr 1	-13,4	€MM		

NOTES

Figure A-2 Economic analysis of catalytic methanation when deoxo process is included, with hydrogen price of 2 €/kg and SNG selling price of 1.90 €/kg.

ECONOMIC ANALYSIS

Project Name
Project Number
Sheet 1

REV	DATE	BY	APVD	REV	DATE	BY	APVD

Owner's Name
Plant Location: Finland
Case Description: Methanation plant

Capital Cost Basis Year: 2006
Units: ○ English ◉ Metric
On Stream: 8 000 hr/yr = 333,33 day/yr

REVENUES AND PRODUCTION COSTS

	M€/yr
Main product (methane) revenue	24,32
Raw materials cost	12,2
Utilities cost	1,9
Consumables cost	0,00109
VCOP	14,2
Salary and overheads	0,9
Maintenance	0,0
Interest	0,08
FCOP	1,0

CAPITAL COSTS

	M€
ISBL Capital Cost	17,8
OSBL Capital Cost	7,1
Engineering Costs	7,5
Contingency	5,0
Total Fixed Capital Cost	37,4
Working Capital	19,040 year 4

Use suitable fractions/expressions

CONSTRUCTION SCHEDULE

Year	% FC	% WC	% FCOP	% VCOP
1	50,00 %	50,00 %		
2	50,00 %	50,00 %		
3			50,00 %	50,00 %
4			100,00 %	100,00 %
5			100,00 %	100,00 %
6			100,00 %	100,00 %
7+			100,00 %	100,00 %

Select percentages according to scheduling of construction, start-up and full operation

ECONOMIC ASSUMPTIONS

Cost of equity	8 %	Debt ratio		Tax rate	24 %
Cost of debt	8 %			Depreciation method	
Cost of capital	8 %			Depreciation period	20 years

CASH FLOW ANALYSIS

All figures in €MM unless indicated

Project year	Cap Ex	Revenue	CCOP	Gr. Profit	Deprcn	Taxbl Inc	Tax Paid	Cash Flow	PV of CF	NPV
1	28,2	0,0	0,0	0,0	0,0	0,0	0,0	-28,2	-26,1	-26,1
2	28,2	0,0	0,0	0,0	0,0	0,0	0,0	-28,2	-24,2	-50,3
3	0,0	12,2	7,6	4,6	0,0	4,6	0,0	4,6	3,6	-46,7
4	0,0	24,3	15,2	9,1	0,0	9,1	1,1	8,0	5,9	-40,8
5	0,0	24,3	15,2	9,1	0,0	9,1	2,2	6,9	4,7	-36,1
6	0,0	24,3	15,2	9,1	0,0	9,1	2,2	6,9	4,4	-31,7
7	0,0	24,3	15,2	9,1	0,0	9,1	2,2	6,9	4,1	-27,6
8	0,0	24,3	15,2	9,1	0,0	9,1	2,2	6,9	3,8	-23,9
9	0,0	24,3	15,2	9,1	0,0	9,1	2,2	6,9	3,5	-20,4
10	0,0	24,3	15,2	9,1	0,0	9,1	2,2	6,9	3,2	-17,2
11	0,0	24,3	15,2	9,1	0,0	9,1	2,2	6,9	3,0	-14,2
12	0,0	24,3	15,2	9,1	0,0	9,1	2,2	6,9	2,8	-11,5
13	0,0	24,3	15,2	9,1	0,0	9,1	2,2	6,9	2,6	-8,9
14	0,0	24,3	15,2	9,1	0,0	9,1	2,2	6,9	2,4	-6,5
15	0,0	24,3	15,2	9,1	0,0	9,1	2,2	6,9	2,2	-4,3
16	0,0	24,3	15,2	9,1	0,0	9,1	2,2	6,9	2,0	-2,3
17	0,0	24,3	15,2	9,1	0,0	9,1	2,2	6,9	1,9	-0,4
18	0,0	24,3	15,2	9,1	0,0	9,1	2,2	6,9	1,7	1,3
19	0,0	24,3	15,2	9,1	0,0	9,1	2,2	6,9	1,6	2,9
20	-19,0	24,3	15,2	9,1	0,0	9,1	2,2	26,0	5,6	8,5

ECONOMIC ANALYSIS

Average cash flow	8,4 €MM/yr	NPV	10 years	-17,2 €MM	IRR	10 years	-0,8%
Simple pay-back period	6,72098429 yrs		15 years	-4,3 €MM		15 years	6,5%
Return on investment (10 yrs)	12,14 %		20 years	8,5 €MM		20 years	10,0%
Return on investment (15 yrs)	13,49 %	NPV to yr	1	-26,1 €MM			

NOTES

Figure A-3 Economic analysis of catalytic methanation without deoxo process, with hydrogen price of 2 €/kg and SNG selling price of 1.90 €/kg.

Project Name
Project Number
Sheet 1

REV	DATE	BY	APVD	REV	DATE	BY	APVD

ECONOMIC ANALYSIS

Owner's Name
Plant Location: Finland
Case Description: Methanation plant

Capital Cost Basis Year: 2006
Units: ○ English ◉ Metric
On Stream: 8 000 hr/yr 333,33 day/yr

REVENUES AND PRODUCTION COSTS

	M€/yr
Main product (methane) revenue	24,32
Raw materials cost	12,2
Utilities cost	1,9
Consumables cost	0,00109
VCOP	14,2
Salary and overheads	0,9
Maintenance	0,0
Interest	0,08
FCOP	1,0

CAPITAL COSTS

	M€
ISBL Capital Cost	9,7
OSBL Capital Cost	3,9
Engineering Costs	4,1
Contingency	2,7
Total Fixed Capital Cost	20,3
Working Capital	19,040 year 4

Use suitable fractions/expressions

CONSTRUCTION SCHEDULE

Year	% FC	% WC	% FCOP	% VCOP
1	50,00 %	50,00 %		
2	50,00 %	50,00 %		
3			50,00 %	50,00 %
4			100,00 %	100,00 %
5			100,00 %	100,00 %
6			100,00 %	100,00 %
7+			100,00 %	100,00 %

Select percentages according to scheduling of construction, start-up and full operation

ECONOMIC ASSUMPTIONS

Cost of equity	8 %	Debt ratio		Tax rate	24 %
Cost of debt	8 %			Depreciation method	
Cost of capital	8 %			Depreciation period	20 years

CASH FLOW ANALYSIS

All figures in €MM unless indicated

Project year	Cap Ex	Revenue	CCOP	Gr. Profit	Deprcn	Taxbl Inc	Tax Paid	Cash Flow	PV of CF	NPV
1	19,7	0,0	0,0	0,0	0,0	0,0	0,0	-19,7	-18,2	-18,2
2	19,7	0,0	0,0	0,0	0,0	0,0	0,0	-19,7	-16,9	-35,1
3	0,0	12,2	7,6	4,6	0,0	4,6	0,0	4,6	3,6	-31,4
4	0,0	24,3	15,2	9,1	0,0	9,1	1,1	8,0	5,9	-25,5
5	0,0	24,3	15,2	9,1	0,0	9,1	2,2	6,9	4,7	-20,8
6	0,0	24,3	15,2	9,1	0,0	9,1	2,2	6,9	4,4	-16,4
7	0,0	24,3	15,2	9,1	0,0	9,1	2,2	6,9	4,1	-12,4
8	0,0	24,3	15,2	9,1	0,0	9,1	2,2	6,9	3,8	-8,6
9	0,0	24,3	15,2	9,1	0,0	9,1	2,2	6,9	3,5	-5,1
10	0,0	24,3	15,2	9,1	0,0	9,1	2,2	6,9	3,2	-1,9
11	0,0	24,3	15,2	9,1	0,0	9,1	2,2	6,9	3,0	1,1
12	0,0	24,3	15,2	9,1	0,0	9,1	2,2	6,9	2,8	3,8
13	0,0	24,3	15,2	9,1	0,0	9,1	2,2	6,9	2,6	6,4
14	0,0	24,3	15,2	9,1	0,0	9,1	2,2	6,9	2,4	8,7
15	0,0	24,3	15,2	9,1	0,0	9,1	2,2	6,9	2,2	10,9
16	0,0	24,3	15,2	9,1	0,0	9,1	2,2	6,9	2,0	12,9
17	0,0	24,3	15,2	9,1	0,0	9,1	2,2	6,9	1,9	14,8
18	0,0	24,3	15,2	9,1	0,0	9,1	2,2	6,9	1,7	16,6
19	0,0	24,3	15,2	9,1	0,0	9,1	2,2	6,9	1,6	18,2
20	-19,0	24,3	15,2	9,1	0,0	9,1	2,2	26,0	5,6	23,7

ECONOMIC ANALYSIS

Average cash flow	8,4 €MM/yr	NPV	10 years	-1,9 €MM	IRR	10 years	6,7%
Simple pay-back period	4,68194699 yrs		15 years	10,9 €MM		15 years	12,7%
Return on investment (10 yrs)	17,43 %		20 years	23,7 €MM		20 years	15,2%
Return on investment (15 yrs)	19,37 %	NPV to yr	1	-18,2 €MM			

NOTES

Figure A-4 Economic analysis of biological methanation when deoxo process is included, with hydrogen price of 4.42 €/kg and biogas selling price of 1.45 €/kg.

ECONOMIC ANALYSIS

Project Name
Project Number
Sheet 1

REV	DATE	BY	APVD	REV	DATE	BY	APVD

Owner's Name
Plant Location: Finland
Case Description: Methanation plant

Capital Cost Basis Year: 2006
Units: ○ English ◉ Metric
On Stream: 8 000 hr/yr 333,33 day/yr

REVENUES AND PRODUCTION COSTS

	M€/yr
Main product (methane) revenue	15,8
Raw materials cost	30,7
Utilities cost	0,6
Consumables cost	0,41
VCOP	31,7
Salary and overheads	0,9
Maintenance	0,0
Interest	0,08
FCOP	1,0

CAPITAL COSTS

	M€
ISBL Capital Cost	16,3
OSBL Capital Cost	6,5
Engineering Costs	6,8
Contingency	4,6
Total Fixed Capital Cost	34,1
Working Capital	-10,831 year 4

Use suitable fractions/expressions

CONSTRUCTION SCHEDULE

Year	% FC	% WC	% FCOP	% VCOP
1	50,00 %	50,00 %		
2	50,00 %	50,00 %		
3			50,00 %	50,00 %
4			100,00 %	100,00 %
5			100,00 %	100,00 %
6			100,00 %	100,00 %
7+			100,00 %	100,00 %

Select percentages according to scheduling of construction, start-up and full operation

ECONOMIC ASSUMPTIONS

Cost of equity	8 %	Debt ratio		Tax rate	24 %
Cost of debt	8 %			Depreciation method	
Cost of capital	8 %			Depreciation period	20 years

CASH FLOW ANALYSIS

All figures in €MM unless indicated

Project year	Cap Ex	Revenue	CCOP	Gr. Profit	Deprcn	Taxbl Inc	Tax Paid	Cash Flow	PV of CF	NPV
1	11,7	0,0	0,0	0,0	0,0	0,0	0,0	-11,7	-10,8	-10,8
2	11,7	0,0	0,0	0,0	0,0	0,0	0,0	-11,7	-10,0	-20,8
3	0,0	7,9	16,4	-8,5	0,0	-8,5	0,0	-8,5	-6,7	-27,5
4	0,0	15,8	32,7	-16,9	0,0	-16,9	-2,0	-14,9	-11,0	-38,5
5	0,0	15,8	32,7	-16,9	0,0	-16,9	-4,1	-12,9	-8,8	-47,2
6	0,0	15,8	32,7	-16,9	0,0	-16,9	-4,1	-12,9	-8,1	-55,4
7	0,0	15,8	32,7	-16,9	0,0	-16,9	-4,1	-12,9	-7,5	-62,9
8	0,0	15,8	32,7	-16,9	0,0	-16,9	-4,1	-12,9	-7,0	-69,8
9	0,0	15,8	32,7	-16,9	0,0	-16,9	-4,1	-12,9	-6,4	-76,3
10	0,0	15,8	32,7	-16,9	0,0	-16,9	-4,1	-12,9	-6,0	-82,2
11	0,0	15,8	32,7	-16,9	0,0	-16,9	-4,1	-12,9	-5,5	-87,8
12	0,0	15,8	32,7	-16,9	0,0	-16,9	-4,1	-12,9	-5,1	-92,9
13	0,0	15,8	32,7	-16,9	0,0	-16,9	-4,1	-12,9	-4,7	-97,6
14	0,0	15,8	32,7	-16,9	0,0	-16,9	-4,1	-12,9	-4,4	-102,0
15	0,0	15,8	32,7	-16,9	0,0	-16,9	-4,1	-12,9	-4,1	-106,1
16	0,0	15,8	32,7	-16,9	0,0	-16,9	-4,1	-12,9	-3,8	-109,8
17	0,0	15,8	32,7	-16,9	0,0	-16,9	-4,1	-12,9	-3,5	-113,3
18	0,0	15,8	32,7	-16,9	0,0	-16,9	-4,1	-12,9	-3,2	-116,5
19	0,0	15,8	32,7	-16,9	0,0	-16,9	-4,1	-12,9	-3,0	-119,5
20	10,8	15,8	32,7	-16,9	0,0	-16,9	-4,1	-23,7	-5,1	-124,6

ECONOMIC ANALYSIS

Average cash flow	-14,1 €MM/yr	NPV	10 years	-82,2 €MM	IRR	10 years	#LUKU!
Simple pay-back period	-1,6488413 yrs		15 years	-106,1 €MM		15 years	#LUKU!
Return on investment (10 yrs)	-54,54 %		20 years	-124,6 €MM		20 years	#LUKU!
Return on investment (15 yrs)	-60,60 %	NPV to yr	1	-10,8 €MM			

NOTES

Figure A-5 Economic analysis of biological methanation when deoxo process is included, with hydrogen price of 2 €/kg and biogas selling price of 1.90 €/kg.

ECONOMIC ANALYSIS

Project Name
Project Number
Sheet 1

REV	DATE	BY	APVD	REV	DATE	BY	APVD

Owner's Name
Plant Location: Finland
Case Description: Methanation plant
Capital Cost Basis Year: 2006
Units: ○ English ◉ Metric
On Stream: 8 000 hr/yr 333,33 day/yr

REVENUES AND PRODUCTION COSTS

	M€/yr
Main product (methane) revenue	20,7
Raw materials cost	12,2
Utilities cost	0,6
Consumables cost	0,41
VCOP	13,2
Salary and overheads	0,9
Maintenance	0,0
Interest	0,08
FCOP	1,0

CAPITAL COSTS

	M€
ISBL Capital Cost	16,3
OSBL Capital Cost	6,5
Engineering Costs	6,8
Contingency	4,6
Total Fixed Capital Cost	34,1
Working Capital	6,922 year 4

Use suitable fractions/expressions

CONSTRUCTION SCHEDULE

Year	% FC	% WC	% FCOP	% VCOP
1	50,00 %	50,00 %		
2	50,00 %	50,00 %		
3			50,00 %	50,00 %
4			100,00 %	100,00 %
5			100,00 %	100,00 %
6			100,00 %	100,00 %
7+			100,00 %	100,00 %

Select percentages according to scheduling of construction, start-up and full operation

ECONOMIC ASSUMPTIONS

Cost of equity	8 %	Debt ratio		Tax rate	24 %
Cost of debt	8 %			Depreciation method	
Cost of capital	8 %			Depreciation period	20 years

CASH FLOW ANALYSIS

All figures in €MM unless indicated

Project year	Cap Ex	Revenue	CCOP	Gr. Profit	Deprcn	Taxbl Inc	Tax Paid	Cash Flow	PV of CF	NPV
1	20,5	0,0	0,0	0,0	0,0	0,0	0,0	-20,5	-19,0	-19,0
2	20,5	0,0	0,0	0,0	0,0	0,0	0,0	-20,5	-17,6	-36,6
3	0,0	10,3	7,1	3,2	0,0	3,2	0,0	3,2	2,5	-34,1
4	0,0	20,7	14,3	6,4	0,0	6,4	0,8	5,6	4,1	-29,9
5	0,0	20,7	14,3	6,4	0,0	6,4	1,5	4,9	3,3	-26,6
6	0,0	20,7	14,3	6,4	0,0	6,4	1,5	4,9	3,1	-23,5
7	0,0	20,7	14,3	6,4	0,0	6,4	1,5	4,9	2,8	-20,7
8	0,0	20,7	14,3	6,4	0,0	6,4	1,5	4,9	2,6	-18,1
9	0,0	20,7	14,3	6,4	0,0	6,4	1,5	4,9	2,4	-15,6
10	0,0	20,7	14,3	6,4	0,0	6,4	1,5	4,9	2,3	-13,4
11	0,0	20,7	14,3	6,4	0,0	6,4	1,5	4,9	2,1	-11,3
12	0,0	20,7	14,3	6,4	0,0	6,4	1,5	4,9	1,9	-9,3
13	0,0	20,7	14,3	6,4	0,0	6,4	1,5	4,9	1,8	-7,5
14	0,0	20,7	14,3	6,4	0,0	6,4	1,5	4,9	1,7	-5,9
15	0,0	20,7	14,3	6,4	0,0	6,4	1,5	4,9	1,5	-4,3
16	0,0	20,7	14,3	6,4	0,0	6,4	1,5	4,9	1,4	-2,9
17	0,0	20,7	14,3	6,4	0,0	6,4	1,5	4,9	1,3	-1,6
18	0,0	20,7	14,3	6,4	0,0	6,4	1,5	4,9	1,2	-0,4
19	0,0	20,7	14,3	6,4	0,0	6,4	1,5	4,9	1,1	0,7
20	-6,9	20,7	14,3	6,4	0,0	6,4	1,5	11,8	2,5	3,3

ECONOMIC ANALYSIS

Average cash flow	5,5 €MM/yr	NPV	10 years	-13,4 €MM	IRR	10 years	-1,5%
Simple pay-back period	7,44562649 yrs		15 years	-4,3 €MM		15 years	6,0%
Return on investment (10 yrs)	11,71 %		20 years	3,3 €MM		20 years	9,1%
Return on investment (15 yrs)	13,01 %	NPV to yr	1	-19,0 €MM			

NOTES

Figure A-6 Economic analysis of biological methanation without deoxo process, with hydrogen price of 2 €/kg and biogas selling price of 1.90 €/kg.

Project Name
Project Number Sheet 1

REV	DATE	BY	APVD	REV	DATE	BY	APVD

ECONOMIC ANALYSIS

Owner's Name
Plant Location Finland
Case Description Methanation plant

Capital Cost Basis Year 2006
Units ○ English ◉ Metric
On Stream 8 000 hr/yr 333,33 day/yr

REVENUES AND PRODUCTION COSTS

	M€/yr
Main product (methane) revenue	20,7
Raw materials cost	12,2
Utilities cost	0,6
Consumables cost	0,41
VCOP	13,2
Salary and overheads	0,9
Maintenance	0,0
Interest	0,08
FCOP	1,0

CAPITAL COSTS

	M€
ISBL Capital Cost	8,1
OSBL Capital Cost	3,2
Engineering Costs	3,4
Contingency	2,3
Total Fixed Capital Cost	17,0
Working Capital	6,922 year 4

Use suitable fractions/expressions

CONSTRUCTION SCHEDULE

Year	% FC	% WC	% FCOP	% VCOP
1	50,00 %	50,00 %		
2	50,00 %	50,00 %		
3			50,00 %	50,00 %
4			100,00 %	100,00 %
5			100,00 %	100,00 %
6			100,00 %	100,00 %
7+			100,00 %	100,00 %

Select percentages according to scheduling of construction, start-up and full operation

ECONOMIC ASSUMPTIONS

Cost of equity 8 % Debt ratio
Cost of debt 8 %
Cost of capital 8 %

Tax rate 24 %
Depreciation method
Depreciation period 20 years

CASH FLOW ANALYSIS

All figures in €MM unless indicated

Project year	Cap Ex	Revenue	CCOP	Gr. Profit	Deprcn	Taxbl Inc	Tax Paid	Cash Flow	PV of CF	NPV
1	12,0	0,0	0,0	0,0	0,0	0,0	0,0	-12,0	-11,1	-11,1
2	12,0	0,0	0,0	0,0	0,0	0,0	0,0	-12,0	-10,3	-21,3
3	0,0	10,3	7,1	3,2	0,0	3,2	0,0	3,2	2,5	-18,8
4	0,0	20,7	14,3	6,4	0,0	6,4	0,8	5,6	4,1	-14,6
5	0,0	20,7	14,3	6,4	0,0	6,4	1,5	4,9	3,3	-11,3
6	0,0	20,7	14,3	6,4	0,0	6,4	1,5	4,9	3,1	-8,3
7	0,0	20,7	14,3	6,4	0,0	6,4	1,5	4,9	2,8	-5,4
8	0,0	20,7	14,3	6,4	0,0	6,4	1,5	4,9	2,6	-2,8
9	0,0	20,7	14,3	6,4	0,0	6,4	1,5	4,9	2,4	-0,3
10	0,0	20,7	14,3	6,4	0,0	6,4	1,5	4,9	2,3	1,9
11	0,0	20,7	14,3	6,4	0,0	6,4	1,5	4,9	2,1	4,0
12	0,0	20,7	14,3	6,4	0,0	6,4	1,5	4,9	1,9	5,9
13	0,0	20,7	14,3	6,4	0,0	6,4	1,5	4,9	1,8	7,7
14	0,0	20,7	14,3	6,4	0,0	6,4	1,5	4,9	1,7	9,4
15	0,0	20,7	14,3	6,4	0,0	6,4	1,5	4,9	1,5	10,9
16	0,0	20,7	14,3	6,4	0,0	6,4	1,5	4,9	1,4	12,3
17	0,0	20,7	14,3	6,4	0,0	6,4	1,5	4,9	1,3	13,7
18	0,0	20,7	14,3	6,4	0,0	6,4	1,5	4,9	1,2	14,9
19	0,0	20,7	14,3	6,4	0,0	6,4	1,5	4,9	1,1	16,0
20	-6,9	20,7	14,3	6,4	0,0	6,4	1,5	11,8	2,5	18,5

ECONOMIC ANALYSIS

Average cash flow	5,5 €MM/yr	NPV	10 years	1,9 €MM	IRR	10 years	10,0%
Simple pay-back period	4,34021793 yrs		15 years	10,9 €MM		15 years	15,5%
Return on investment (10 yrs)	20,09 %		20 years	18,5 €MM		20 years	17,4%
Return on investment (15 yrs)	22,33 %	NPV to yr	1	-11,1 €MM			

NOTES